

# Geometric and probabilistic descriptions of chaotic phase space transport

Shane Ross

Dept. of Engineering Science and Mechanics, Virginia Tech

[www.shaneros.com](http://www.shaneros.com)

In collaboration with Piyush Grover, Carmine Senatore, Phanindra Tallapragada, Pankaj Kumar, Mohsen Gheisarieha, David Schmale, Francois Lekien, Mark Stremler

School and Conference on Computational Methods in Dynamics, ICTP, July 2011



MultiSTEPS: MultiScale Transport in  
Environmental & Physiological Systems,  
[www.multisteps.esm.vt.edu](http://www.multisteps.esm.vt.edu)



# Motivation: application to real data

- Many systems defined from data or large-scale simulations
  - experimental measurements, observations
- e.g., from fluid dynamics, biology, social sciences
- Aperiodic, finite-time, finite resolution
  - in general, no fixed points, periodic orbits, or other invariant sets (or their stable and unstable manifolds) to organize phase space

## Motivation: application to real data

- Perhaps can find appropriate analogs to the objects; adapt previous results to this setting
- Try some numerical explorations; see what merit furthers study

# Chaotic phase space transport via lobe dynamics

- As our dynamical system, we consider a discrete map<sup>1</sup>

$$f : \mathcal{M} \longrightarrow \mathcal{M},$$

e.g.,  $f = \phi_t^{t+T}$ , where  $\mathcal{M}$  is a differentiable, orientable, two-dimensional manifold e.g.,  $\mathbb{R}^2$ ,  $S^2$

- To understand the transport of points under the map  $f$ , we consider the **invariant manifolds of unstable fixed points**

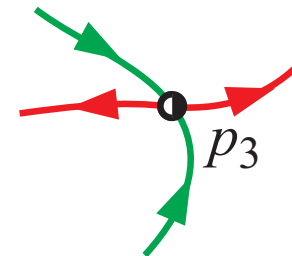
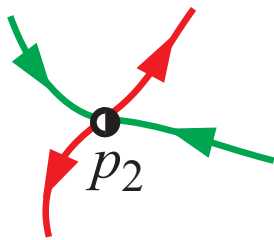
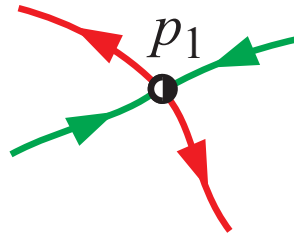
- Let  $p_i, i = 1, \dots, N_p$ , denote a collection of saddle-type hyperbolic fixed points for  $f$ .

---

<sup>1</sup>Following Rom-Kedar and Wiggins [1990]

# Partition phase space into regions

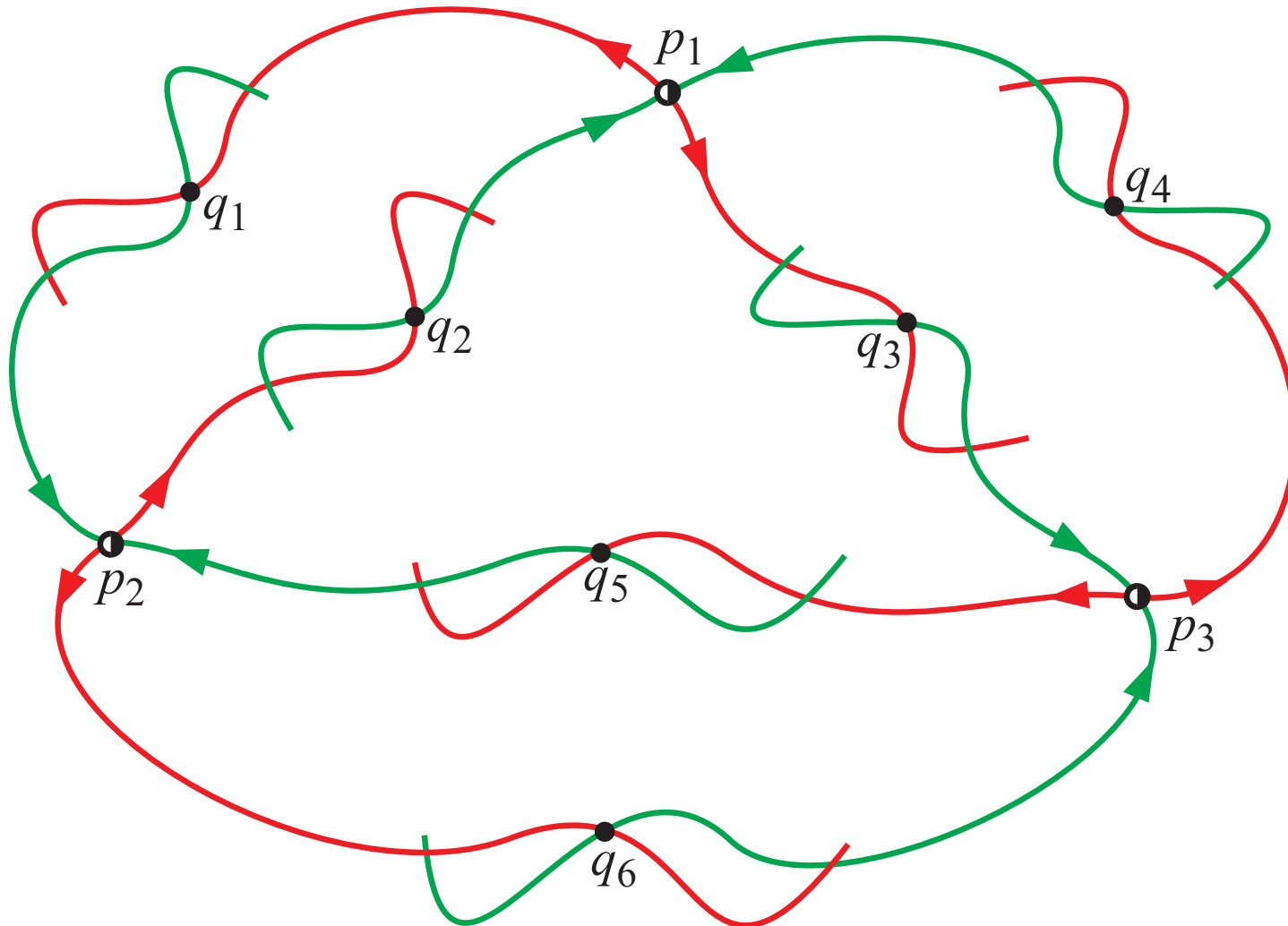
- Natural way to partition phase space
  - Pieces of  $W^u(p_i)$  and  $W^s(p_i)$  partition  $\mathcal{M}$ .



Unstable and stable manifolds in **red** and **green**, resp.

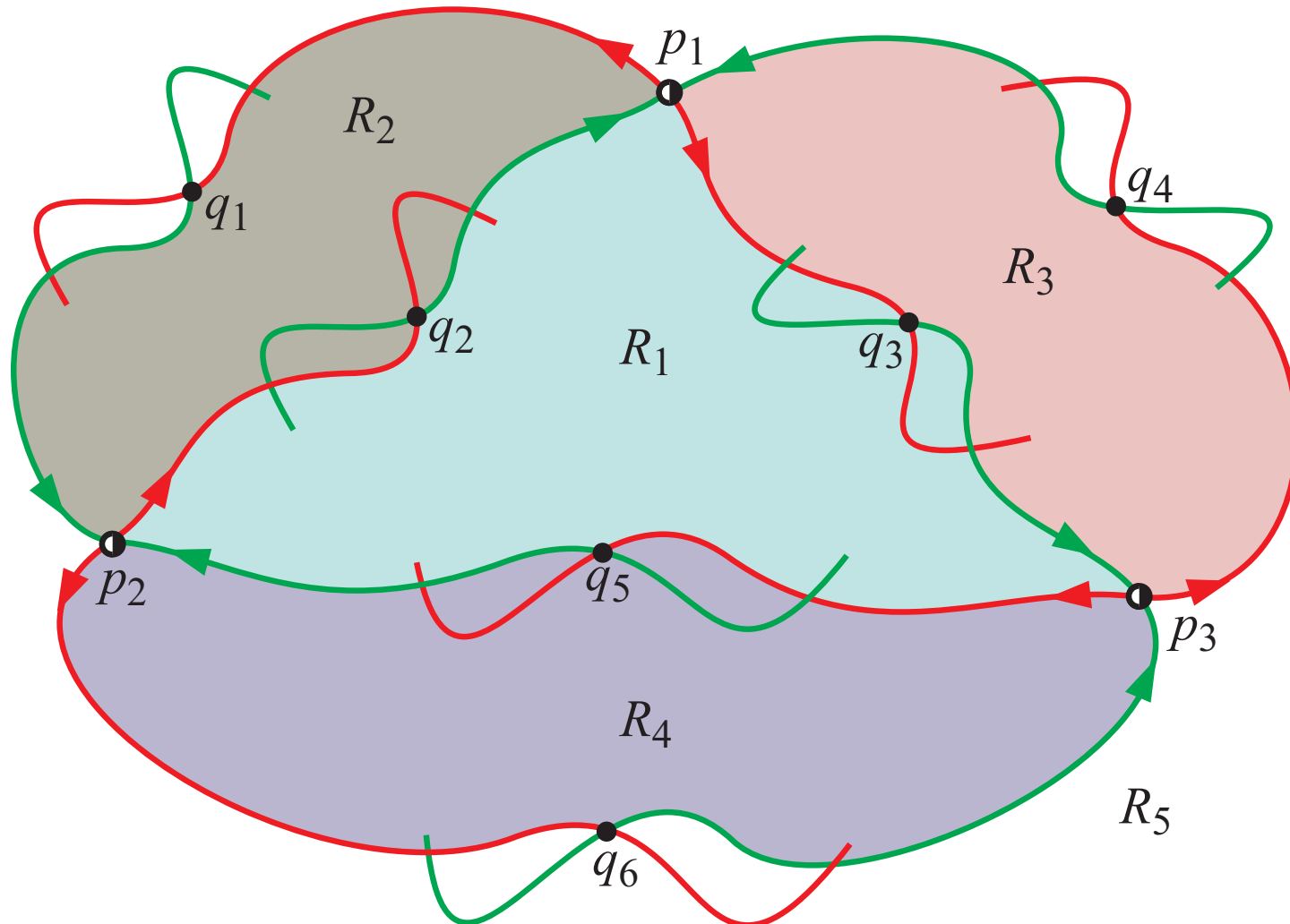
# Partition phase space into regions

- Intersection of unstable and stable manifolds define **boundaries**.



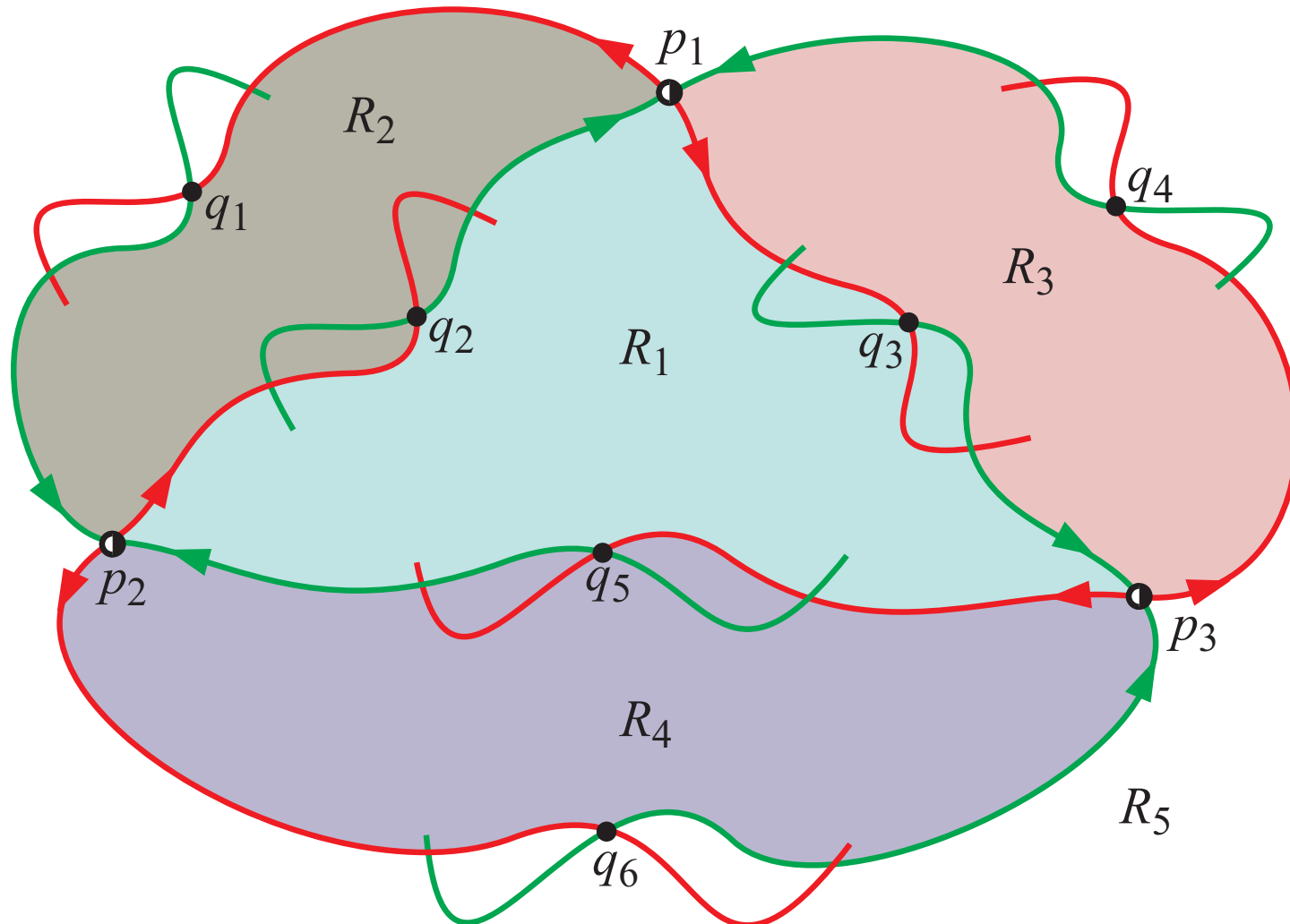
# Partition phase space into regions

- These boundaries divide the phase space into **regions**.



# Label mobile subregions: 'atoms' of transport

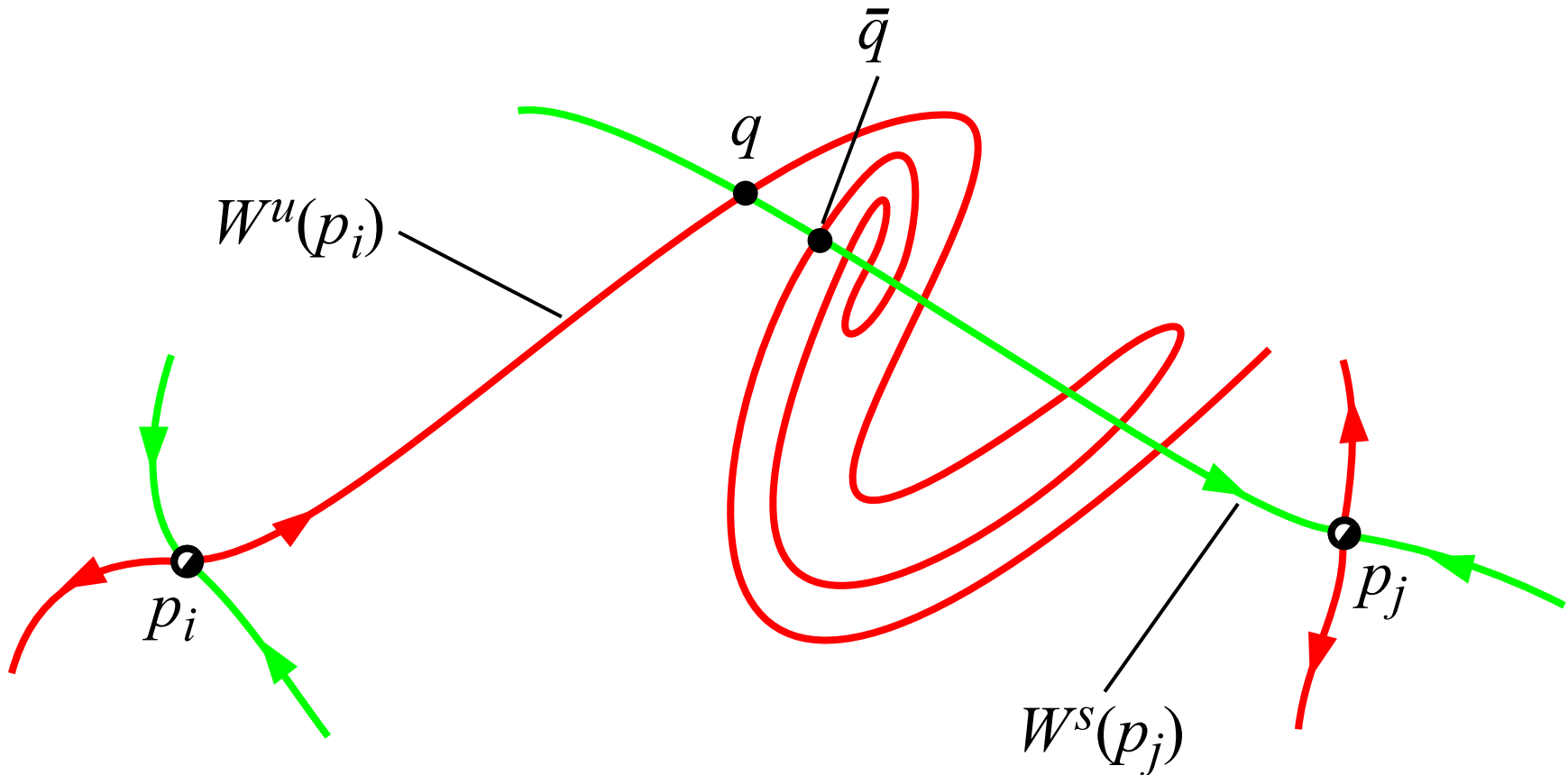
- Can label mobile subregions based on their past and future whereabouts under one iterate of the map, e.g.,  $(\dots, R_3, R_3, [R_1], R_1, R_2, \dots)$





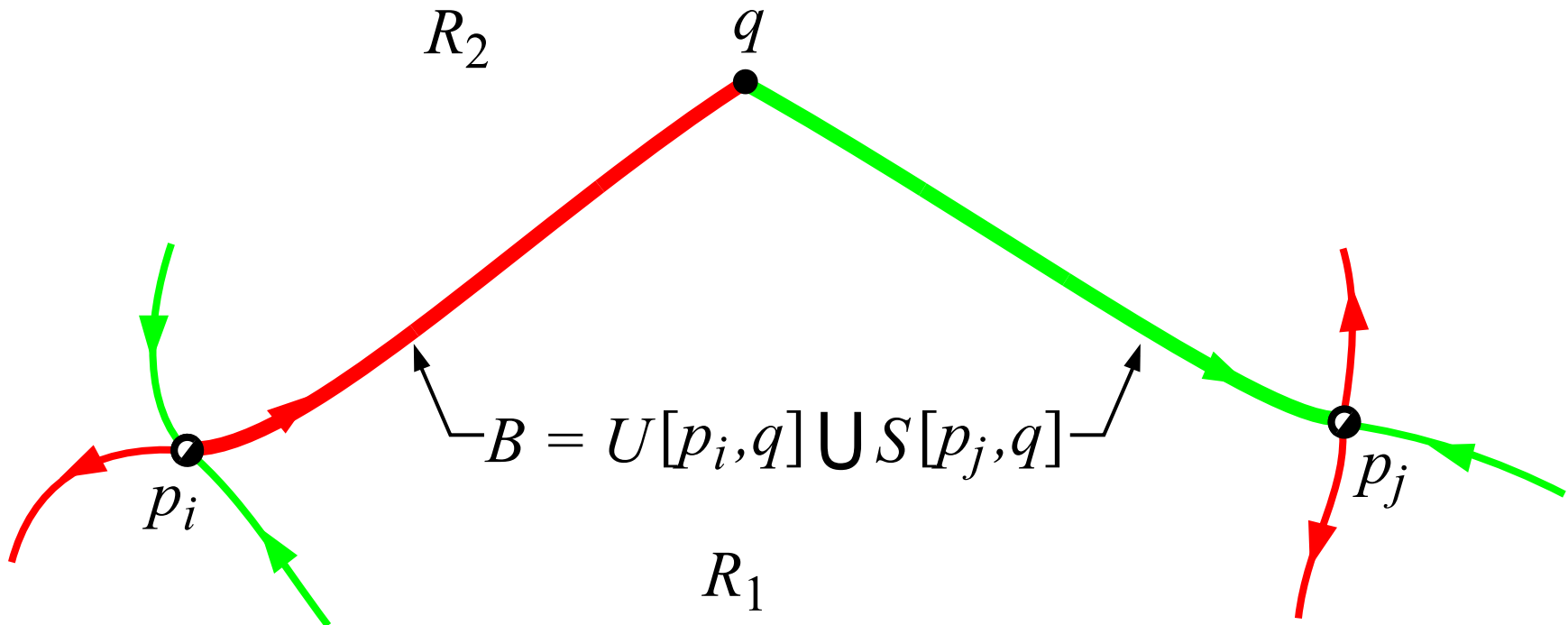
# Primary intersection points (pips) and boundaries

- $q$  is a primary intersection point (pip),  $\bar{q}$  is not a pip.



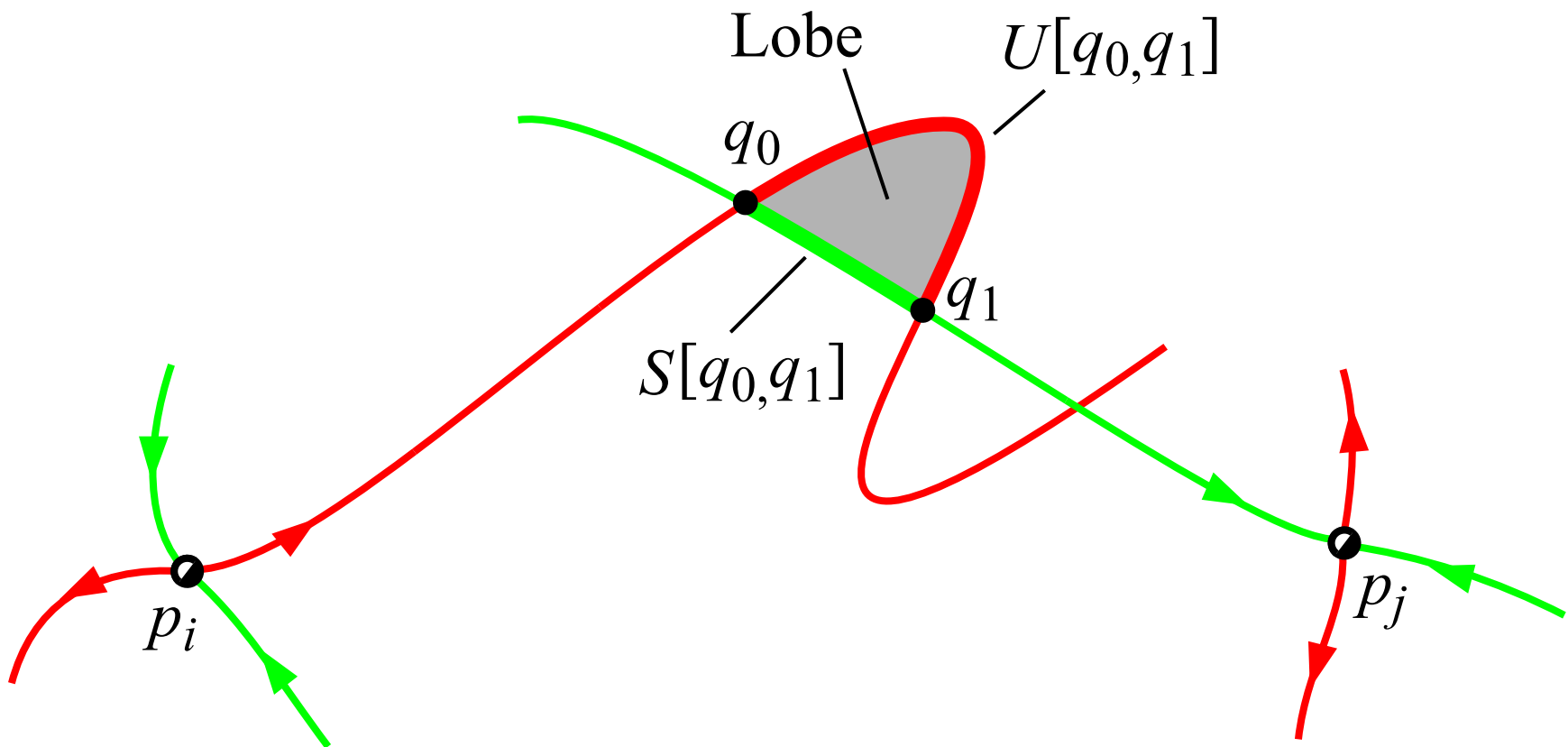
# Primary intersection points (pips) and boundaries

- Suppose  $W^u(p_i)$  and  $W^s(p_j)$  intersect in the pip  $q$ . Define  $B \equiv U[p_i, q] \cup S[p_j, q]$  as a **boundary** between “two sides,”  $R_1$  and  $R_2$ .



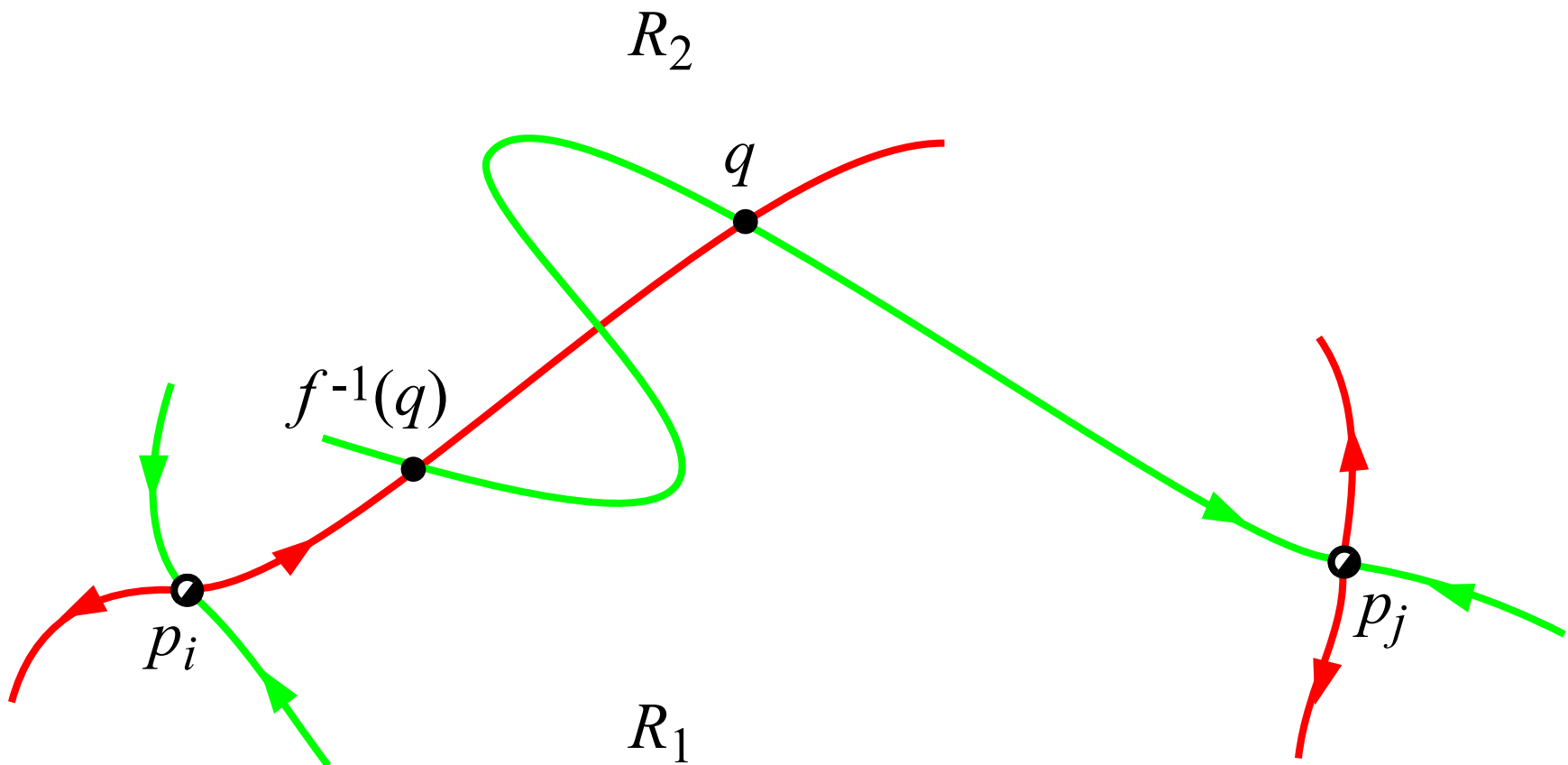
# Lobes: the mobile subregions

- Let  $q_0, q_1 \in W^u(p_i) \cap W^s(p_j)$  be two adjacent pips, i.e., there are no other pips on  $U[q_0, q_1]$  and  $S[q_0, q_1]$ . The region interior to  $U[q_0, q_1] \cup S[q_0, q_1]$  is a **lobe**.



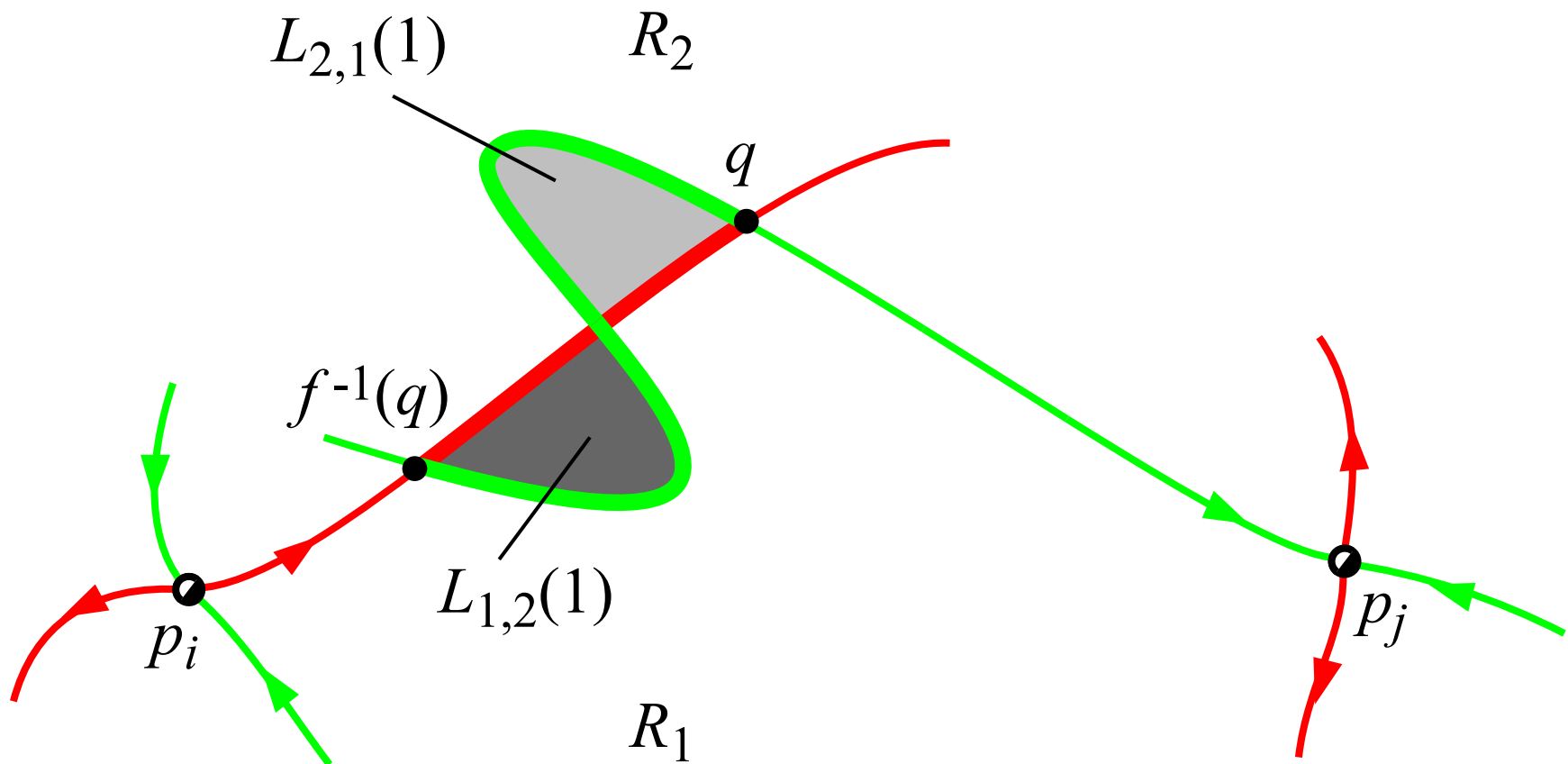
# Lobe dynamics: transport across a boundary $B$

- $f^{-1}(q)$  is a pip.  $f$  is orientation-preserving  $\Rightarrow$  there's *at least one* pip on  $U[f^{-1}(q), q]$  where the  $W^u(p_i), W^s(p_j)$  intersection is topologically transverse.



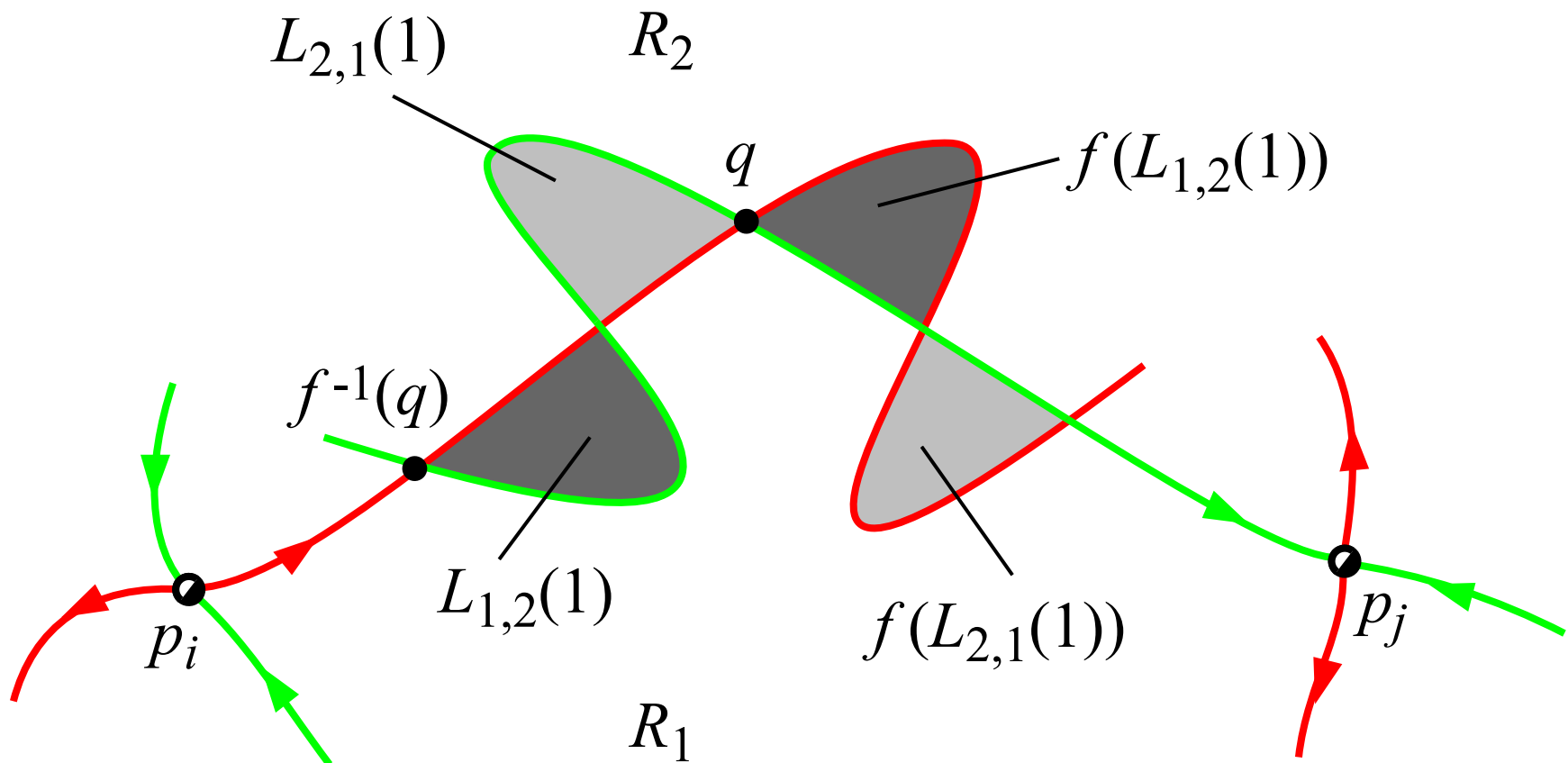
# Lobe dynamics: transport across a boundary $B$

- $U[f^{-1}(q), q] \cup S[f^{-1}(q), q]$  forms boundary of two lobes; one in  $R_1$ , labeled  $L_{1,2}(1)$ , or equivalently  $([R_1], R_2)$ , where  $f(([R_1], R_2)) = (R_1, [R_2])$ , etc. for  $L_{2,1}(1)$



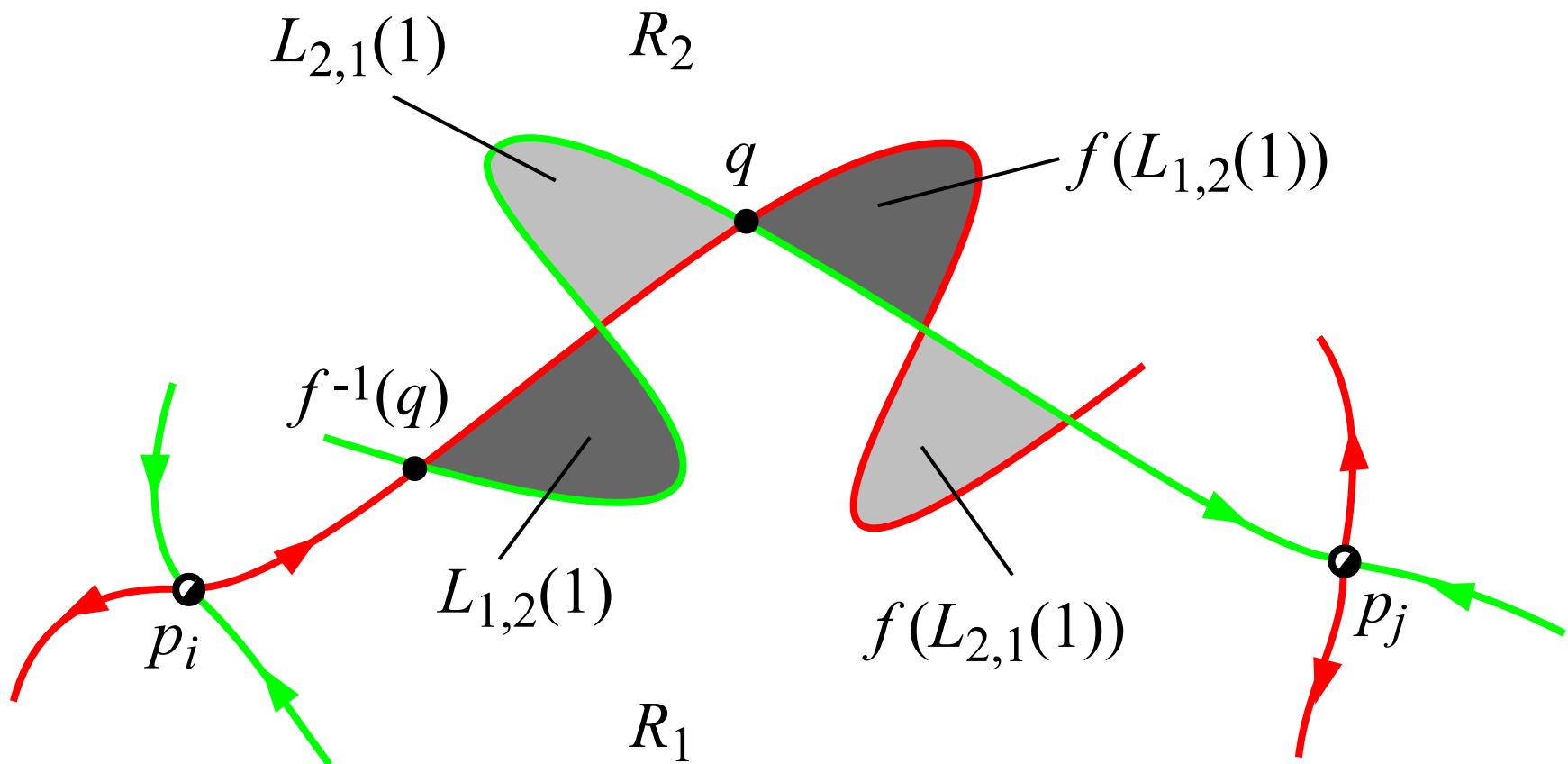
# Lobe dynamics: transport across a boundary $B$

- Under one iteration of  $f$ , *only points in  $L_{1,2}(1)$  can move from  $R_1$  into  $R_2$  by crossing  $B$ , etc.*
- The two lobes  $L_{1,2}(1)$  and  $L_{2,1}(1)$  are called a **turnstile**.



# Lobe dynamics: transport across a boundary $B$

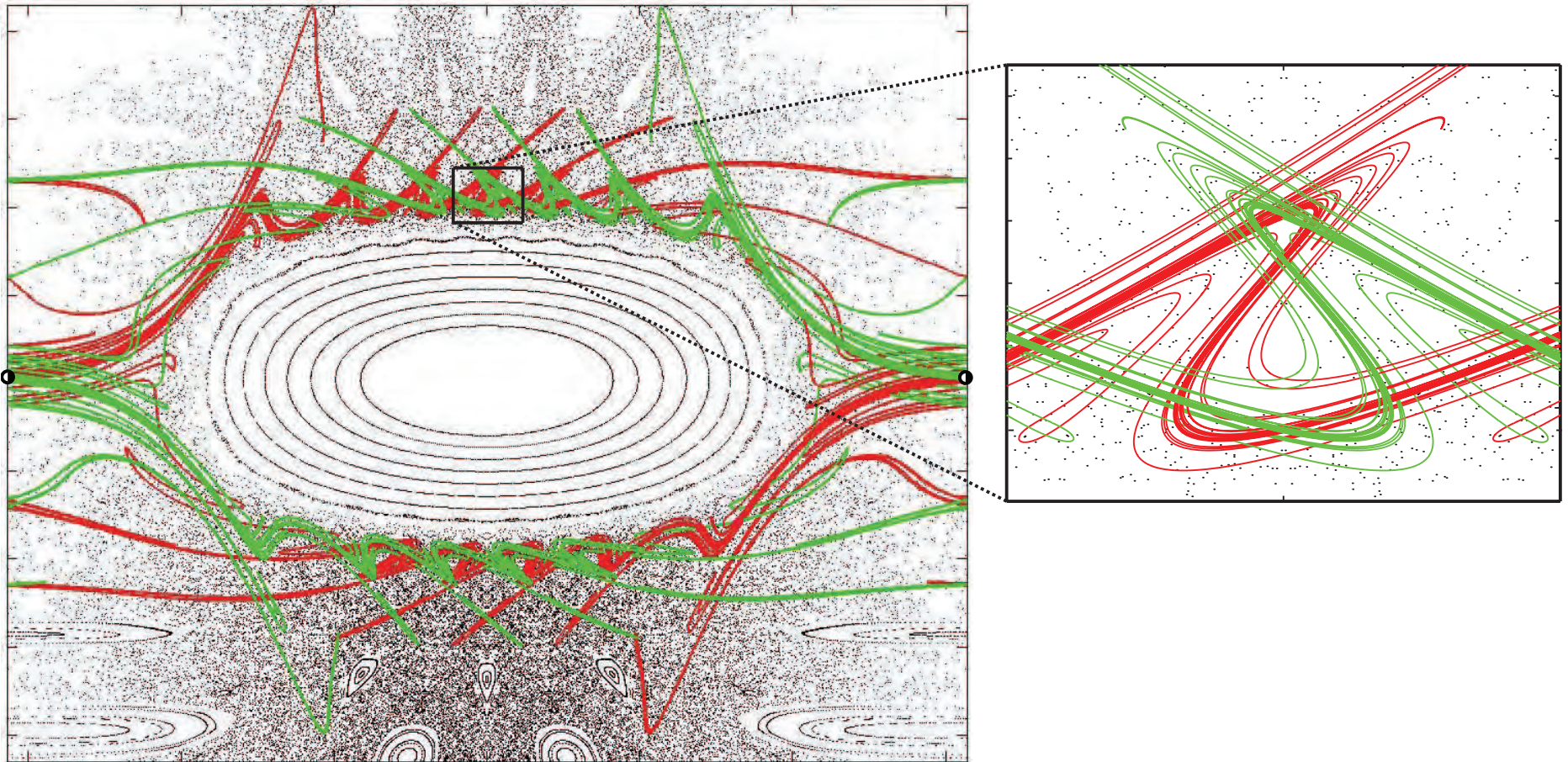
- Essence of lobe dynamics: the dynamics associated with crossing  $B$  is reduced to the dynamics of the turnstile lobes associated with  $B$ .





# Identifying atoms of transport by itinerary

- In a complicated system, can still identify manifolds ...

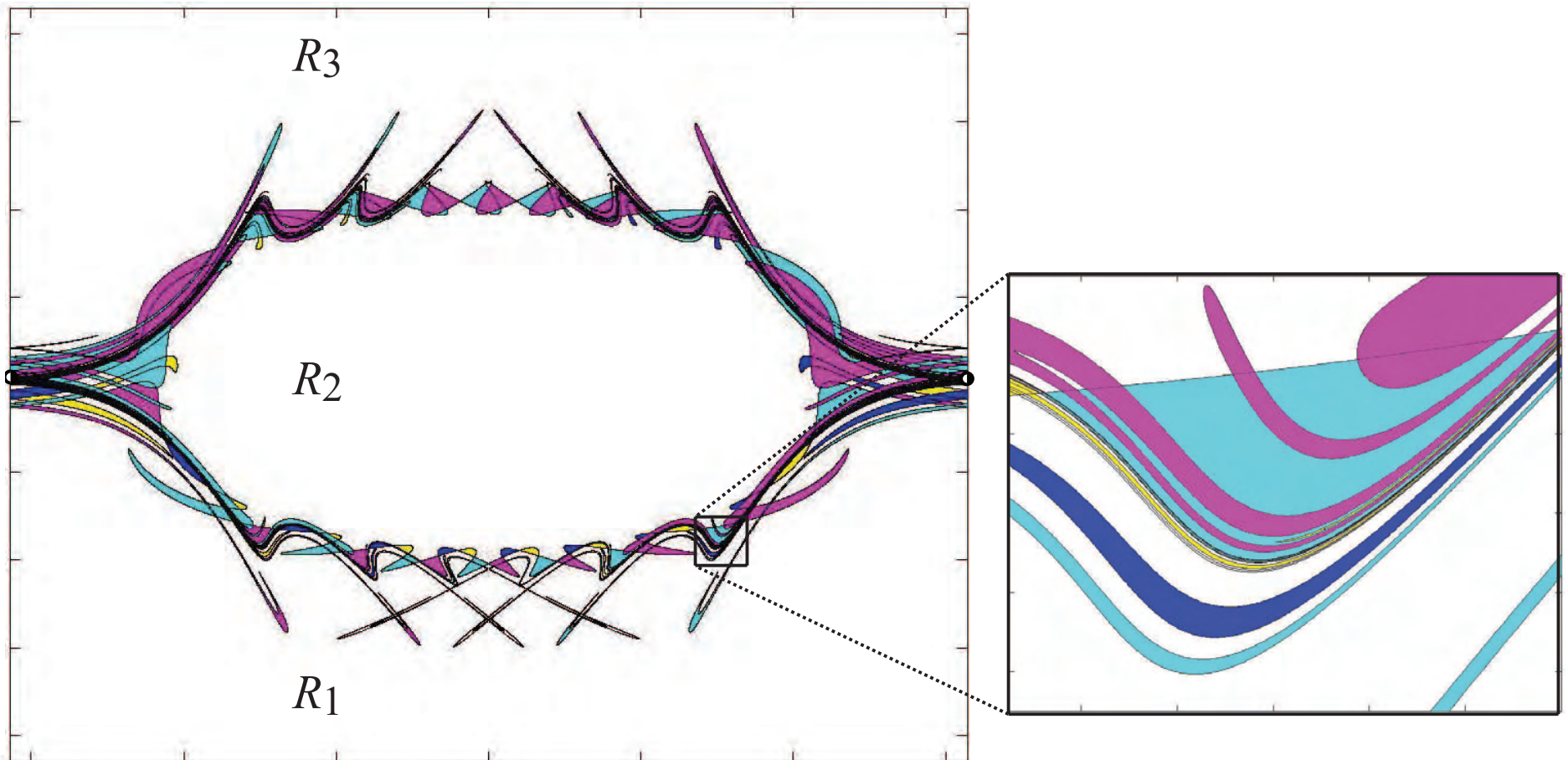


Unstable and stable manifolds in **red** and **green**, resp.



# Identifying atoms of transport by itinerary

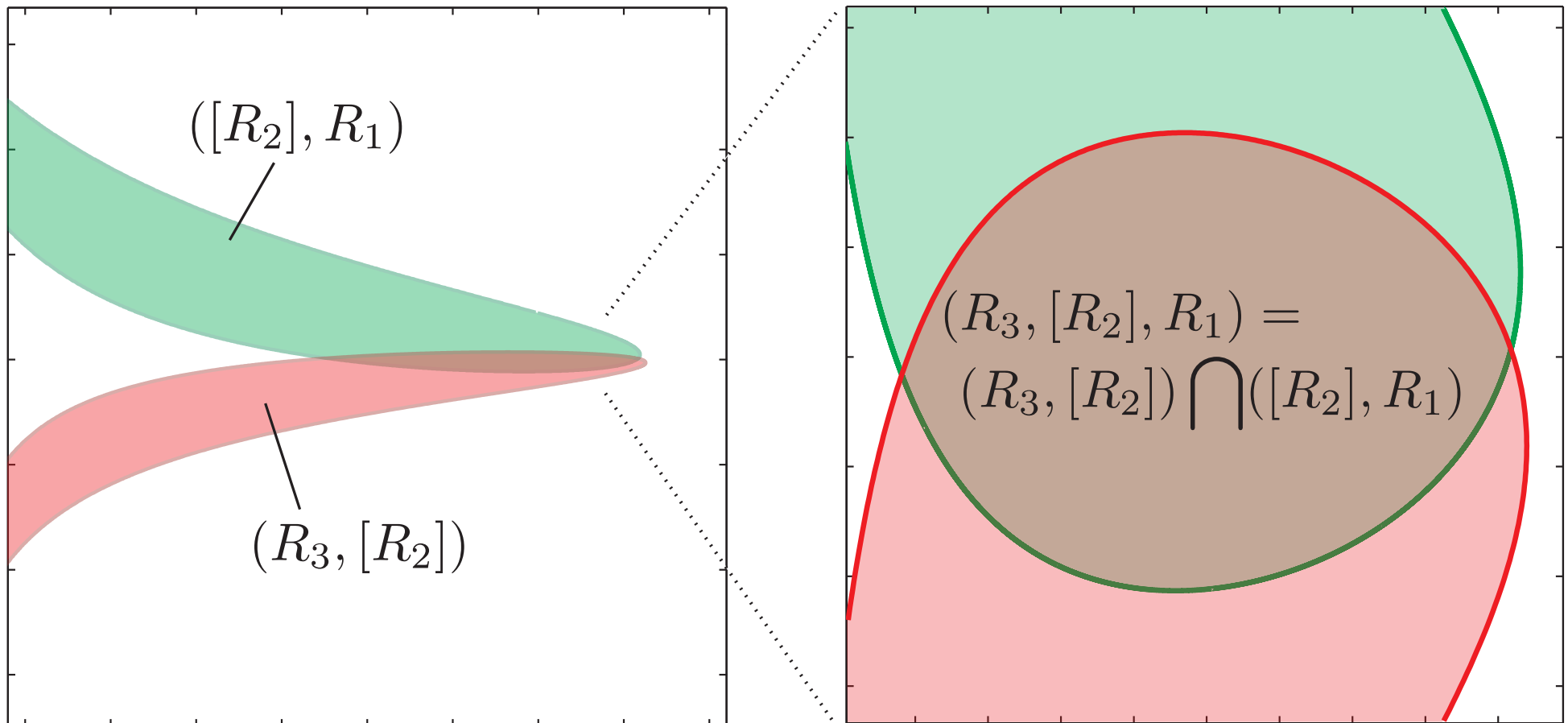
□ ... and lobes



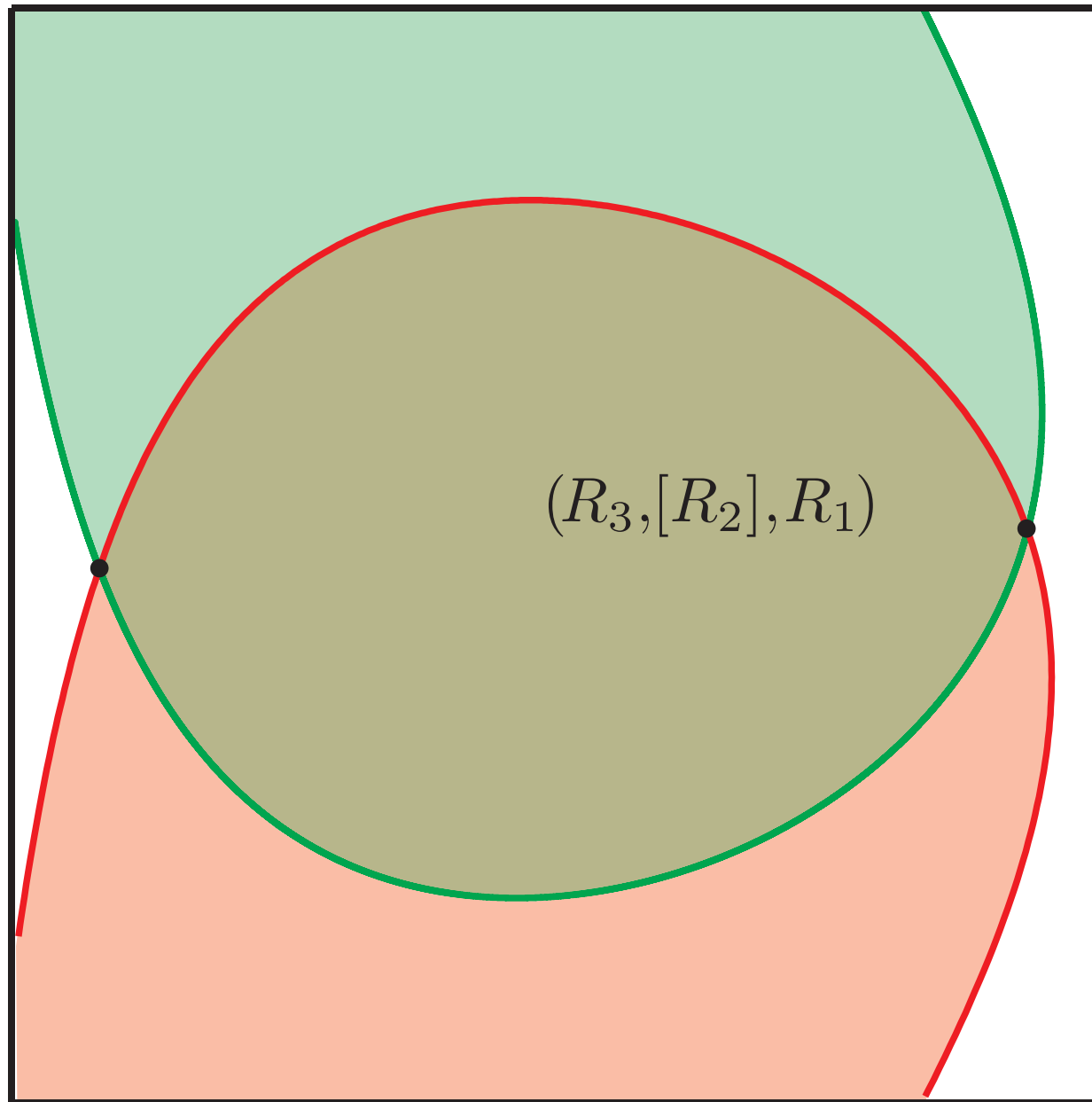
Significant amount of fine, filamentary structure.

# Identifying atoms of transport by itinerary

- e.g., with three regions  $\{R_1, R_2, R_3\}$ , label lobe intersections accordingly.
- Denote the intersection  $(R_3, [R_2]) \cap ([R_2], R_1)$  by  $(R_3, [R_2], R_1)$

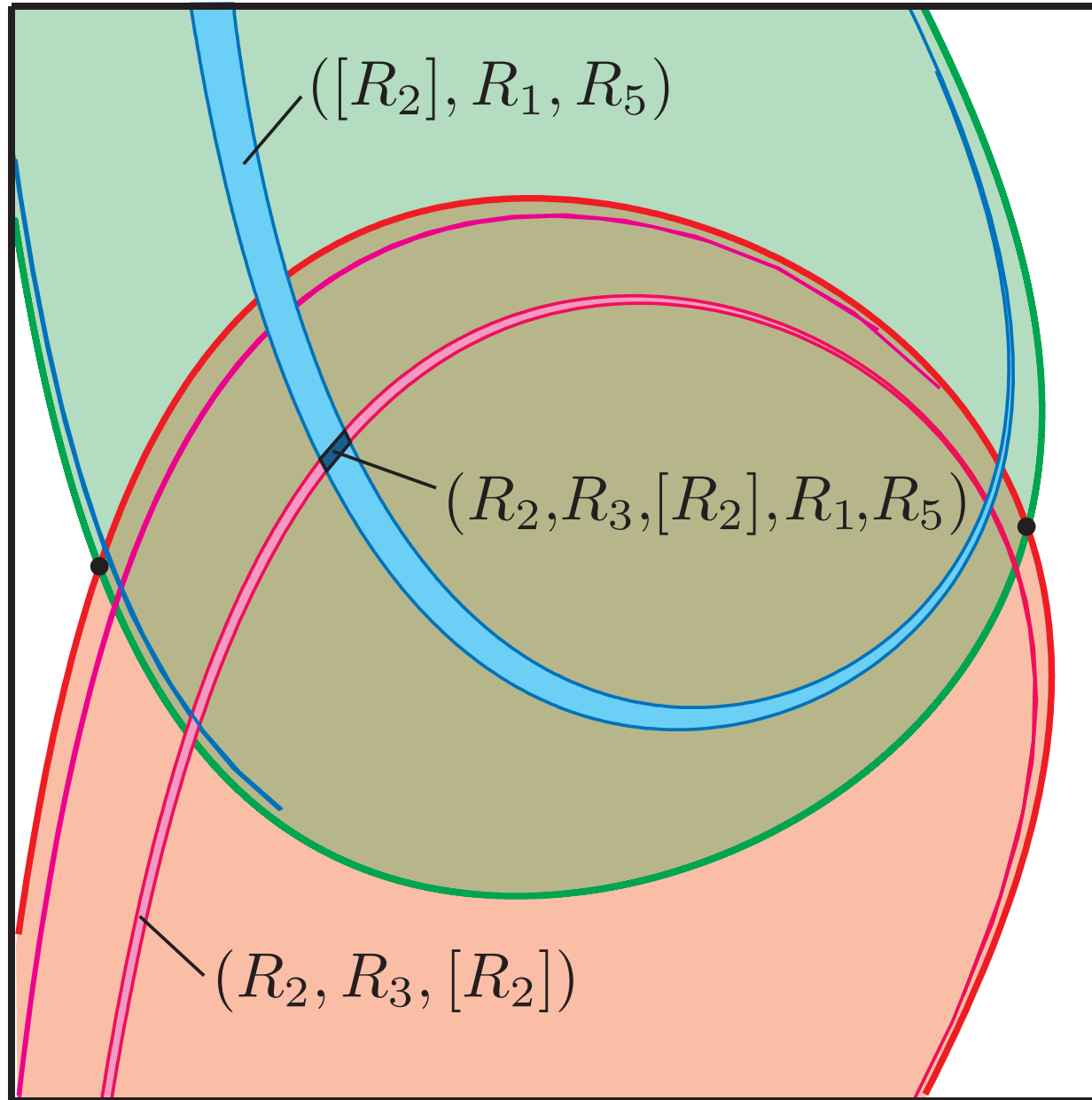


# Identifying atoms of transport by itinerary



Longer itineraries...

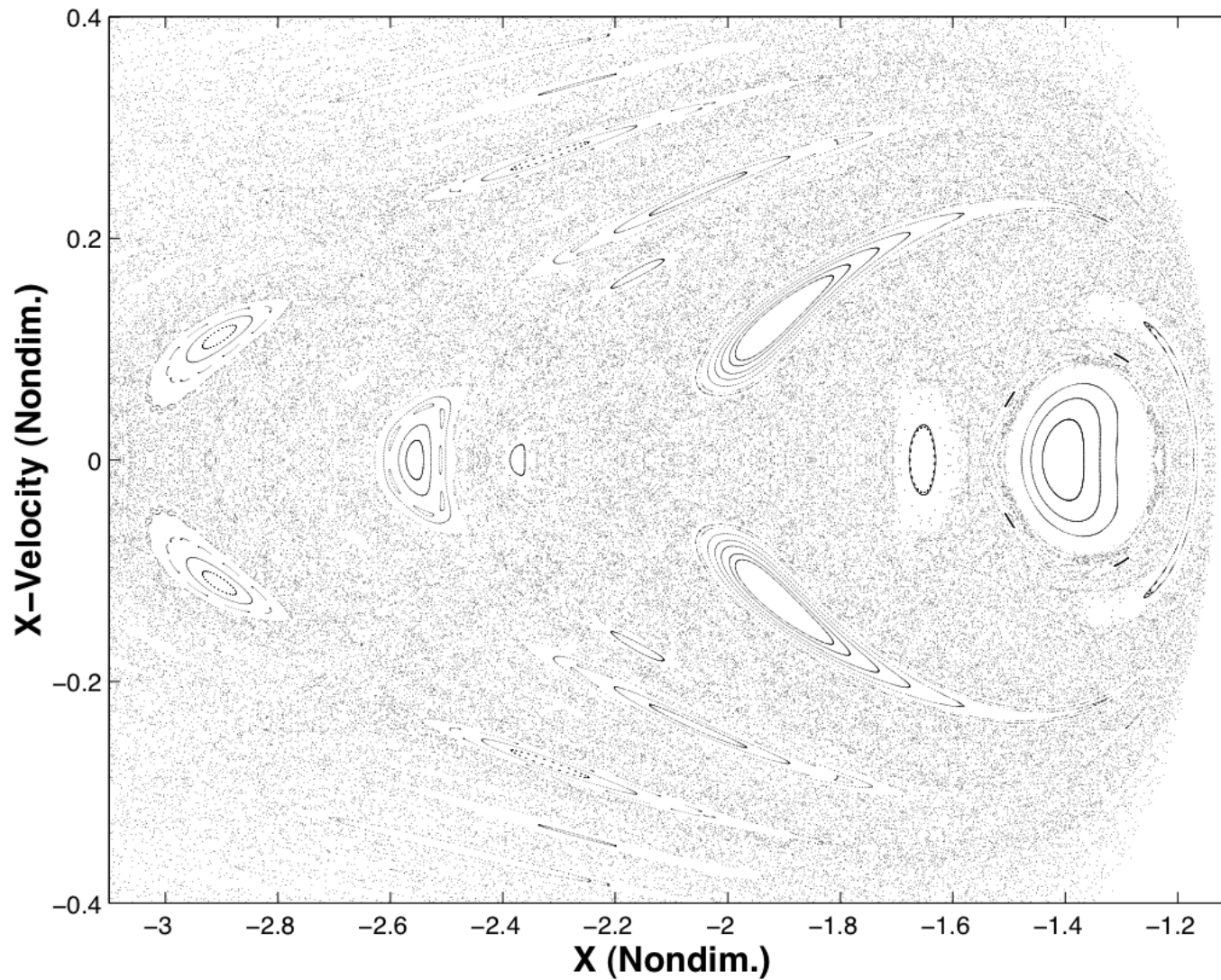
# Identifying atoms of transport by itinerary



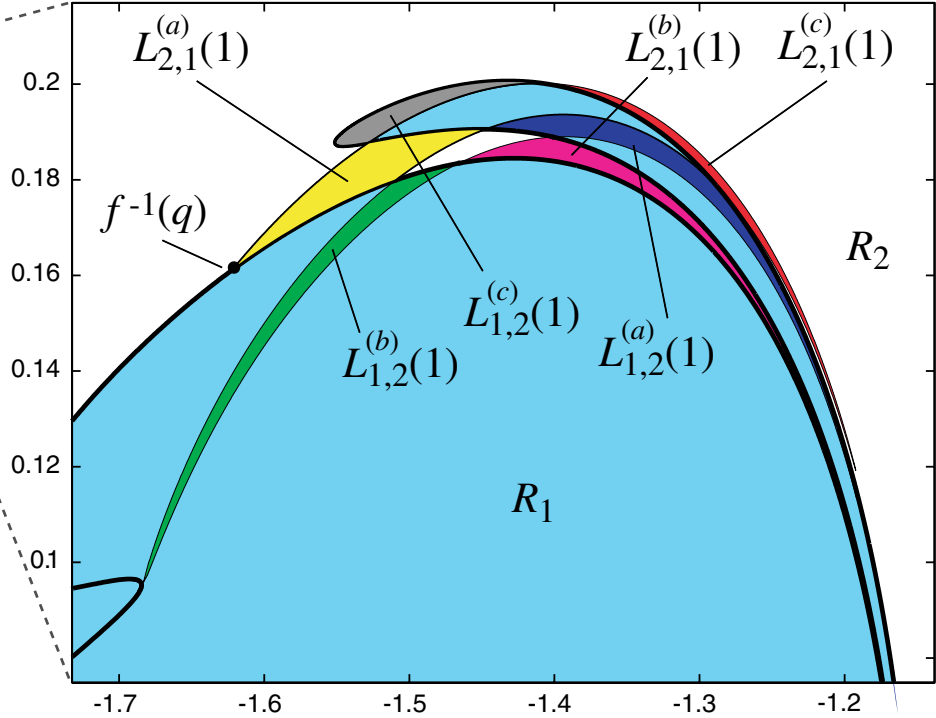
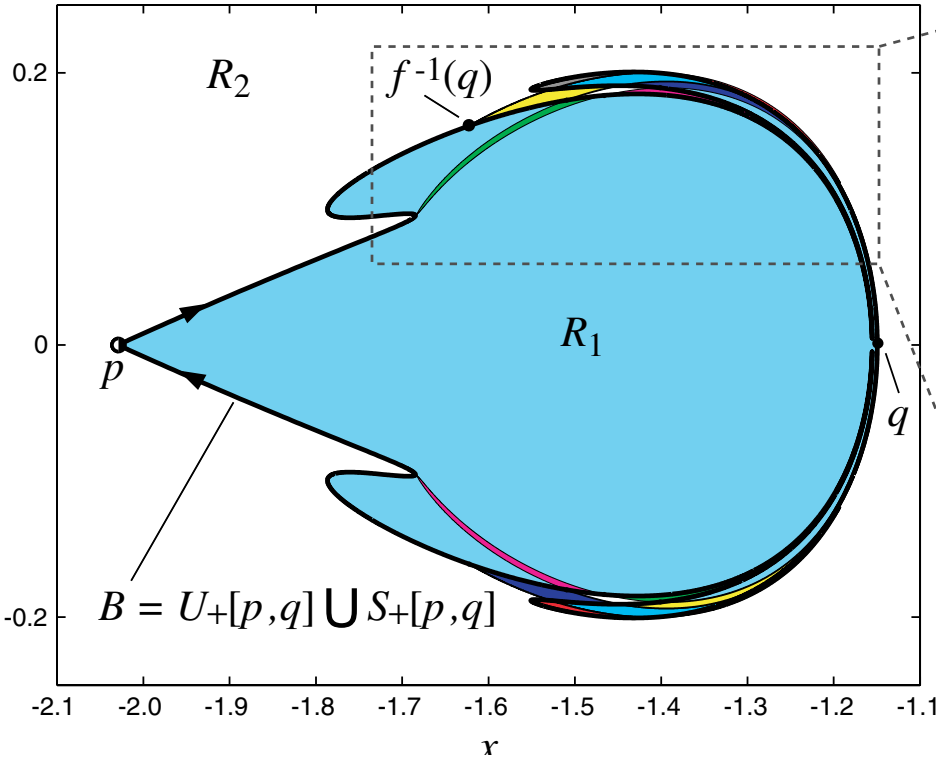
... correspond to smaller pieces of phase space; horseshoe dynamics, etc

# Lobe Dynamics: example

- rest. 3-body problem: chaotic sea contains unstable fixed points.



# Compute a boundary

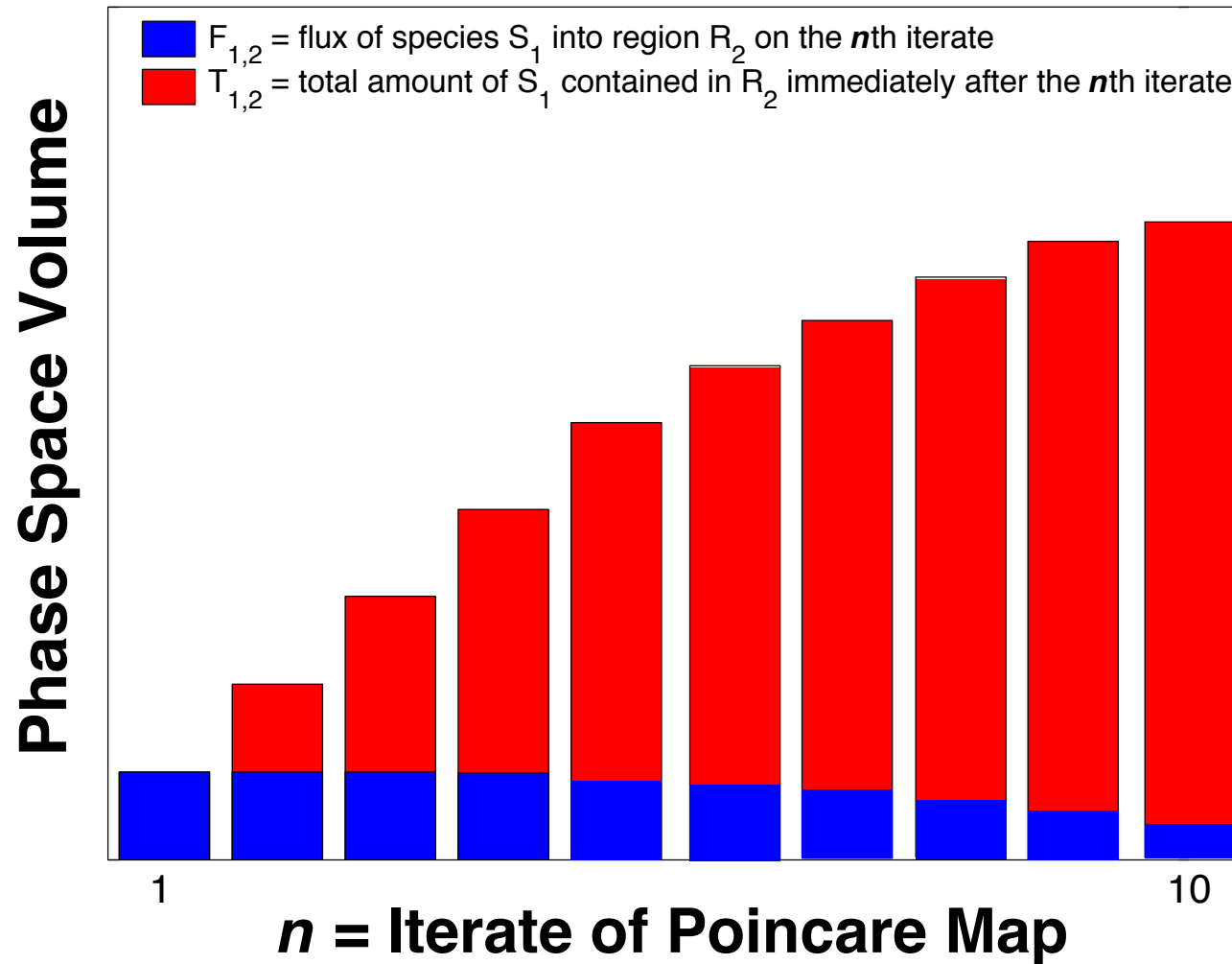


# Transport btwn Two Regions

- The evolution of a lobe of species  $S_1$  into  $R_2$

# Transport btwn Two Regions

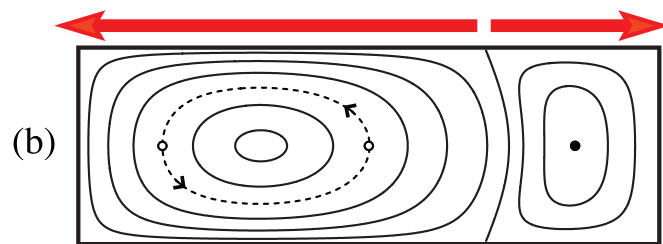
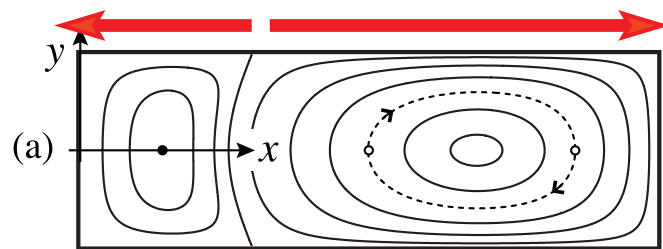
## Species Distribution: Species $S_1$ in Region $R_2$





# Lobe dynamics: fluid example

□ Fluid example: time-periodic Stokes flow



streamlines

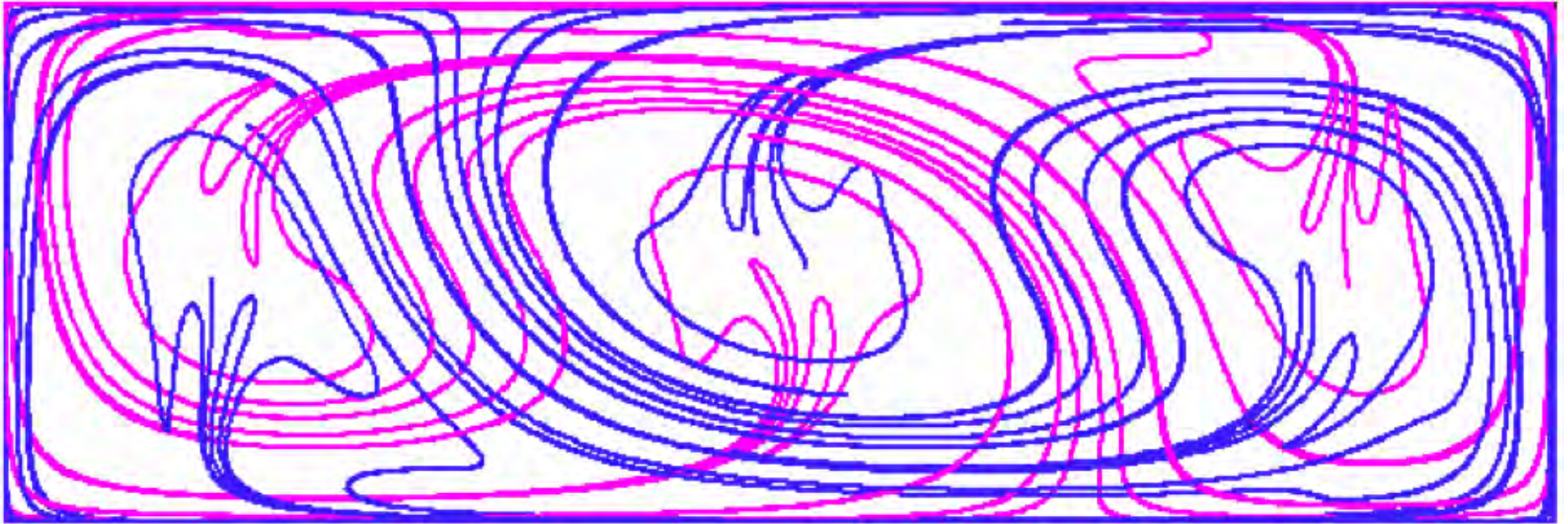
tracer blob

## Lid-driven cavity flow

- Model for microfluidic mixer
- System has parameter  $\tau_f$ , which we treat as a bifurcation parameter  
— critical point  $\tau_f^* = 1$ ; above and next few slides show  $\tau_f > 1$

# Lobe dynamics: fluid example

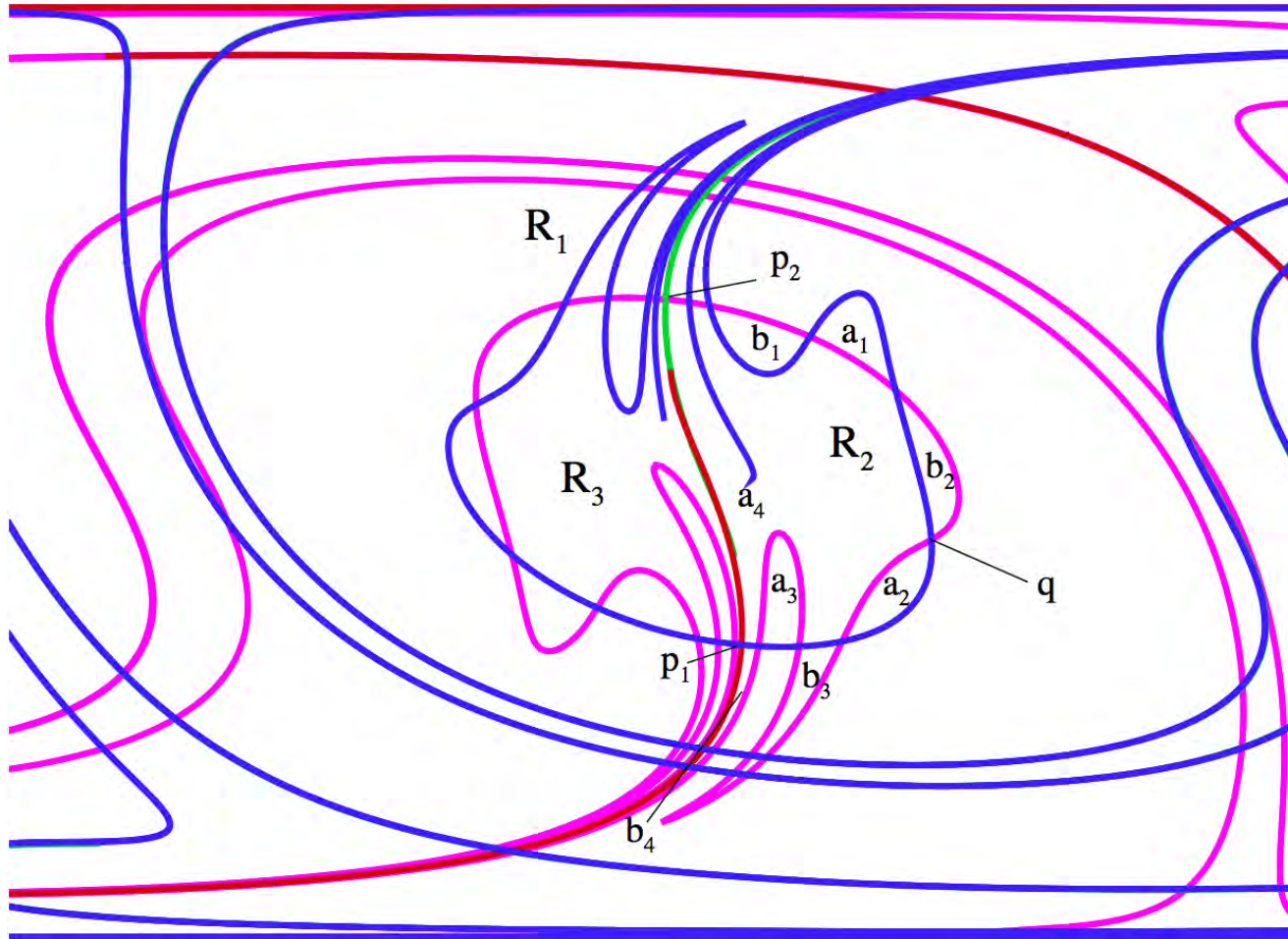
- Fluid example: Poincaré map



some invariant manifolds of saddles

# Lobe dynamics: fluid example

□ Fluid example: Poincaré map



regions and lobes labeled

# Stable/unstable manifolds and lobes in fluids

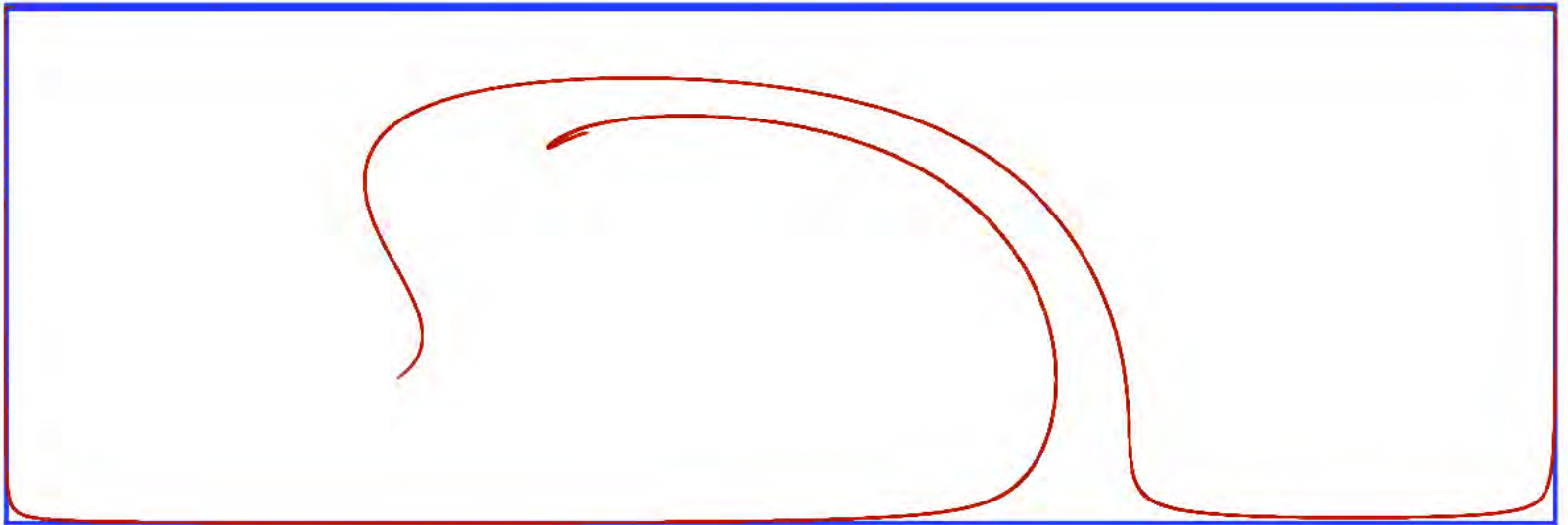
□ Fluid example: Poincaré map



material blob at  $t = 0$

# Stable/unstable manifolds and lobes in fluids

- Fluid example: Poincaré map

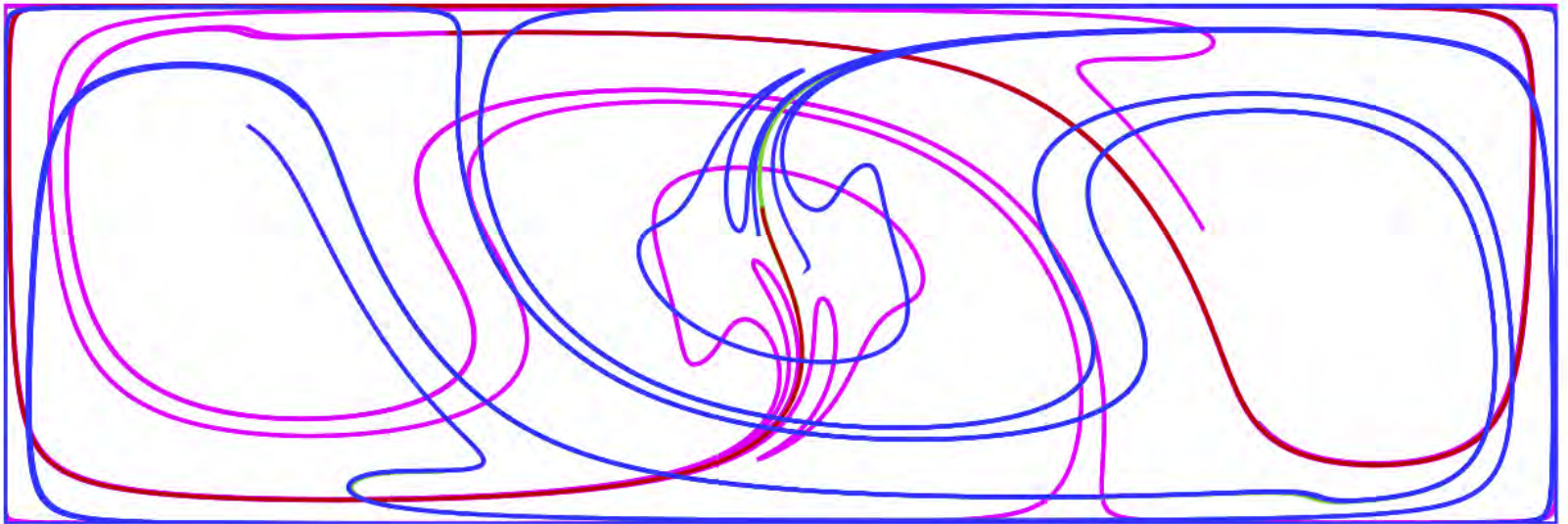


material blob at  $t = 5$



# Stable/unstable manifolds and lobes in fluids

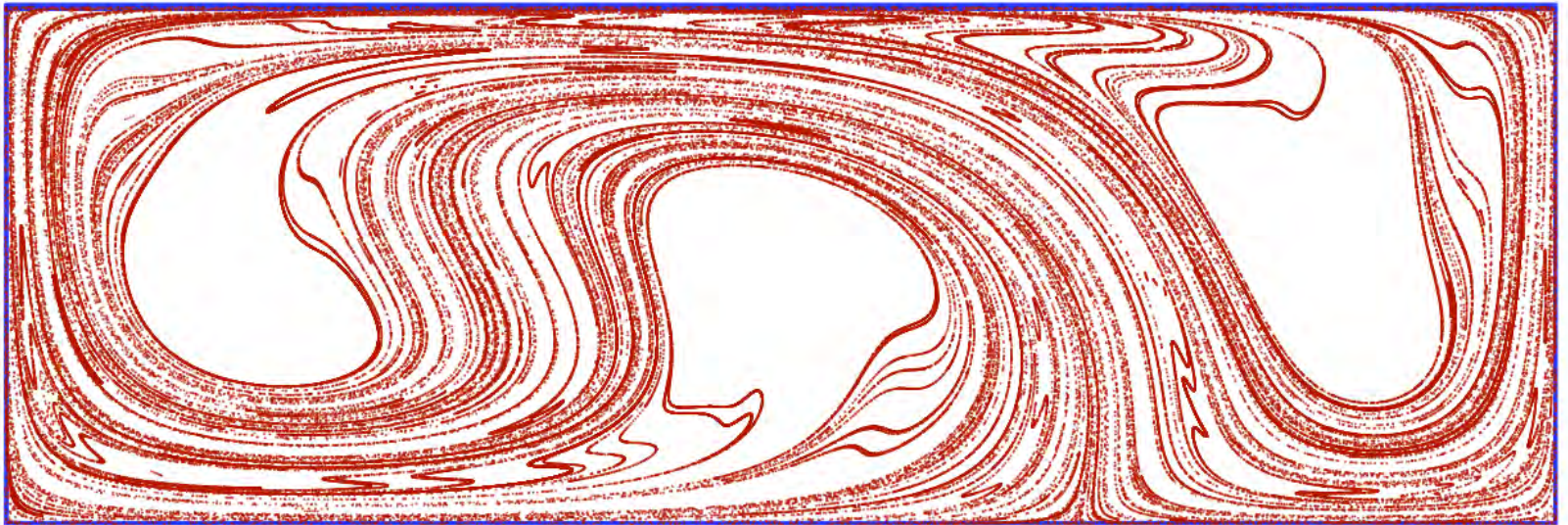
- Fluid example: Poincaré map



some invariant manifolds of saddles

# Stable/unstable manifolds and lobes in fluids

- Fluid example: Poincaré map



material blob at  $t = 10$



# Stable/unstable manifolds and lobes in fluids

- Fluid example: Poincaré map

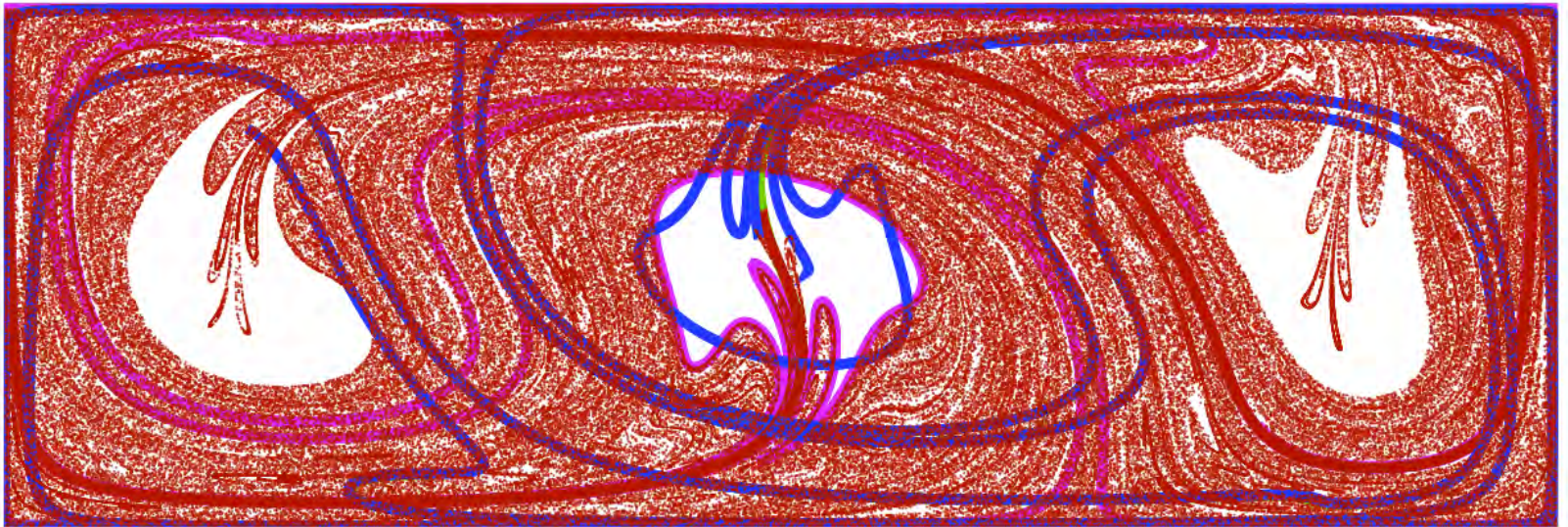


material blob at  $t = 15$



# Stable/unstable manifolds and lobes in fluids

- Fluid example: Poincaré map



material blob and manifolds

# Stable/unstable manifolds and lobes in fluids

- Fluid example: Poincaré map

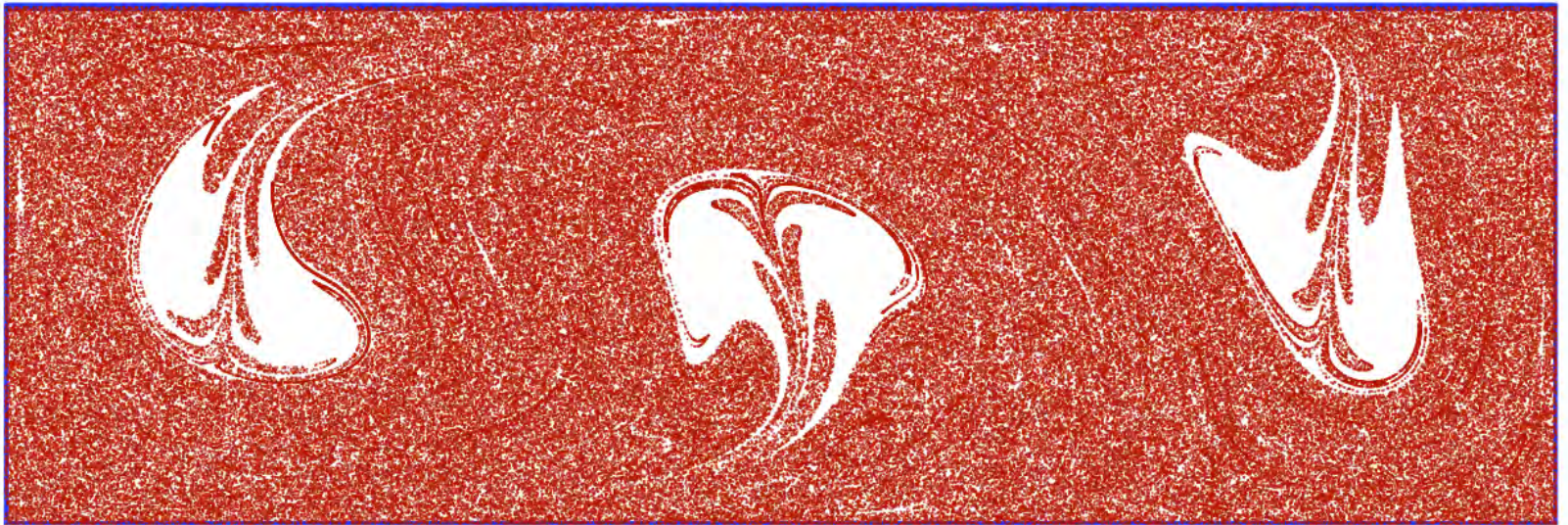


material blob at  $t = 20$



# Stable/unstable manifolds and lobes in fluids

- Fluid example: Poincaré map

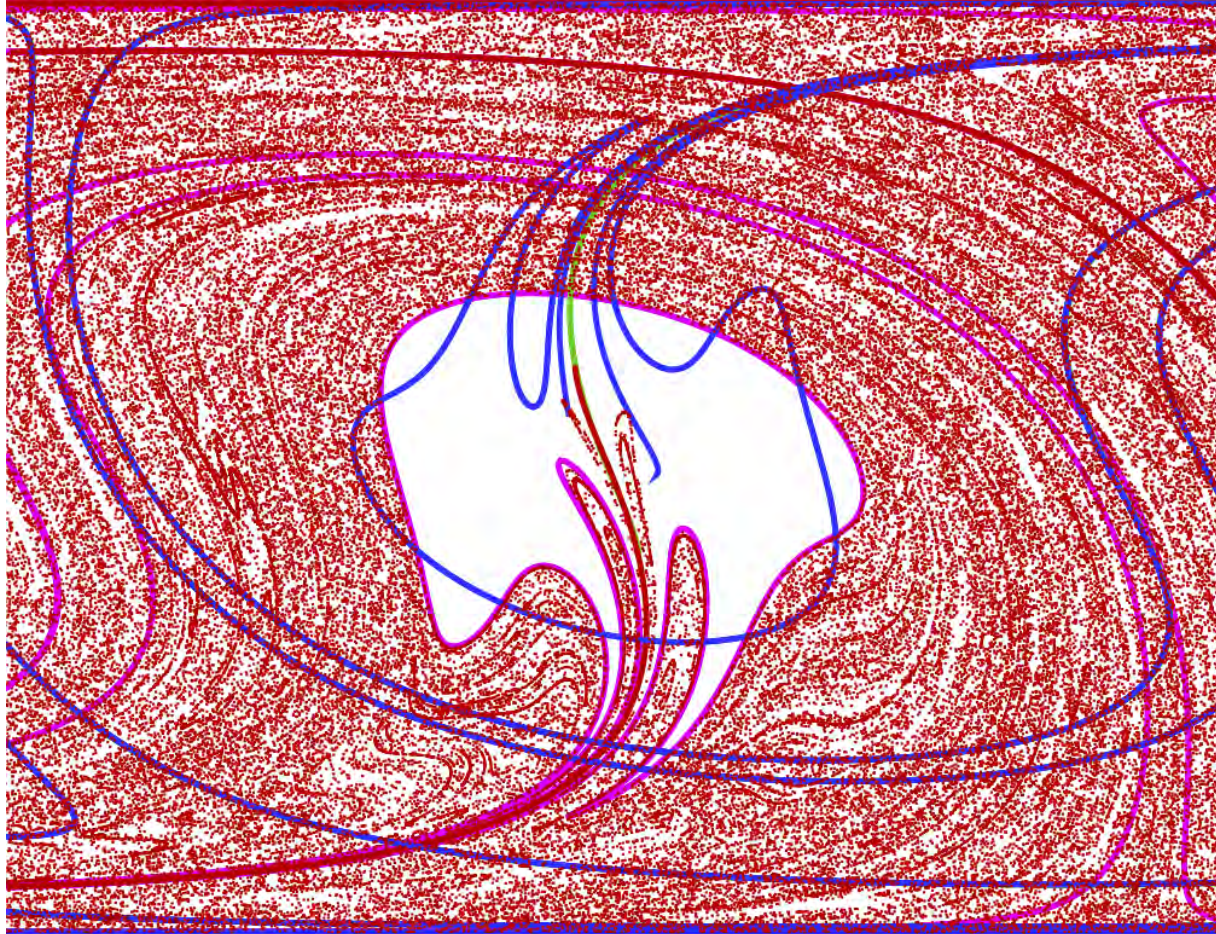


material blob at  $t = 25$



# Stable/unstable manifolds and lobes in fluids

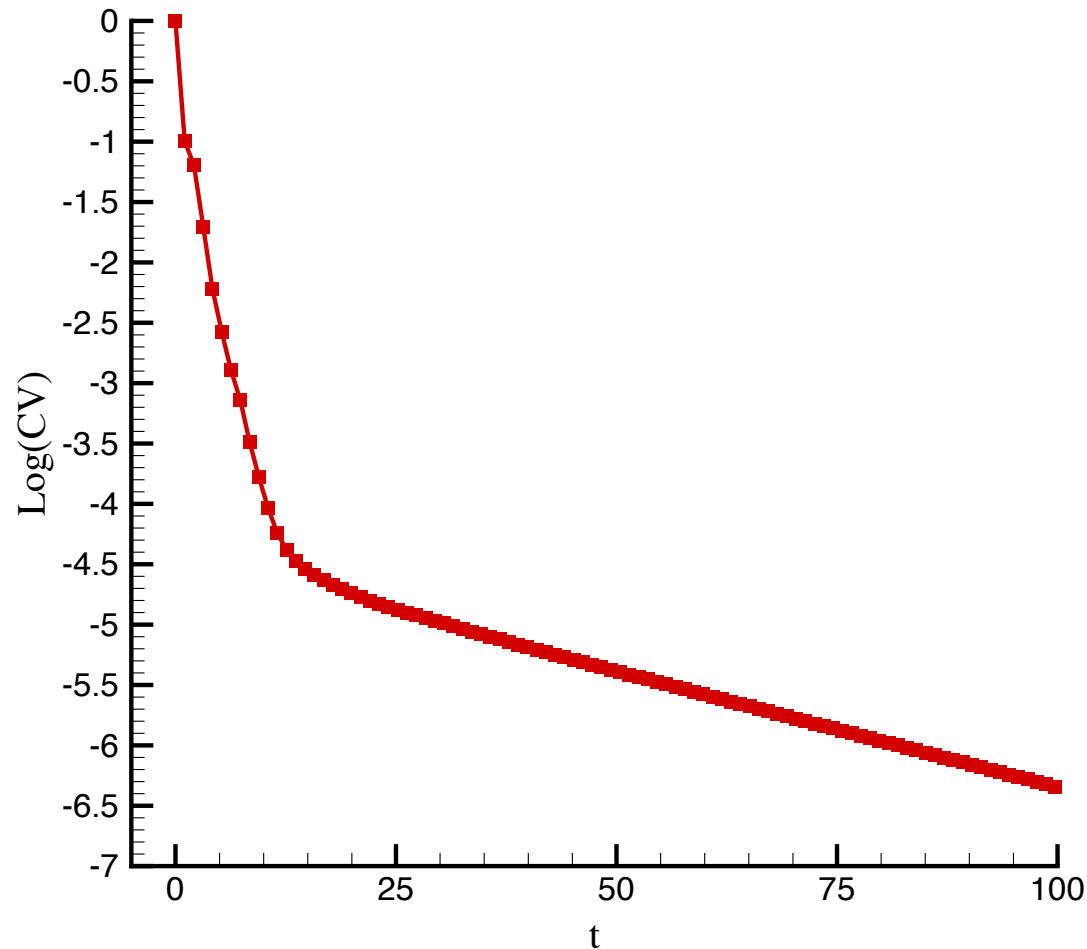
□ Fluid example: Poincaré map



- Saddle manifolds and lobe dynamics provide template for motion

# Stable/unstable manifolds and lobes in fluids

□ Concentration variance; a measure of homogenization

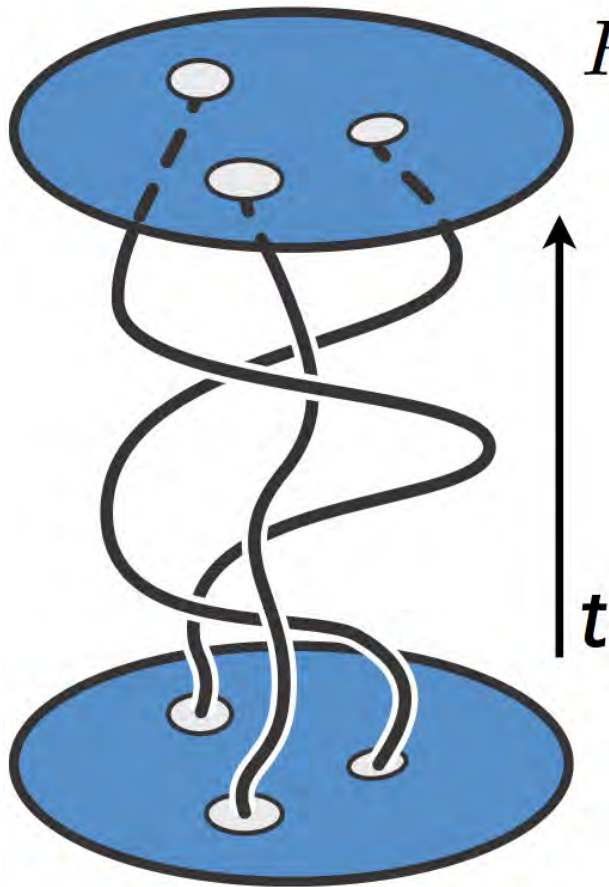


- Homogenization has two exponential rates: slower one related to lobes



# Braiding of stirrers

- Large-scale braiding provides the faster scale  
— and an alternative point-of-view

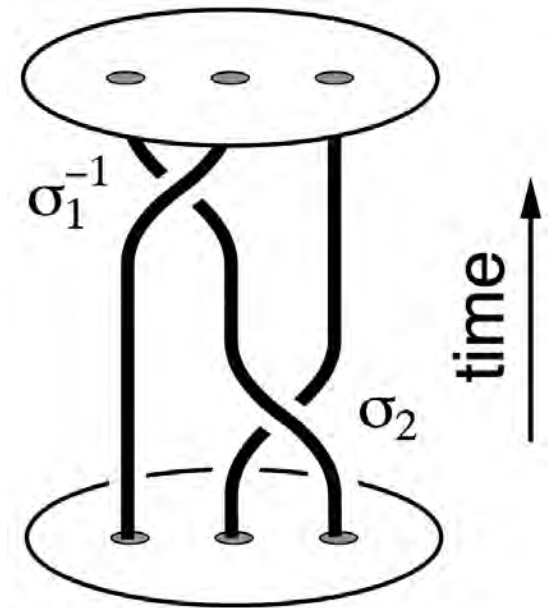


$R_N$  : 2D fluid region with  $N$  stirring ‘rods’

- stirrers move on periodic orbits
- stirrers = solid objects or *fluid particles*
- stirrer motions generate diffeomorphism  
 $f : R_N \rightarrow R_N$
- stirrer trajectories generate braids  
in 2+1 dimensional space-time

# Thurston-Nielsen classification theorem

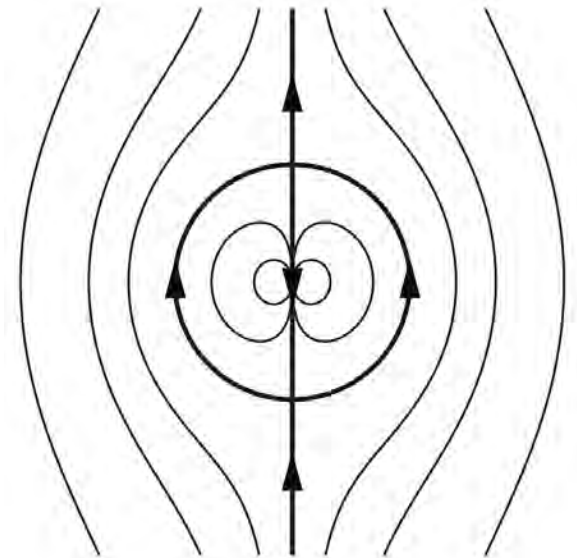
- Thurston (1988) Bull. Am. Math. Soc.
- A stirrer motion  $f$  is isotopic to a stirrer motion  $g$  of one of three types (i) finite order (f.o.): the  $n$ th iterate of  $g$  is the identity (ii) pseudo-Anosov (pA):  $g$  has dense orbits, Markov partition with transition matrix  $A$ , topological entropy  $h_{\text{TN}}(g) = \log(\lambda_{\text{PF}}(A))$ , where  $\lambda_{\text{PF}}(A) > 1 =$  Perron-Frobenius eigenvalue of  $A$  (iii) reducible:  $g$  contains both f.o. and pA regions
- $h_{\text{TN}}$  computed from 'braid word', e.g.,  $\sigma_{-1}\sigma_2$
- $\log(\lambda_{\text{PF}}(A))$  provides a **lower bound** on the true topological entropy
- i.e., non-trivial material lines grow like  $l \sim l_0 \lambda^n$ , where  $\lambda \geq \lambda_{\text{TN}}$



# Identifying 'ghost rods': periodic points

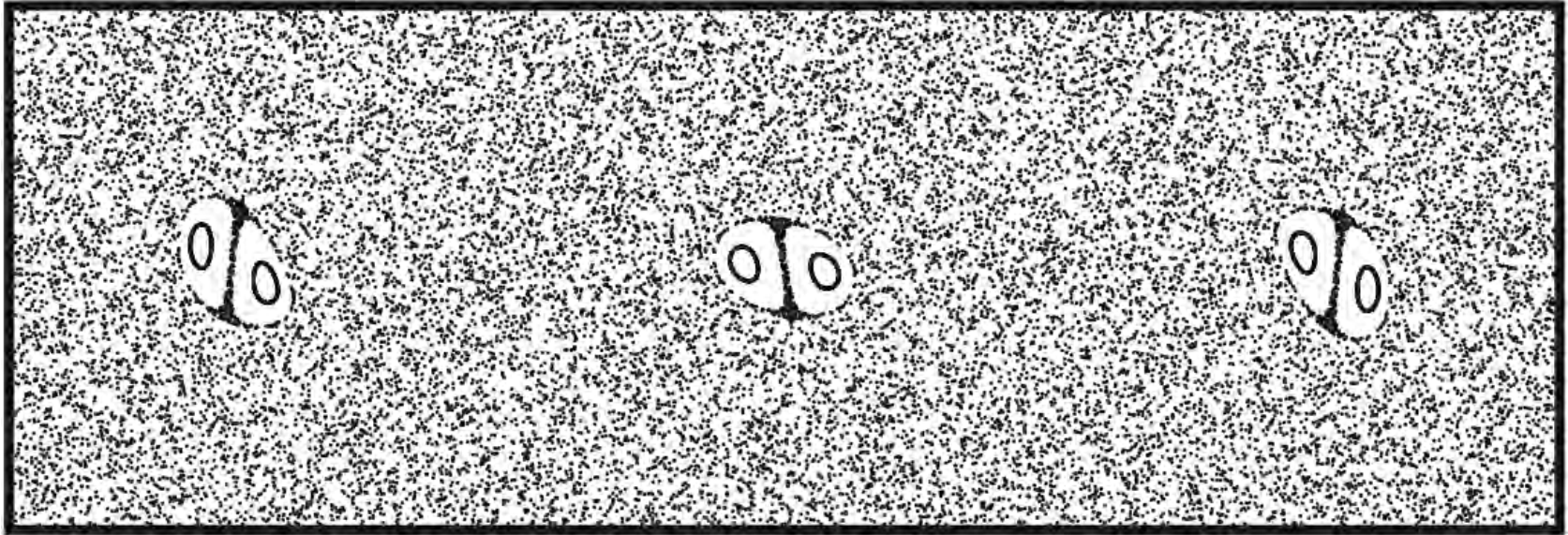
tracer blob for  $\tau_f > 1$

- For  $\tau_f > 1$ , groups of elliptic and saddle periodic points of period 3  
— streamlines around groups resemble fluid motion around a solid rod  $\Rightarrow$
- At  $\tau_f = 1$ , points merge into parabolic points
- Below  $\tau_f < 1$ , periodic points vanish



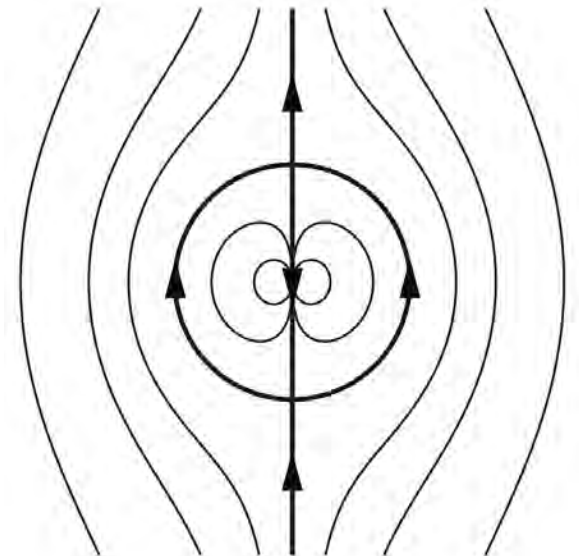


# Identifying 'ghost rods': periodic points

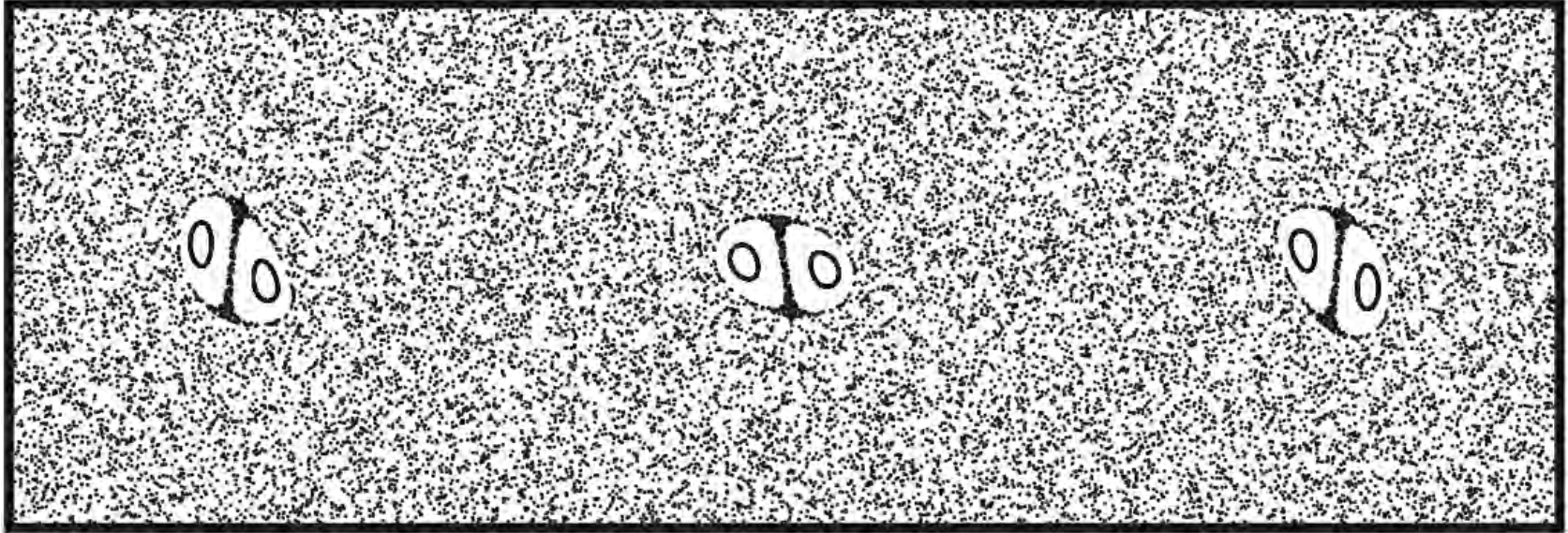


Poincaré section for  $\tau_f > 1$

- For  $\tau_f > 1$ , groups of elliptic and saddle periodic points of period 3  
— streamlines around groups resemble fluid motion around a solid rod  $\Rightarrow$
- At  $\tau_f = 1$ , points merge into parabolic points
- Below  $\tau_f < 1$ , periodic points vanish

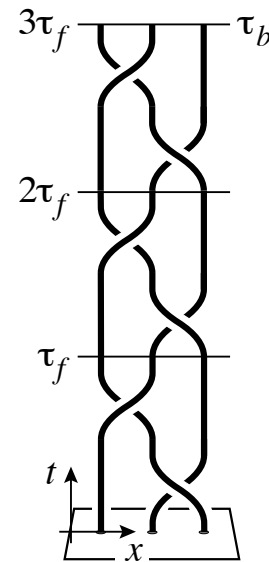


# Identifying 'ghost rods': periodic points

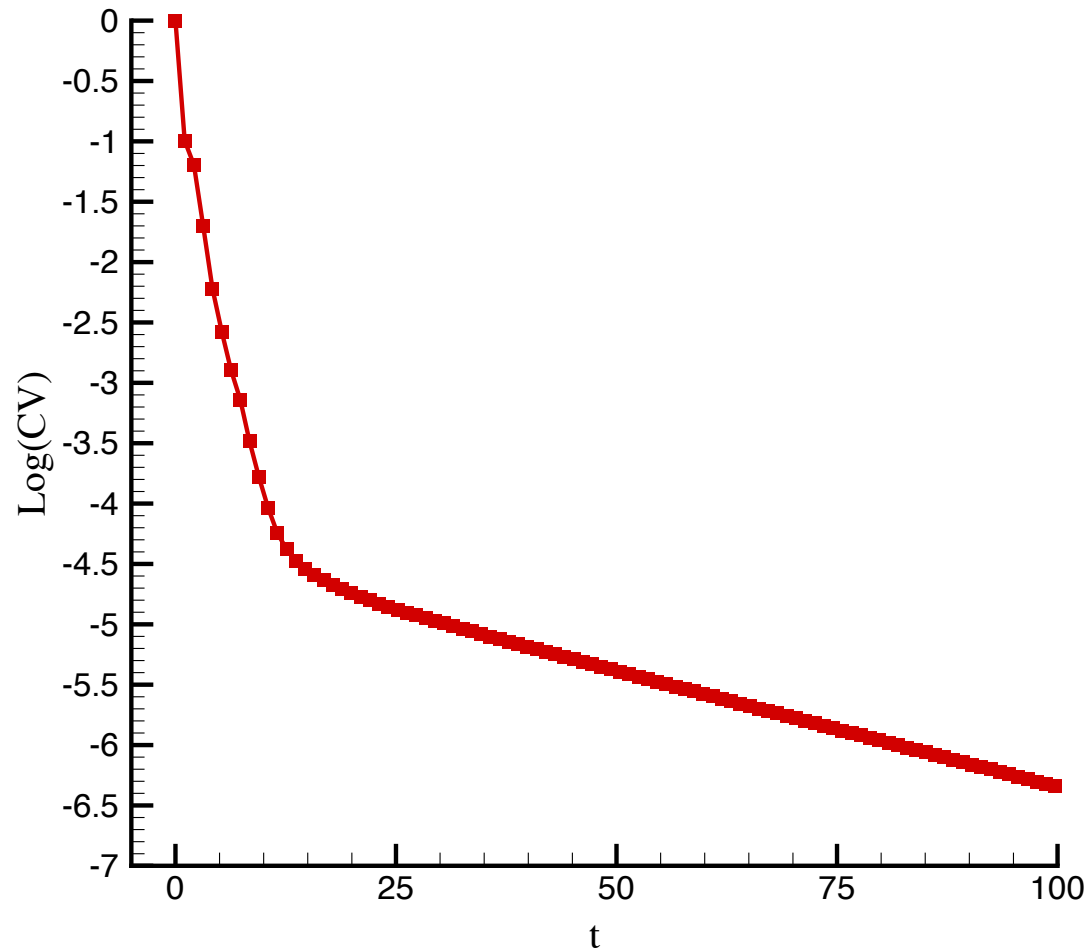


Poincaré section for  $\tau_f > 1$

- Periodic points of period 3  $\Rightarrow$  act as 'ghost rods'
- Their braid  $\Rightarrow h_{\text{TN}} = 0.96242$  from TNCT
- Actual  $h_{\text{flow}} \approx 0.964$
- $\Rightarrow h_{\text{TN}}$  is an excellent lower bound



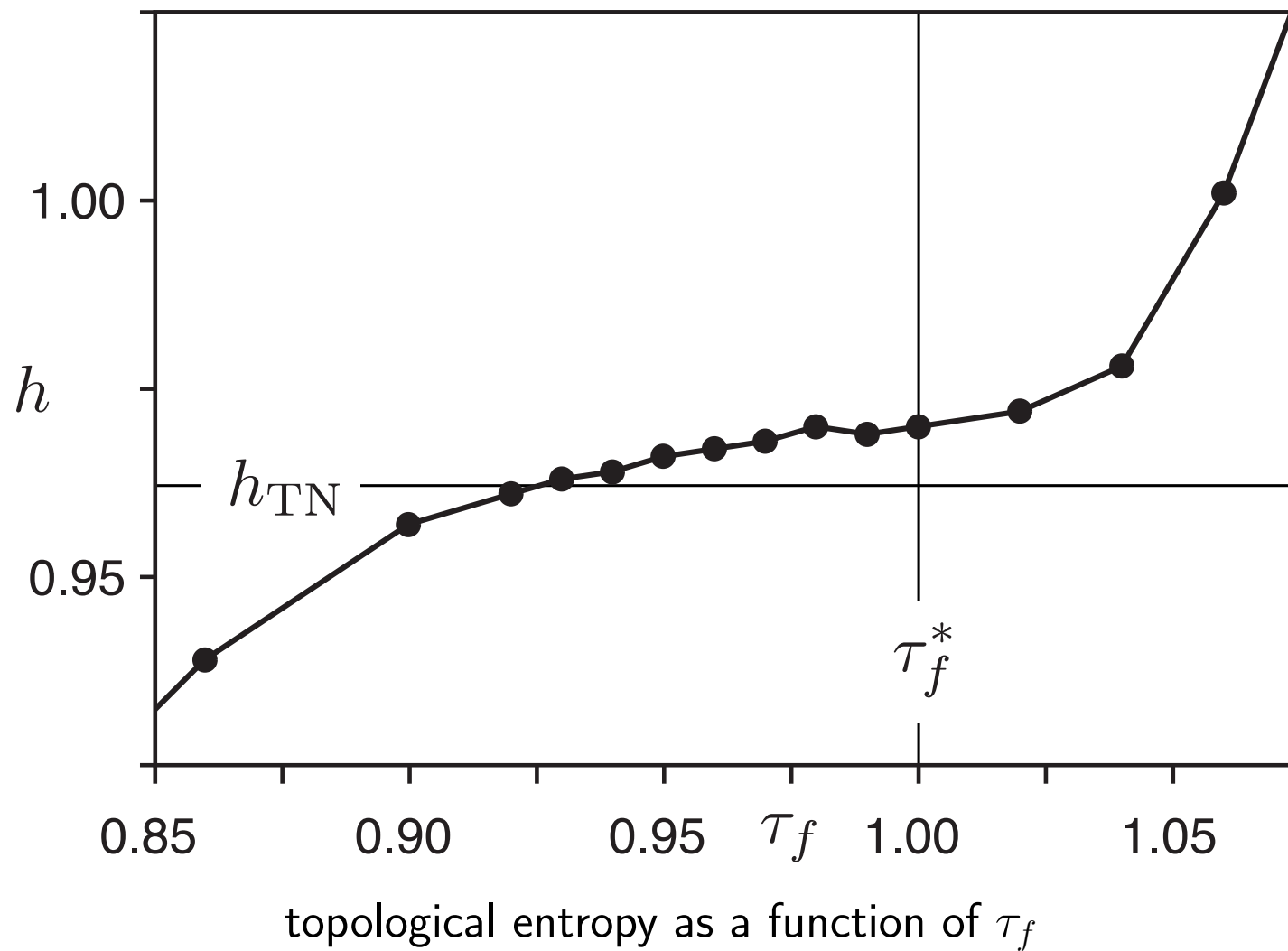
# Identifying 'ghost rods': periodic points



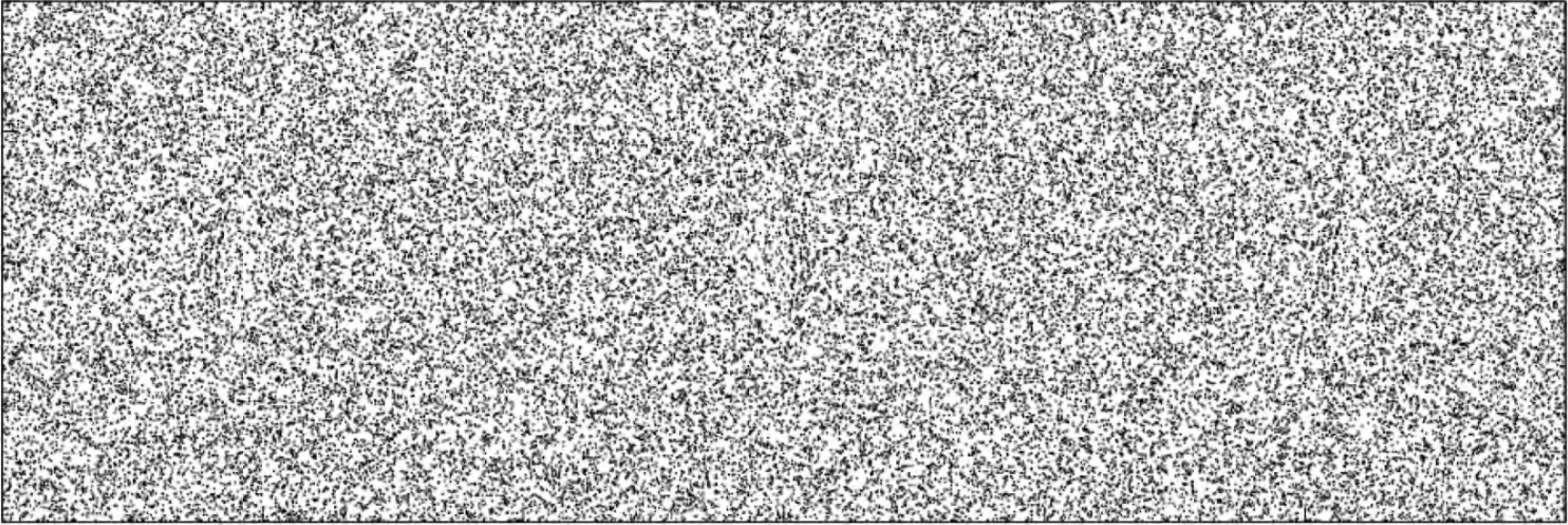
- Homogenization has two exponential rates: slower one related to lobes
- **Fast rate due to braiding of 'ghost rods'!**



# Topological entropy continuity across critical point



# Identifying 'ghost rods'?



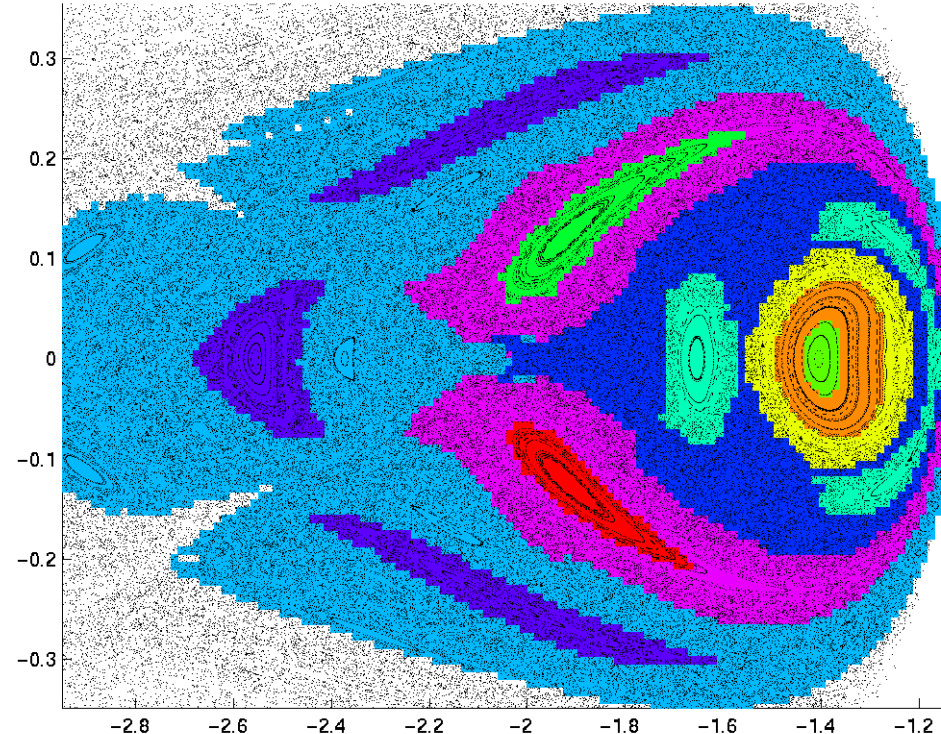
Poincaré section for  $\tau_f < 1 \Rightarrow$  no obvious structure!

- Note the absence of any elliptical islands
- No periodic orbits of low period were found
- Is the phase space featureless?

# Almost-invariant set (AIS) approach

- Take probabilistic point of view (recall, e.g., Oliver Junge's talk)
- Partition phase space into **loosely coupled regions**

AISs  $\approx$  “Leaky” regions with a long residence time<sup>2</sup>



3-body problem phase space is divided into several invariant and almost-invariant sets.

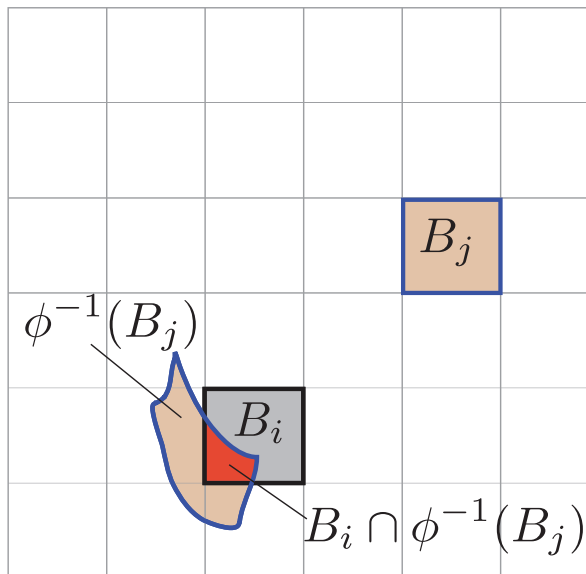
<sup>2</sup>Dellnitz, Junge, Koon, Lekien, Lo, Marsden, Padberg, Preis, Ross, Thiere [2005] Int. J. Bif. Chaos

# Almost-invariant set (AIS) approach

- Create box partition of phase space  $\mathcal{B} = \{B_1, \dots, B_q\}$ , with  $q$  large
- Consider a  $q$ -by- $q$  **transition (Ulam) matrix**,  $P$ , for our dynamical system, where

$$P_{ij} = \frac{m(B_i \cap f^{-1}(B_j))}{m(B_i)},$$

the *transition probability* from  $B_i$  to  $B_j$  using, e.g.,  $f = \phi_t^{t+T}$



- $P$  approximates our dynamical system via a finite state Markov chain.



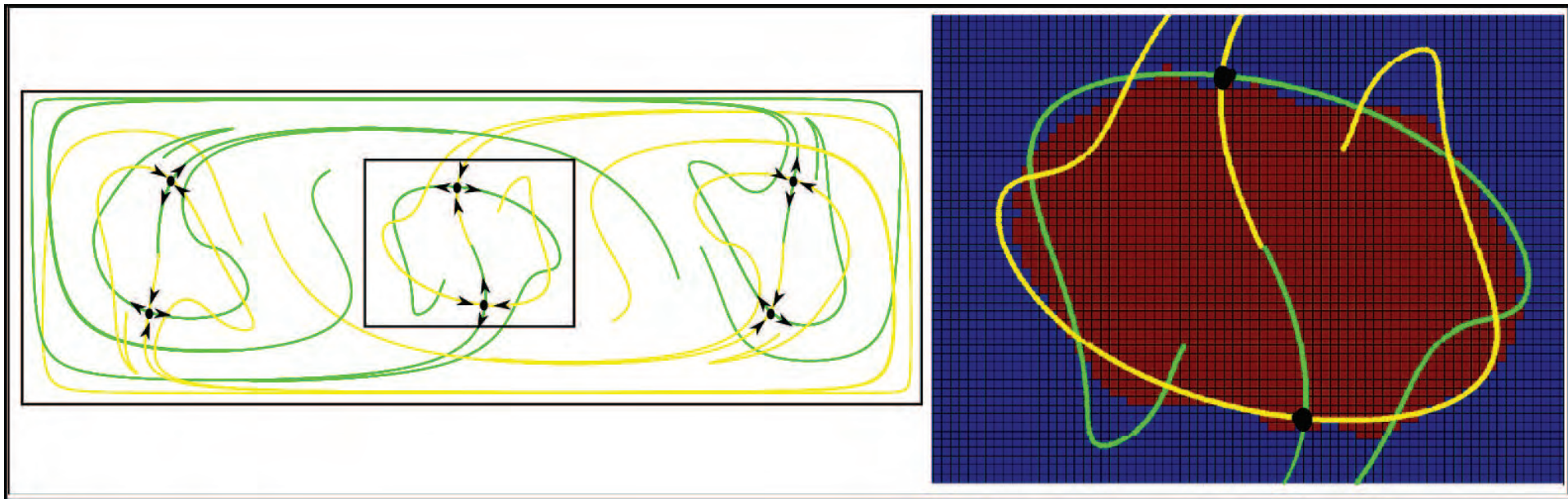
# Almost-invariant set (AIS) approach

- A set  $B$  is called almost invariant over the interval  $[t, t + T]$  if

$$\rho(B) = \frac{m(B \cap \phi^{-1}(B))}{m(B)} \approx 1.$$

- Can maximize value of  $\rho$  over all possible combinations of sets  $B \in \mathcal{B}$ .
- In practice, AIS or relatedly, almost-cyclic sets (ACS), identified via **eigenvectors** (of eigenvalues with  $|\lambda| \approx 1$ ) of  $P$  or graph-partitioning
- Appropriate for non-autonomous, aperiodic, finite-time settings

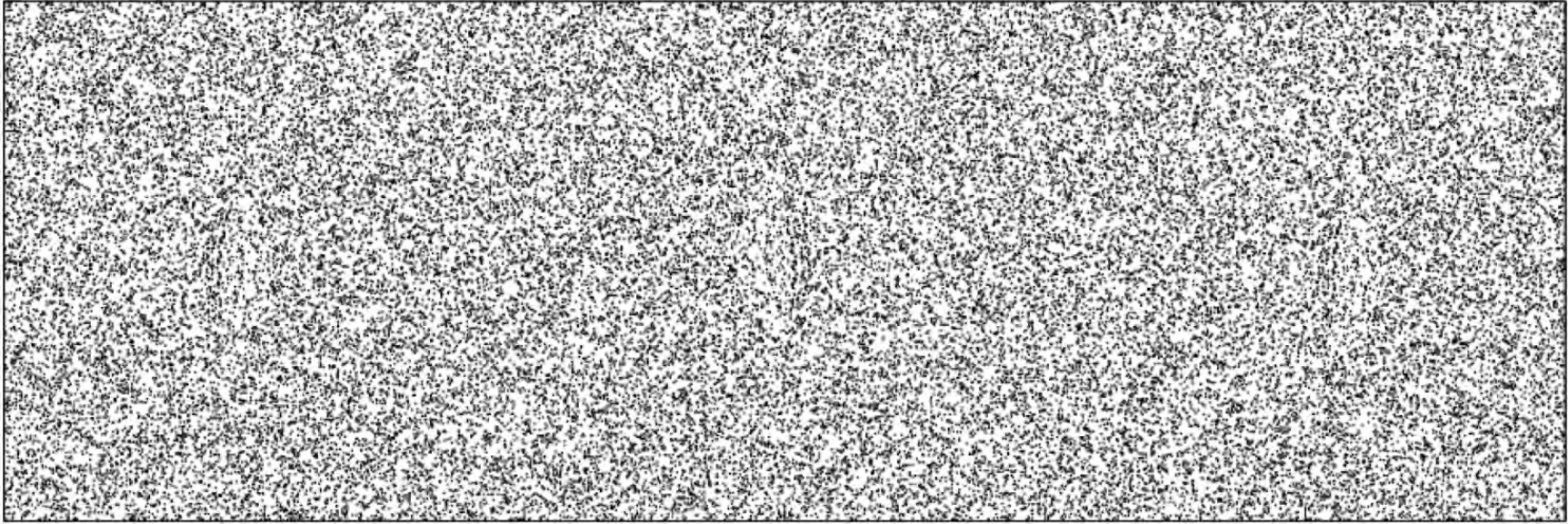
# Identifying 'ghost rods': almost-cyclic sets



- Return to  $\tau_f > 1$  case, where periodic points and manifolds exist
- Agreement between AIS boundaries and manifolds of periodic points
- Known previously<sup>3</sup> and applies to more general objects than periodic points, i.e. normally hyperbolic invariant manifolds (NHIMs)

<sup>3</sup>Dellnitz, Junge, Lo, Marsden, Padberg, Preis, Ross, Thiere [2005] Phys. Rev. Lett.; Dellnitz, Junge, Koon, Lekien, Lo, Marsden, Padberg, Preis, Ross, Thiere [2005] Int. J. Bif. Chaos

# Identifying 'ghost rods': almost-cyclic sets

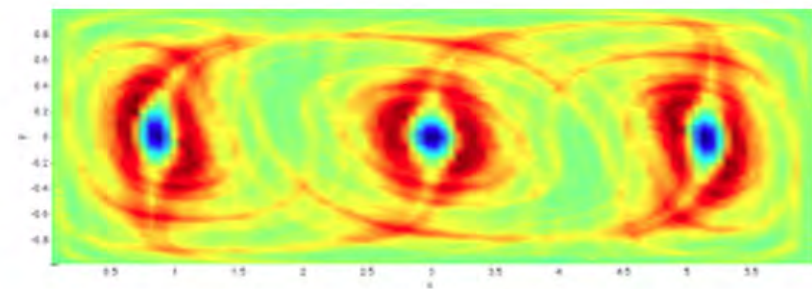
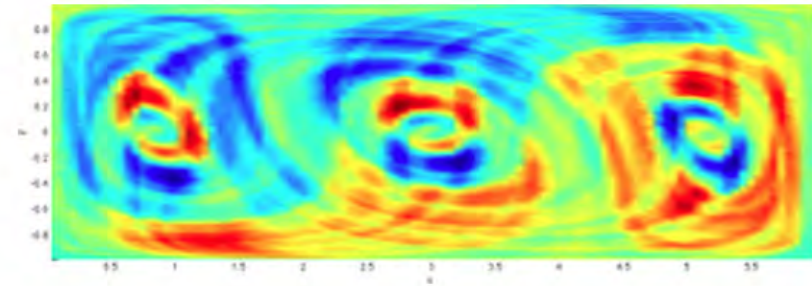
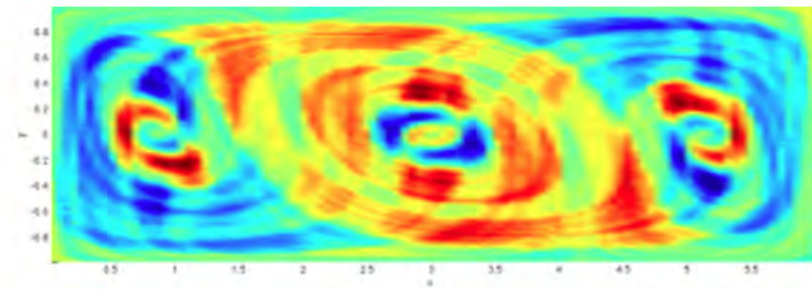
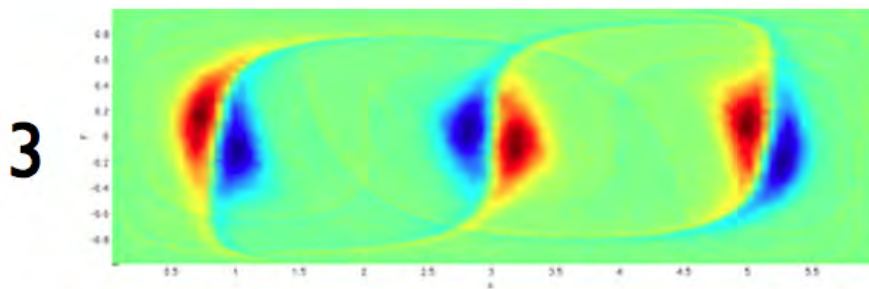
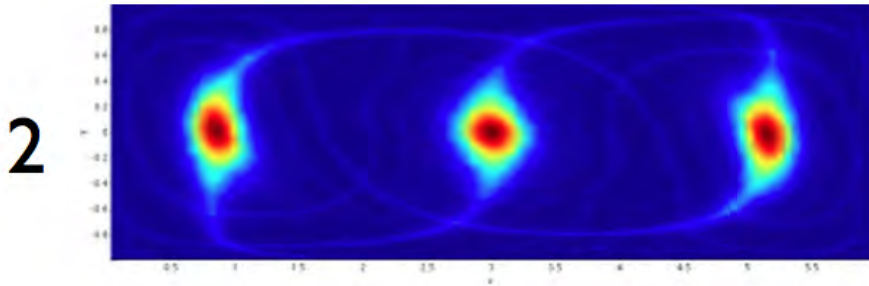
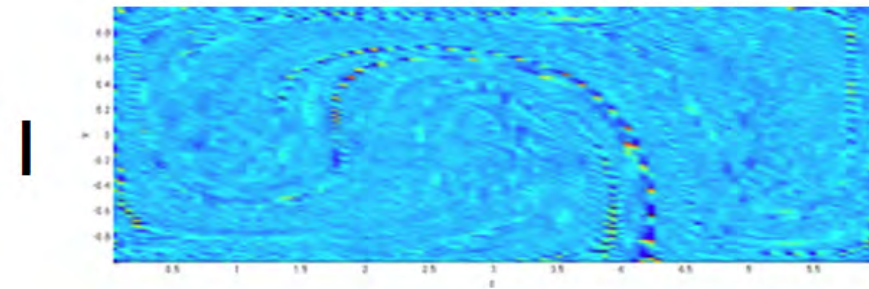


Poincaré section for  $\tau_f < 1 \Rightarrow$  no obvious structure!

- Return to  $\tau_f < 1$  case, where no periodic orbits of low period known
- Is the phase space featureless?
- Consider transition matrix  $P_t^{t+\tau_f}$  induced by Poincaré map  $\phi_t^{t+\tau_f}$

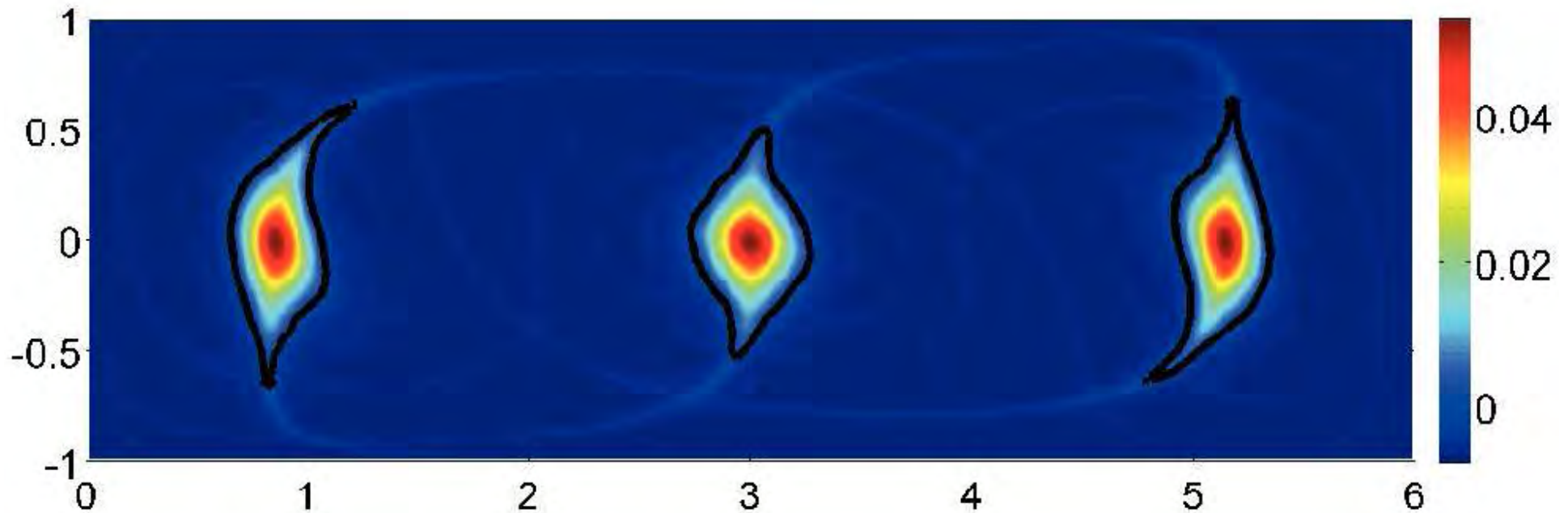


# Identifying 'ghost rods': almost-cyclic sets



Top six eigenvalues for  $\tau_f = 0.99 < \tau_f^*$

# Identifying 'ghost rods': almost-cyclic sets



The zero contour (black) is the boundary between the two almost-invariant sets.

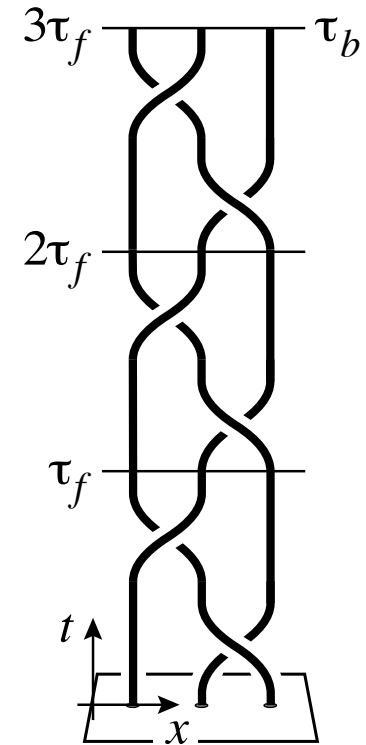
- Three-component AIS made of 3 almost-cyclic sets (ACSs) of period 3
- ACS effectively replace compact region bounded by saddle manifolds
- Also a remnant of the global 'stable and unstable manifolds' of the saddle points, even there are no more saddle points

# Identifying ‘ghost rods’: almost-cyclic sets

Almost-cyclic sets stirring the surrounding fluid like ‘ghost rods’  
— **works even when periodic orbits are absent!**

Movie shown is second eigenvector for  $P_t^{t+\tau_f}$  for  $t \in [0, \tau_f)$

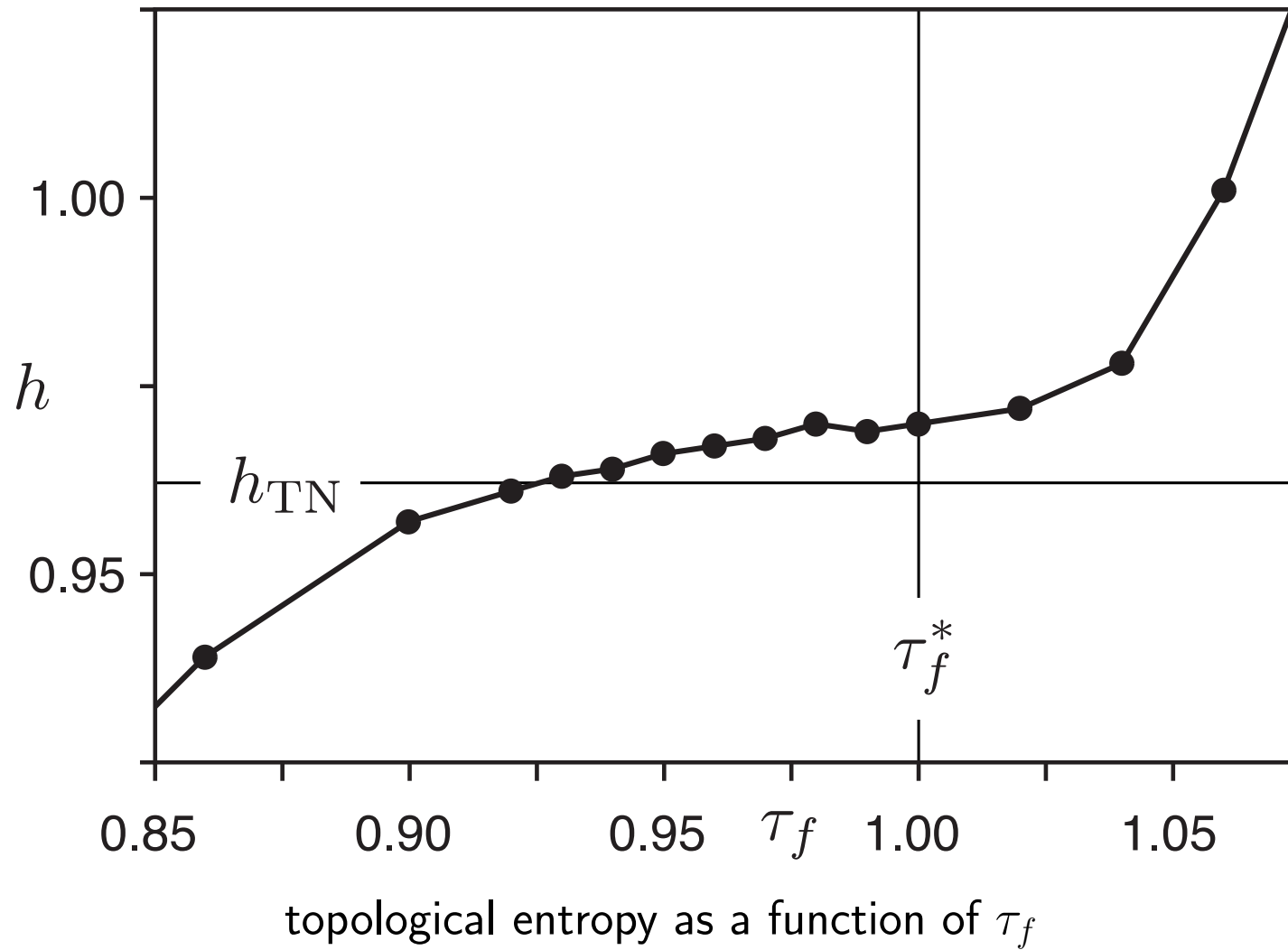
# Identifying 'ghost rods': almost-cyclic sets



- Braid of ACSs gives lower bound of entropy via Thurston-Nielsen
- One only needs approximately cyclic blobs of fluid
  - Even though the theorems require exactly periodic points!
  - Stremler, Ross, Grover, Kumar [2011] Phys. Rev. Lett.

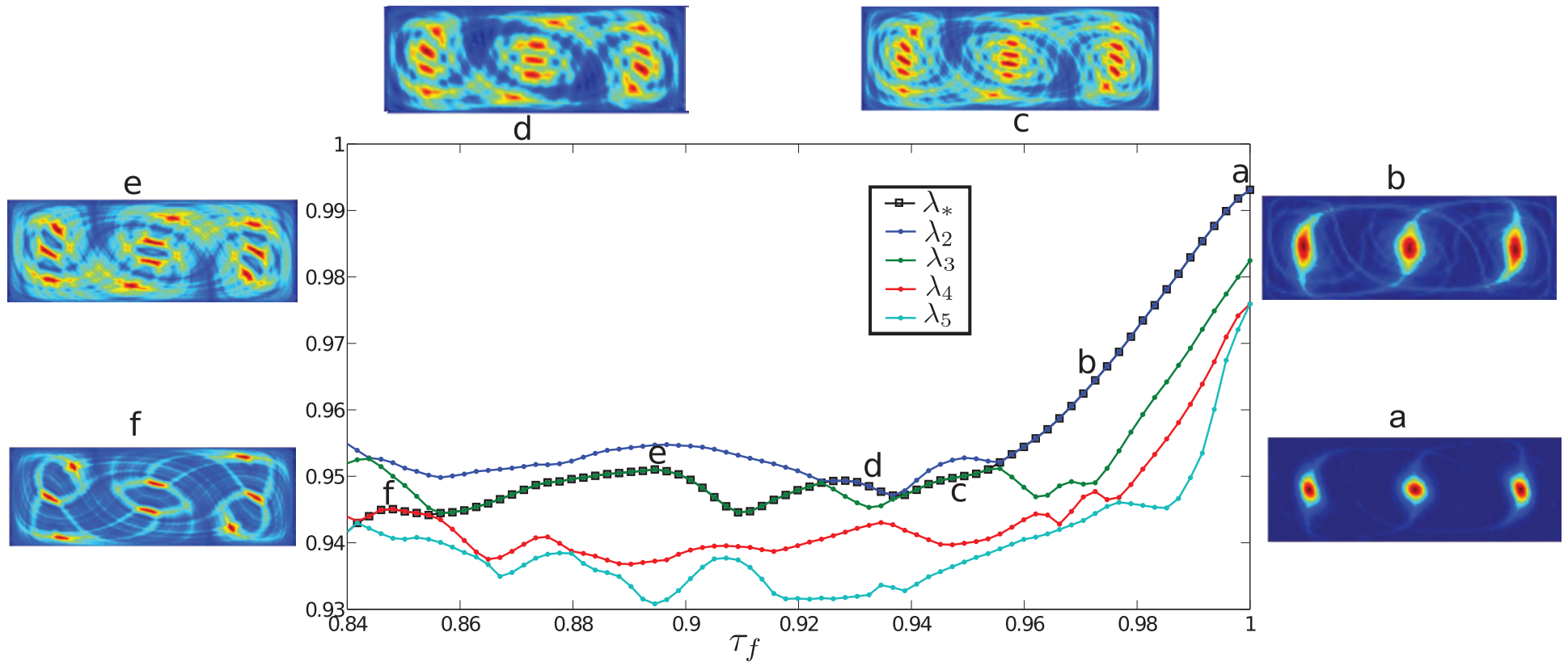


# Topological entropy vs. bifurcation parameter



- $h_{\text{TN}}$  shown for ACS braid on 3 strands

# Eigenvalues/eigenvectors vs. bifurcation parameter



Movie shows change in eigenvector branch, marked with '-□-' above, as parameter decreases from a to f  $\Rightarrow$

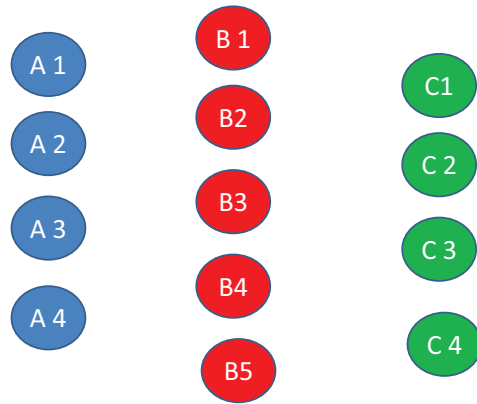
# Bifurcation of ACSs

For example, braid on 13 strands for  $\tau_f = 0.92$

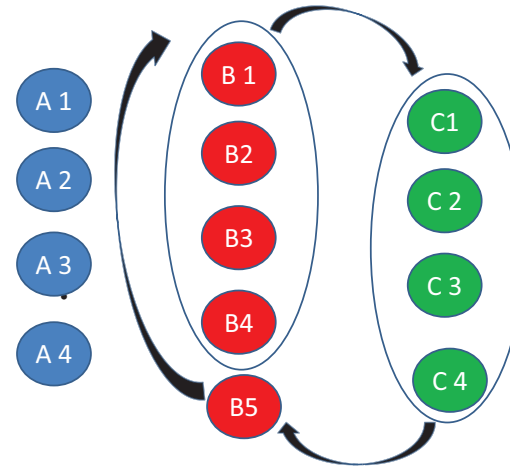
Movie shown is second eigenvector for  $P_t^{t+\tau_f}$  for  $t \in [0, \tau_f)$

Thurston-Nielsen for this braid provides lower bound on topological entropy

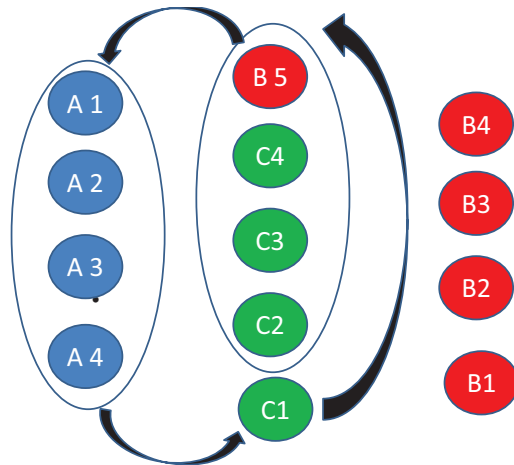
# Bifurcation of ACSs



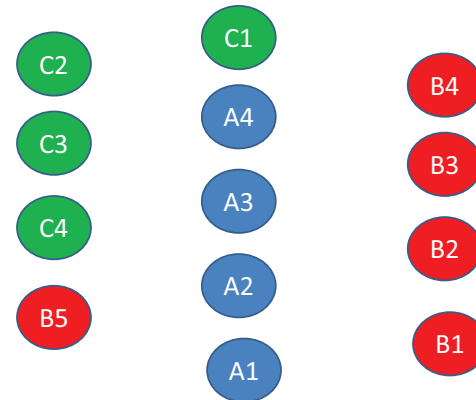
(a) Initial state



(b) First half-period

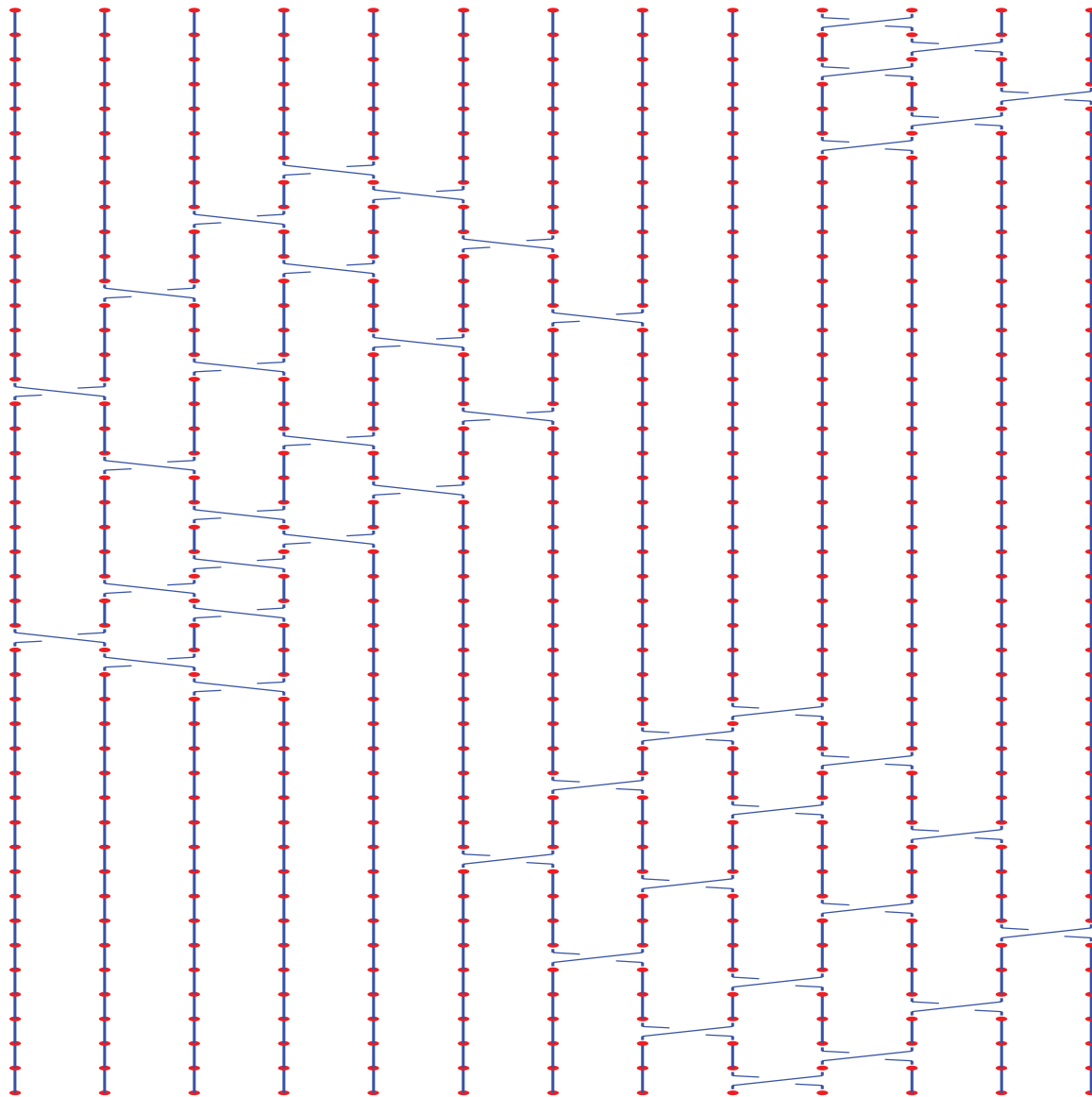


(c) Second half-period



(d) State after 1 period

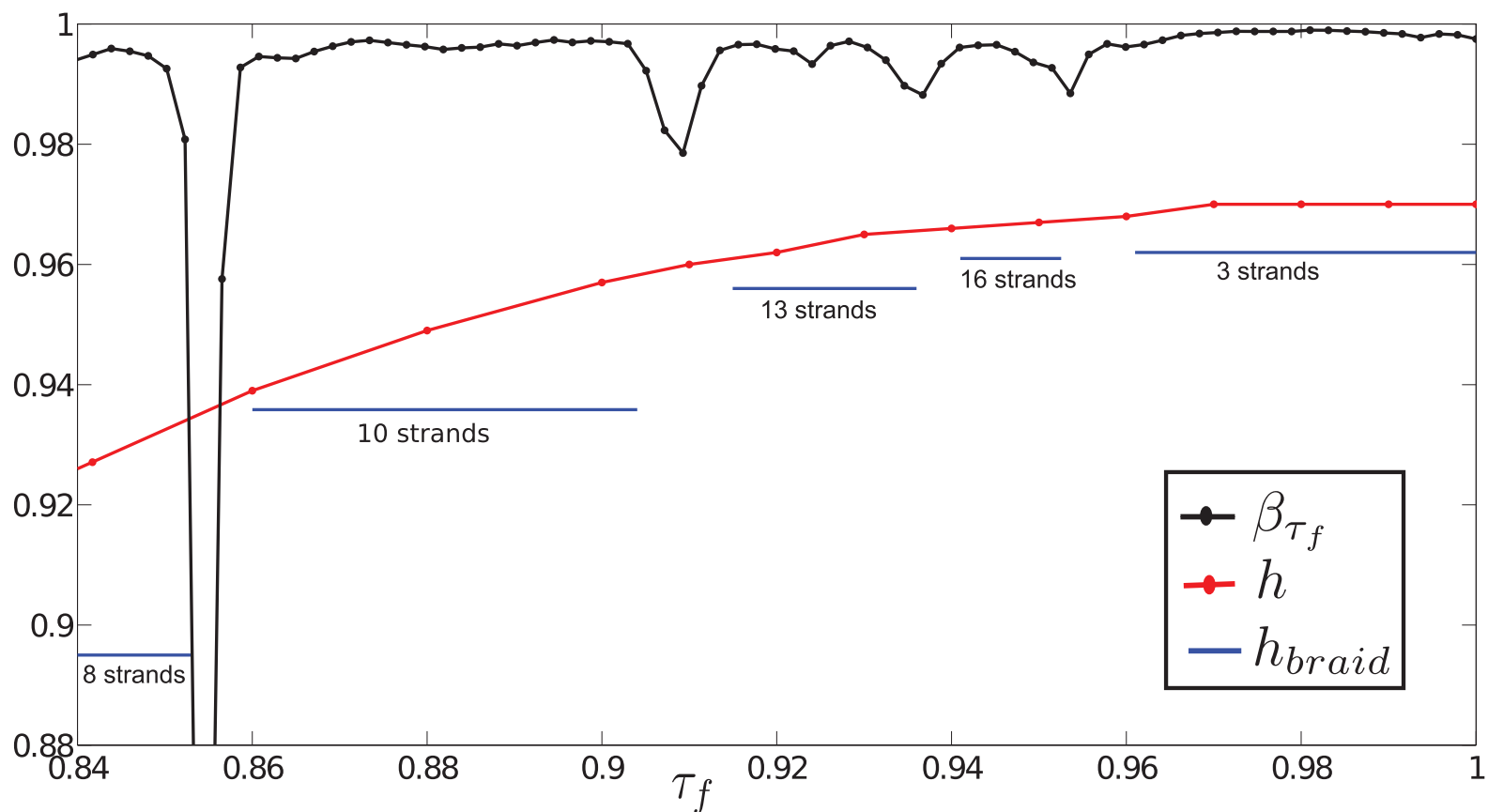
# Bifurcation of ACSs



representation of braid



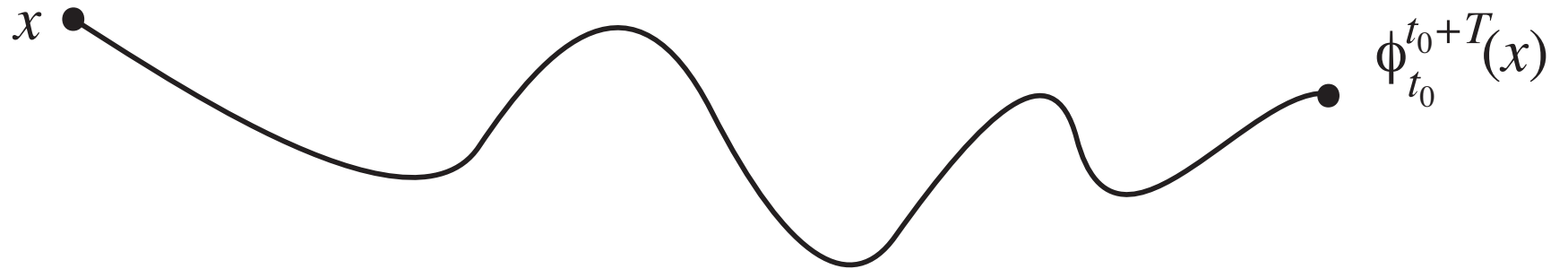
# Sequence of ACS braids bounds entropy



For various braids of ACSs, the calculated entropy is given, bounding from below the true topological entropy over the range where the braid exists

# Aperiodic, finite-time setting

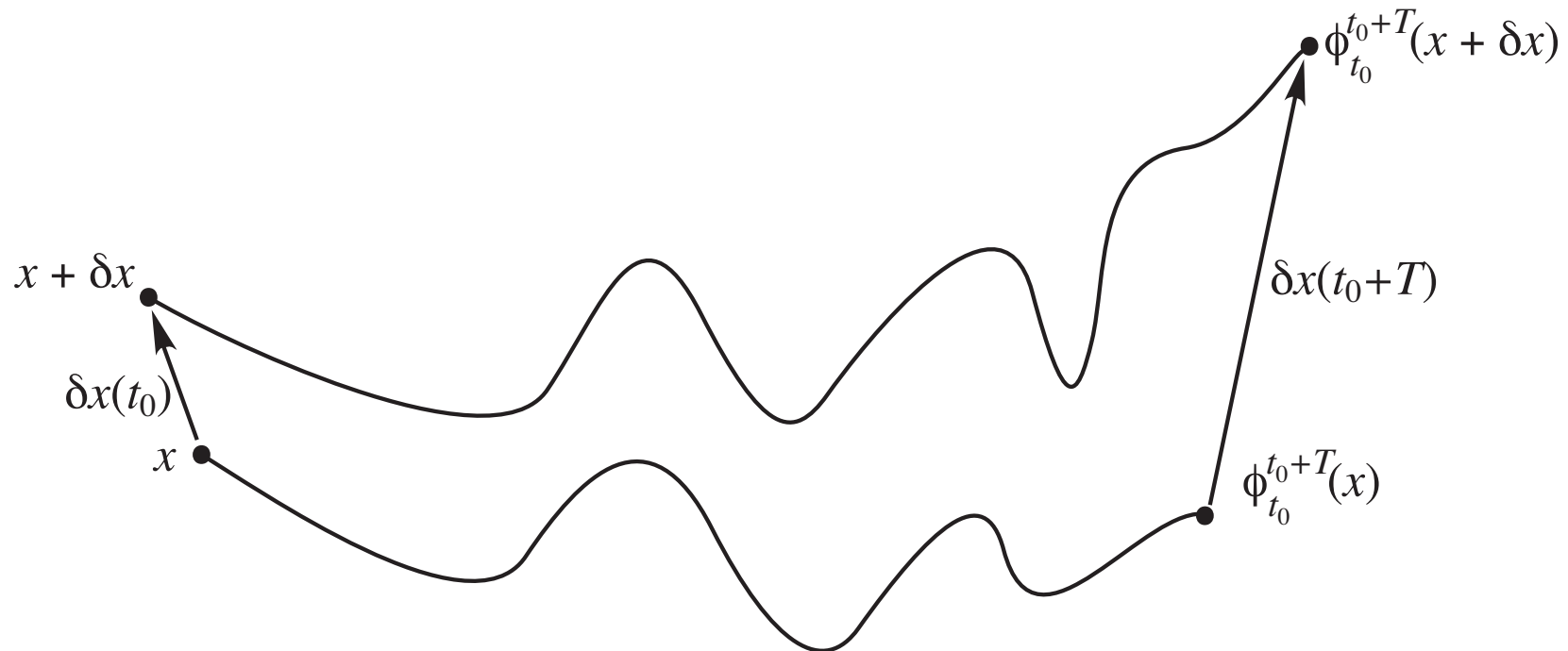
- Data-driven, finite-time, aperiodic setting
- How do we get at transport?
- Recall the flow,  $x \mapsto \phi_t^{t+T}(x)$



# Identify regions of high sensitivity of initial conditions

- Small initial perturbations  $\delta x(t)$  grow like

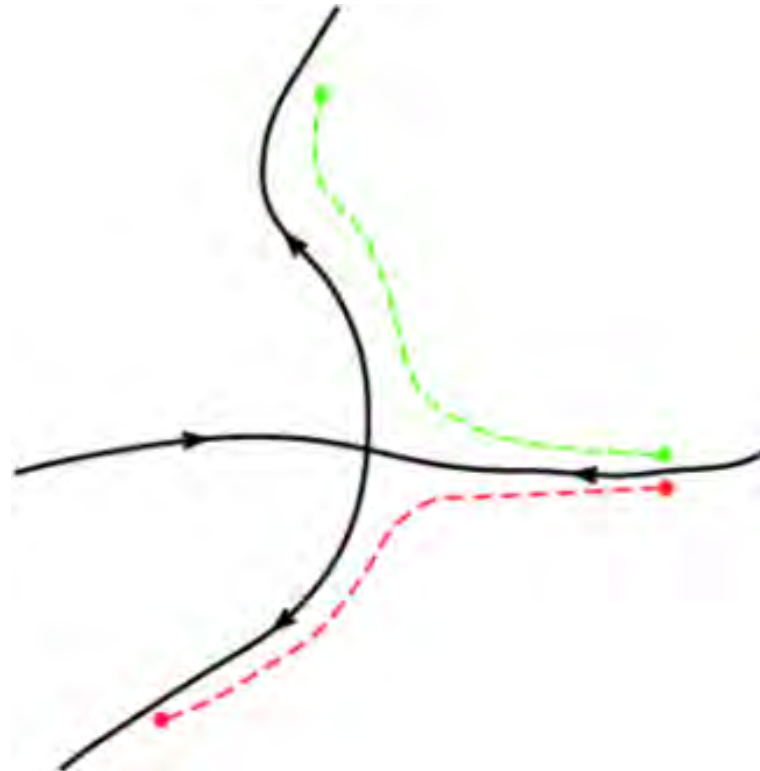
$$\begin{aligned}\delta x(t + T) &= \phi_t^{t+T}(x + \delta x(t)) - \phi_t^{t+T}(x) \\ &= \frac{d\phi_t^{t+T}(x)}{dx} \delta x(t) + O(\|\delta x(t)\|^2)\end{aligned}$$



# Identify regions of high sensitivity of initial conditions

- Small initial perturbations  $\delta x(t)$  grow like

$$\begin{aligned}\delta x(t + T) &= \phi_t^{t+T}(x + \delta x(t)) - \phi_t^{t+T}(x) \\ &= \frac{d\phi_t^{t+T}(x)}{dx} \delta x(t) + O(\|\delta x(t)\|^2)\end{aligned}$$



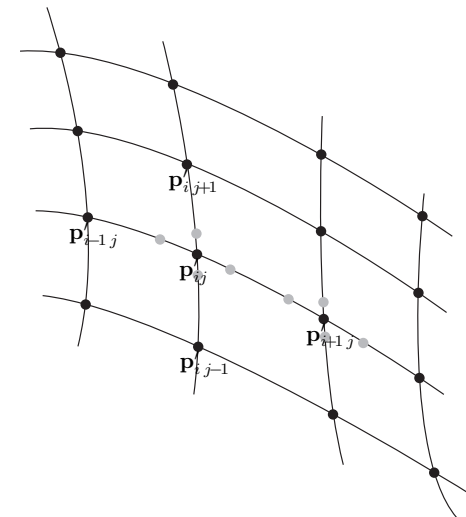
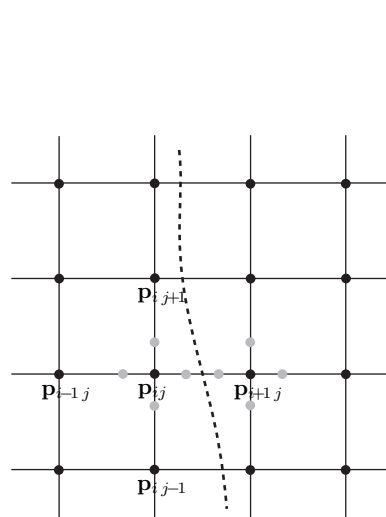
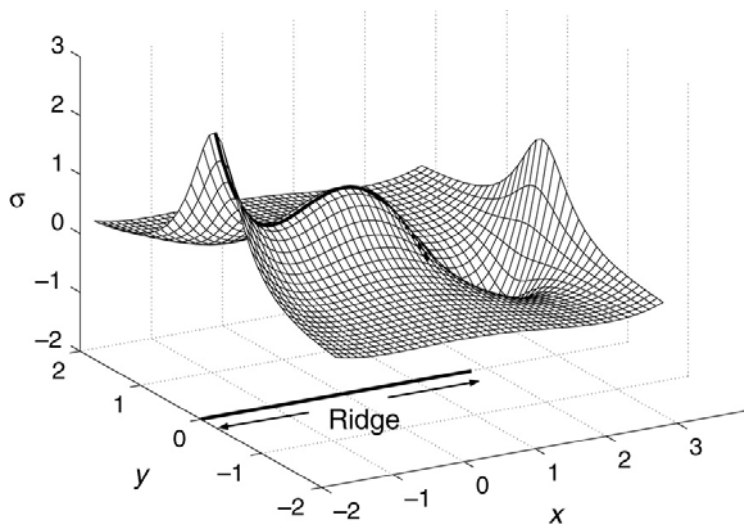
# Invariant manifold analogs: FTLE-LCS approach

- The finite-time Lyapunov exponent (FTLE),

$$\sigma_t^T(x) = \frac{1}{|T|} \log \left\| \frac{d\phi_t^{t+T}(x)}{dx} \right\|$$

measures the maximum stretching rate over the interval  $T$  of trajectories starting near the point  $x$  at time  $t$

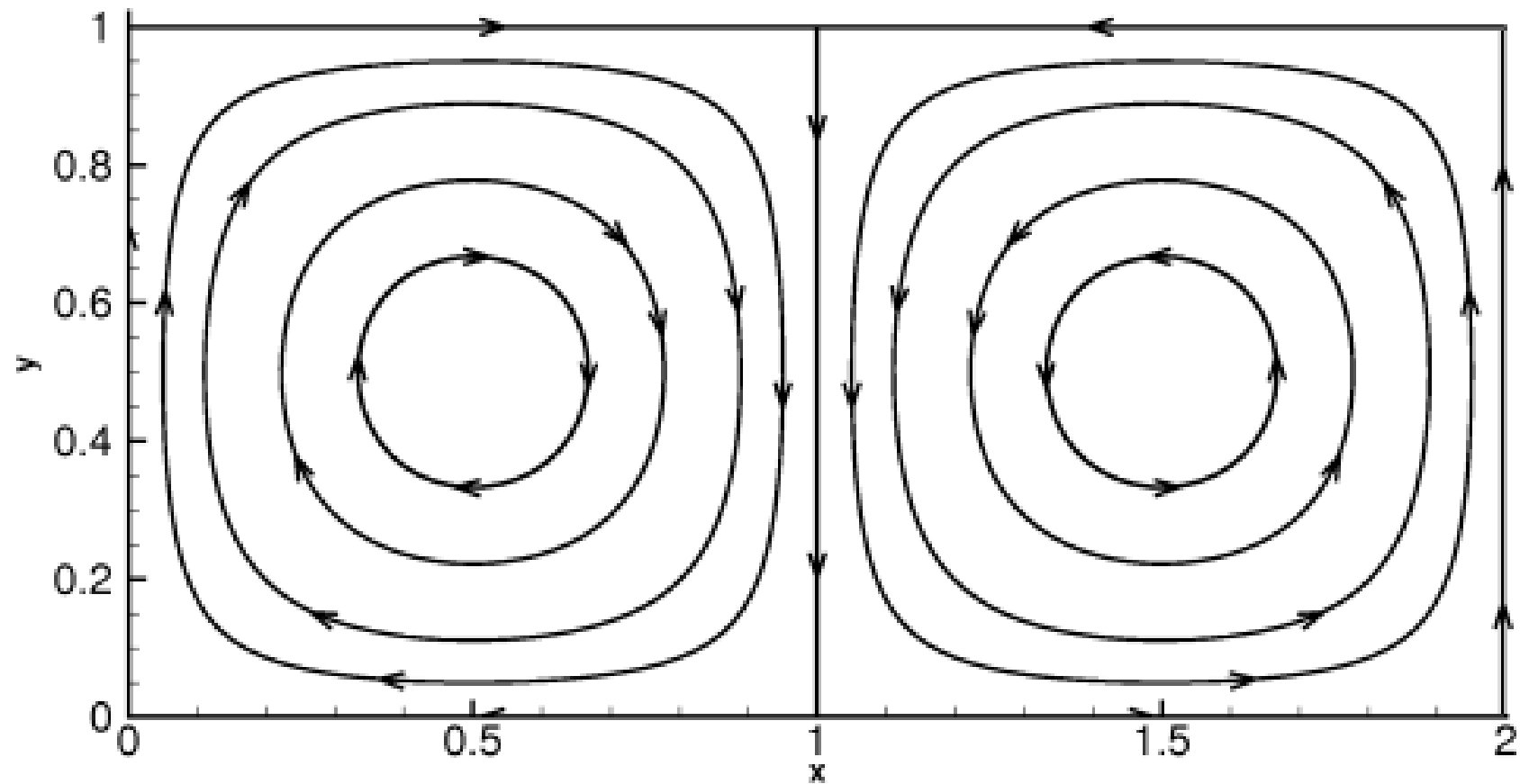
- Ridges of  $\sigma_t^T$  are candidate hyperbolic codim-1 surfaces; finite-time analogs of stable/unstable manifolds; Lagrangian coherent structures<sup>4</sup>



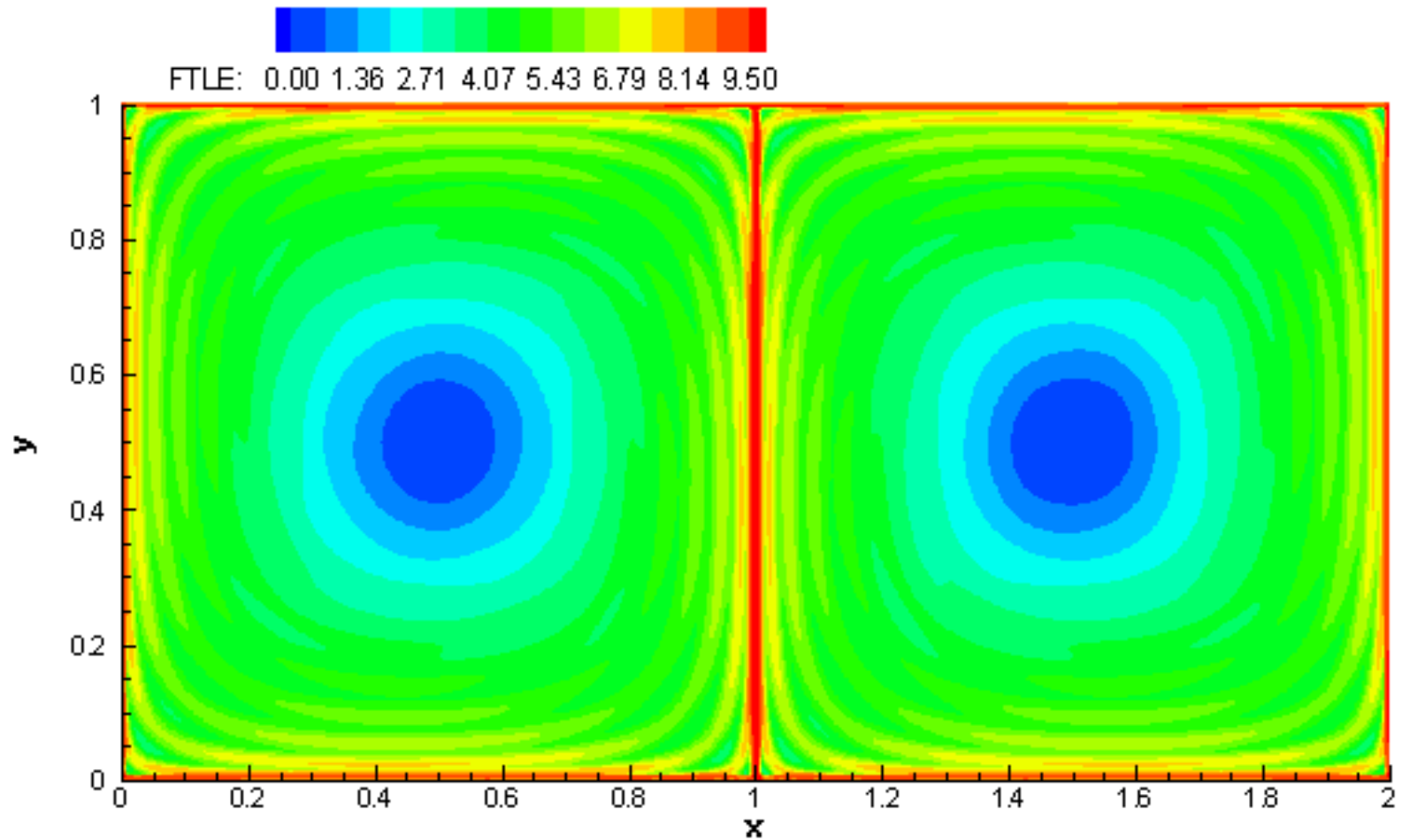
<sup>4</sup>cf. Bowman, 1999; Haller & Yuan, 2000; Haller, 2001; Shadden, Lekien, Marsden, 2005



# Invariant manifold analogs: FTLE-LCS approach



# Invariant manifold analogs: FTLE-LCS approach

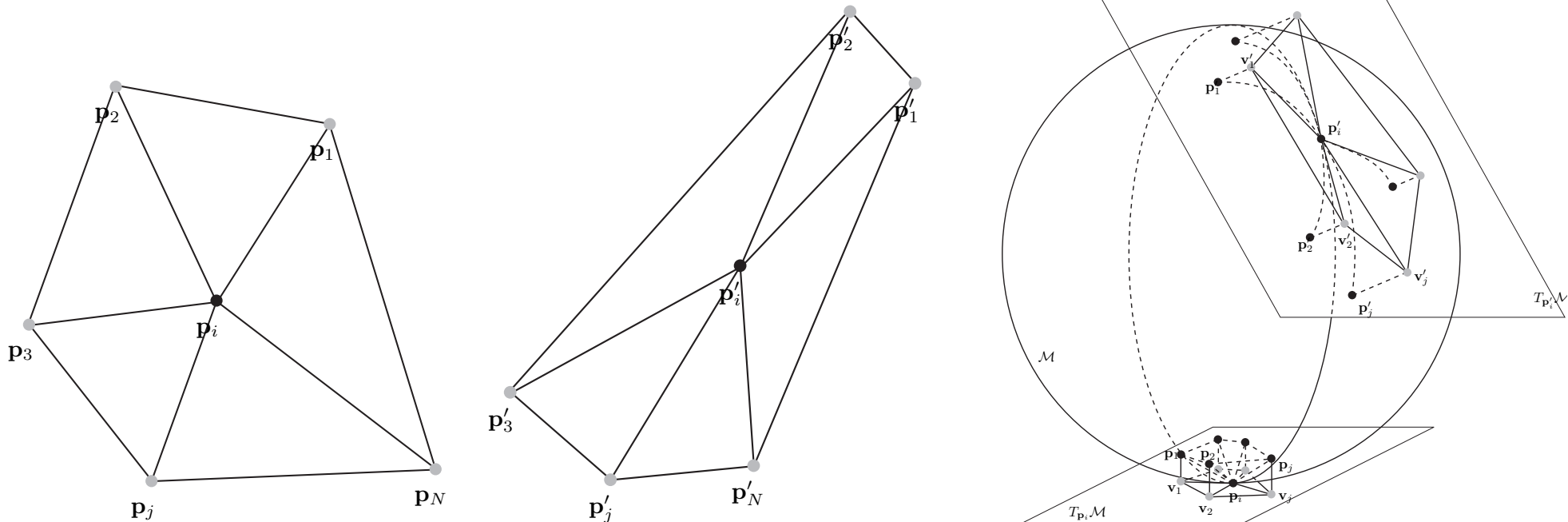


# Invariant manifold analogs: FTLE-LCS approach

- We can define the FTLE for Riemannian manifolds<sup>3</sup>

$$\sigma_t^T(x) = \frac{1}{|T|} \ln \left\| D\phi_t^{t+T} \right\| \doteq \frac{1}{|T|} \log \left( \max_{y \neq 0} \frac{\left\| D\phi_t^{t+T}(y) \right\|}{\|y\|} \right)$$

with  $y$  a small perturbation in the tangent space at  $x$ .



<sup>3</sup>Lekien & Ross [2010] Chaos

# Transport barriers: LCS

- Ridges correspond to dynamical barriers<sup>3</sup> or Lagrangian coherent structures (LCS): repelling surfaces for  $T > 0$ , attracting for  $T < 0$

cylinder

Moebius strip

Each frame has a different initial time  $t$

---

<sup>3</sup>Lekien & Ross [2010] Chaos

# Atmospheric flows: Antarctic polar vortex

ozone data



# Atmospheric flows: Antarctic polar vortex

ozone data + LCSs (red = repelling, blue = attracting)

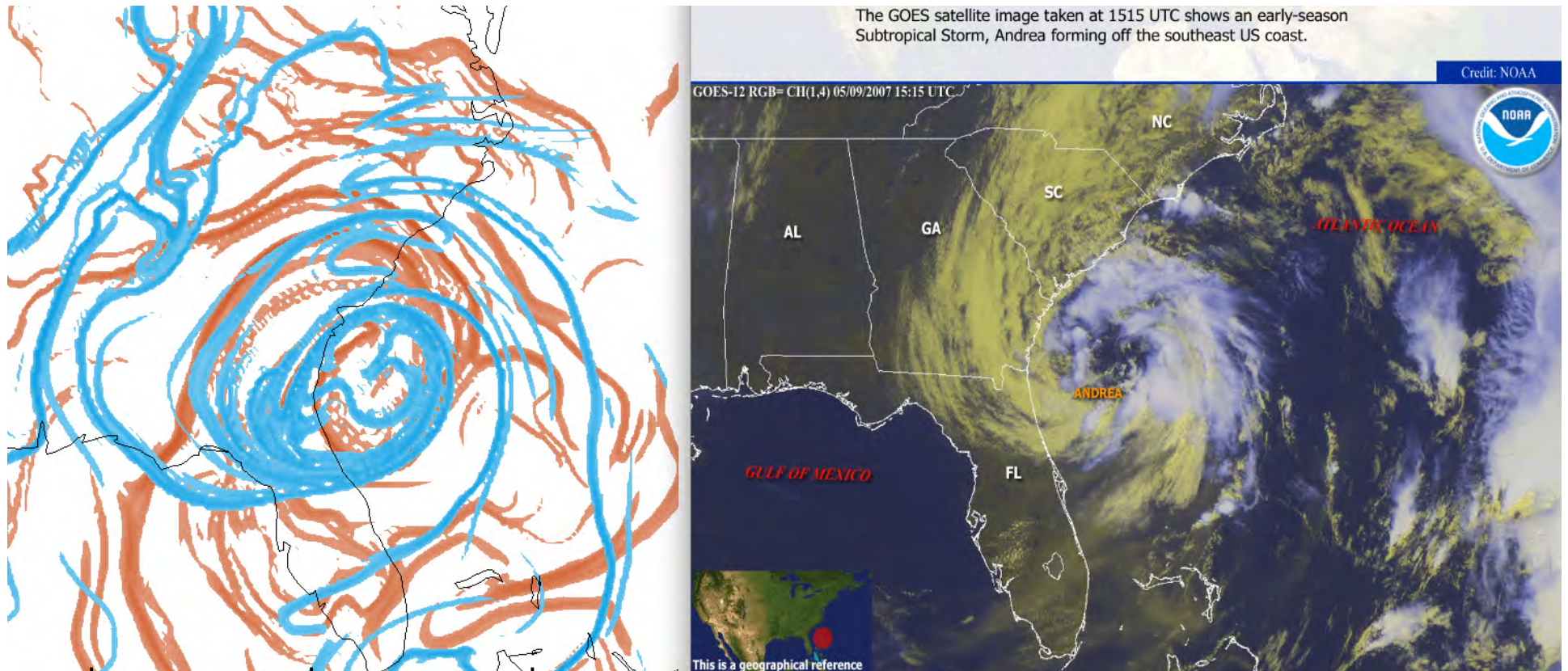
# Atmospheric flows: Antarctic polar vortex

air masses on either side of a repelling LCS

# Atmospheric flows: continental U.S.

LCSs: orange = repelling, blue = attracting

# Atmospheric flows and lobe dynamics



orange = repelling LCSs, blue = attracting LCSs

satellite

## Hurricane Andrea, 2007

cf. Sapsis & Haller [2009], Du Toit & Marsden [2010], Lekien & Ross [2010], Tallapragada & Ross [2011]

# Atmospheric flows and lobe dynamics



Hurricane Andrea at one snapshot; LCS shown (orange = repelling, blue = attracting)

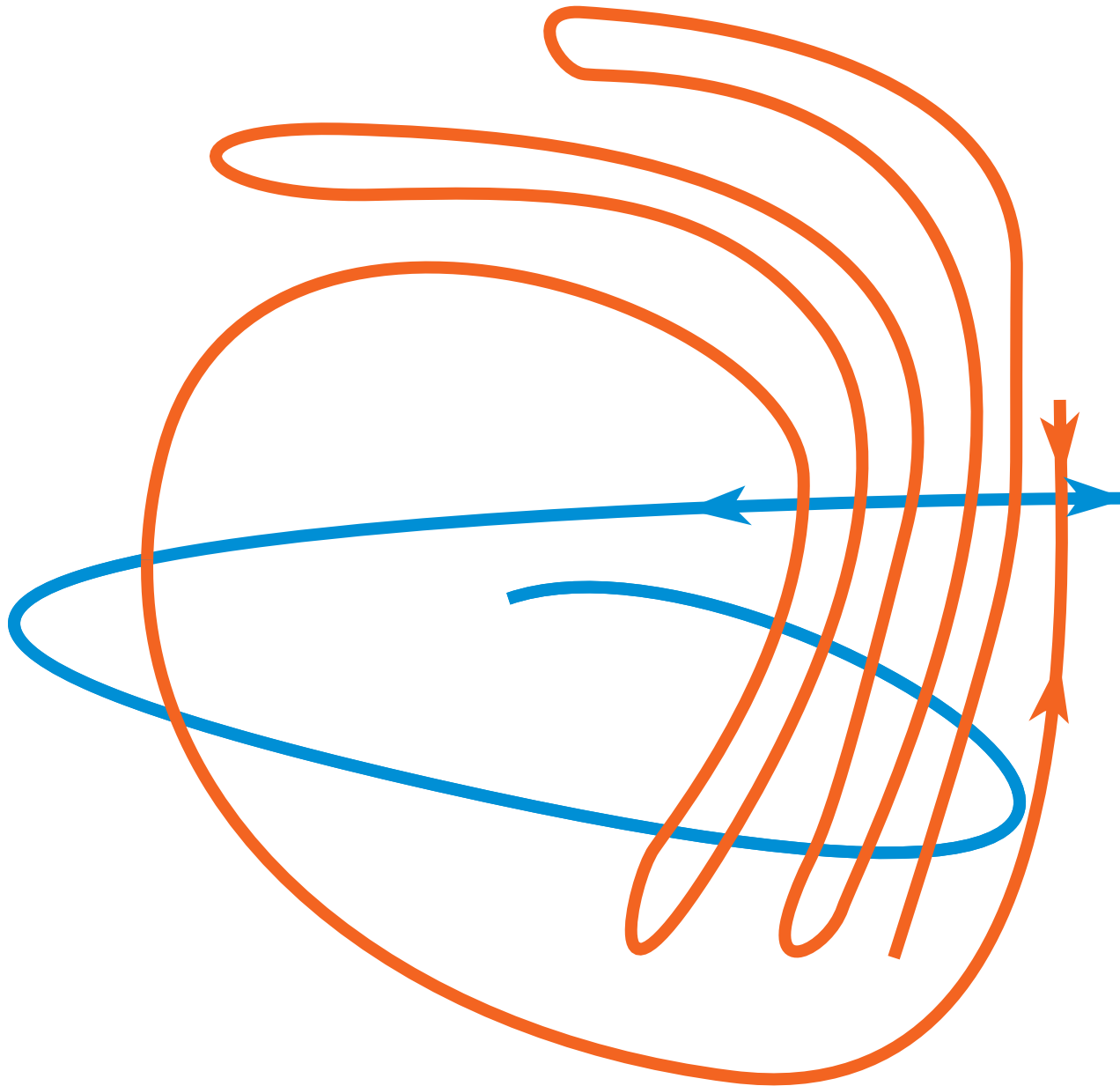


# Atmospheric flows and lobe dynamics



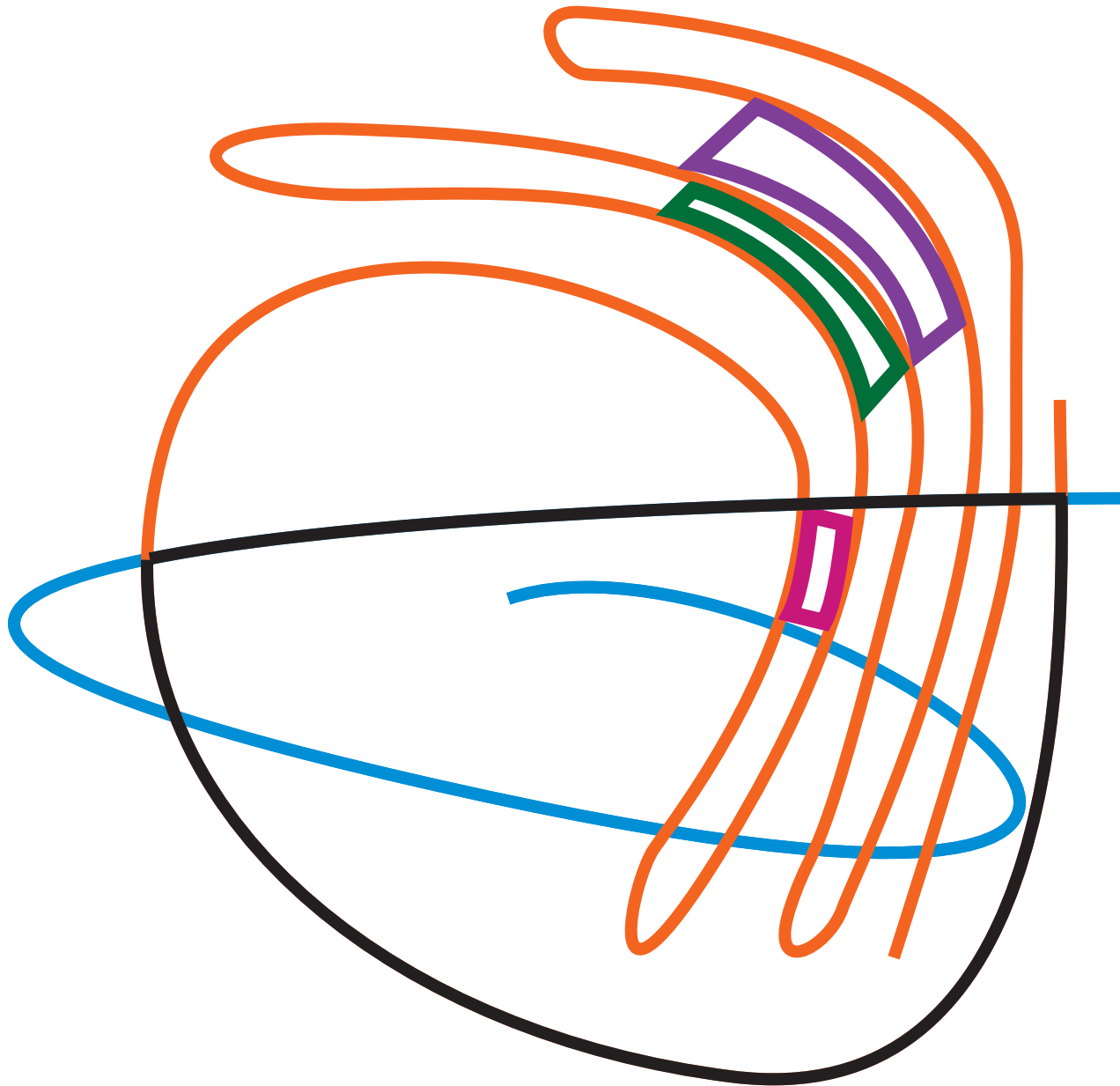
orange = repelling (stable manifold),    blue = attracting (unstable manifold)

# Atmospheric flows and lobe dynamics



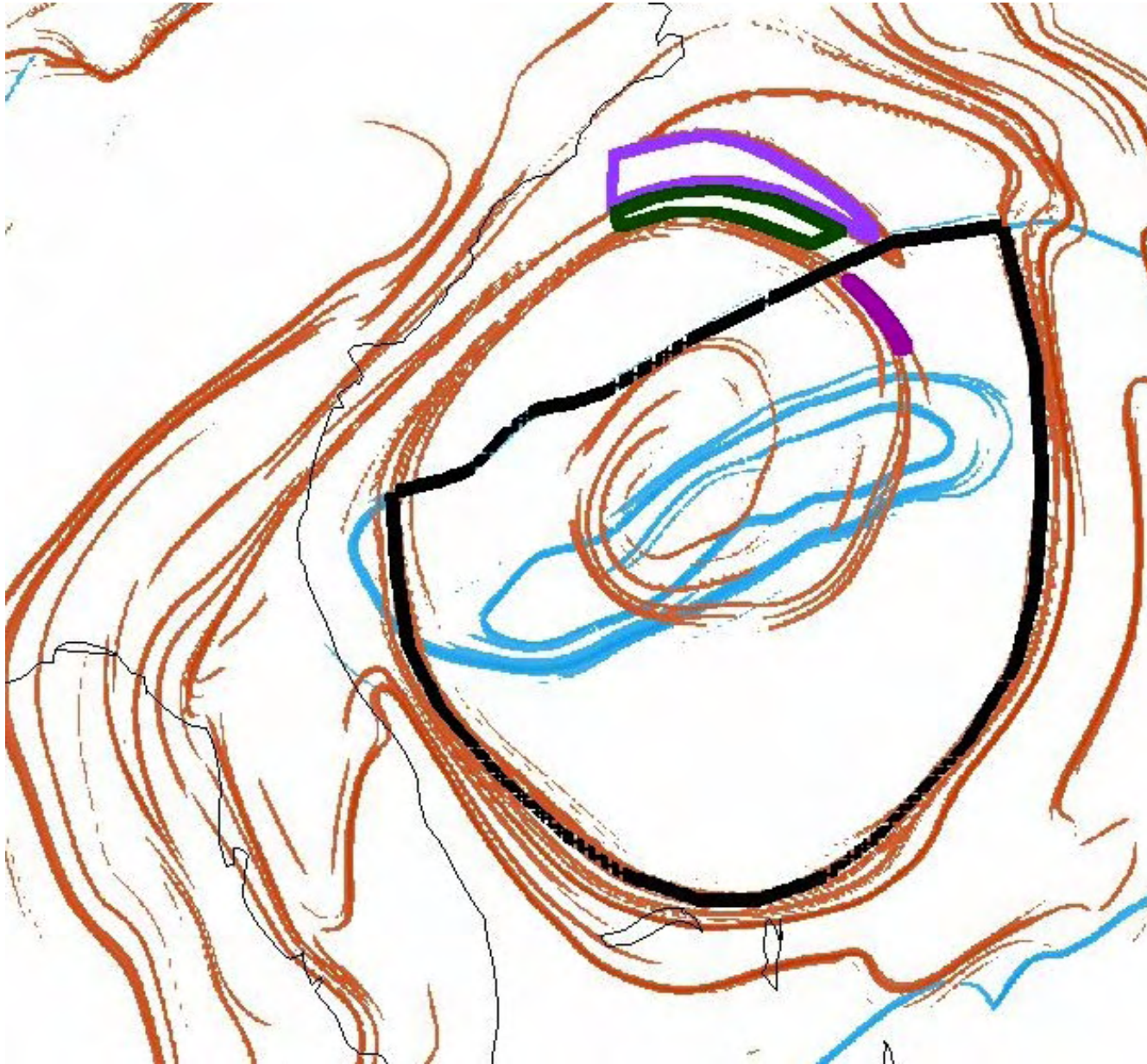
orange = repelling (stable manifold), blue = attracting (unstable manifold)

# Atmospheric flows and lobe dynamics



Portions of lobes colored; magenta = outgoing, green = incoming, purple = stays out

# Atmospheric flows and lobe dynamics



Portions of lobes colored; magenta = outgoing, green = incoming, purple = stays out

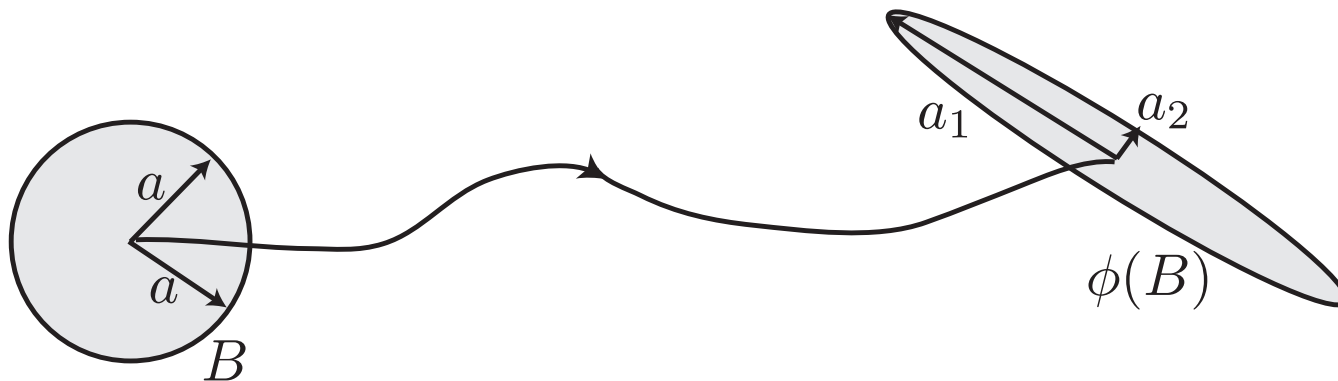
# Atmospheric flows and lobe dynamics

Sets behave as lobe dynamics dictates



# Coherent sets and set-based definition of FTLE

- Consider, e.g., a flow  $\phi_t^{t+T}$  in  $(x_1, x_2) \in \mathbb{R}^2$ .
- Treat the evolution of set  $B \subset \mathbb{R}^2$  as evolution of two random variables  $X_1$  and  $X_2$  defined by probability density function  $f(x_1, x_2)$ , initially uniform on  $B$ ,  $f = \frac{1}{\mu(B)} \mathcal{X}_B$ , with  $\mathcal{X}_B$  the characteristic function of  $B$ .
- Under the action of the flow  $\phi_t^{t+T}$ ,  $f$  is mapped to  $Pf$  where  $P$  is the associated Perron-Frobenius operator.
- Let  $I(f)$  be the covariance of  $f$  and  $I(Pf)$  the covariance of  $Pf$ .



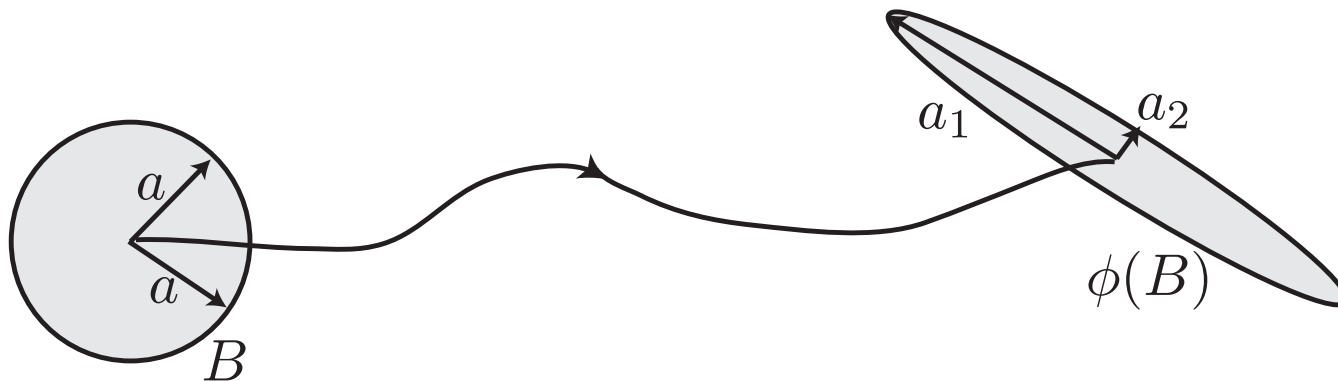
Deformation of a disk under the flow during  $[t, t + T]$

# Coherent sets and set-based definition of FTLE

- **Definition.** The **covariance-based FTLE** of  $B$  is

$$\sigma_I(B, t, T) = \frac{1}{|T|} \log \left( \frac{\sqrt{\lambda_{max}(I(Pf))}}{\sqrt{\lambda_{max}(I(f))}} \right).$$

- Reduces to usual definition of FTLE in the limit that the linearization approximation (i.e., line-stretching method) is valid

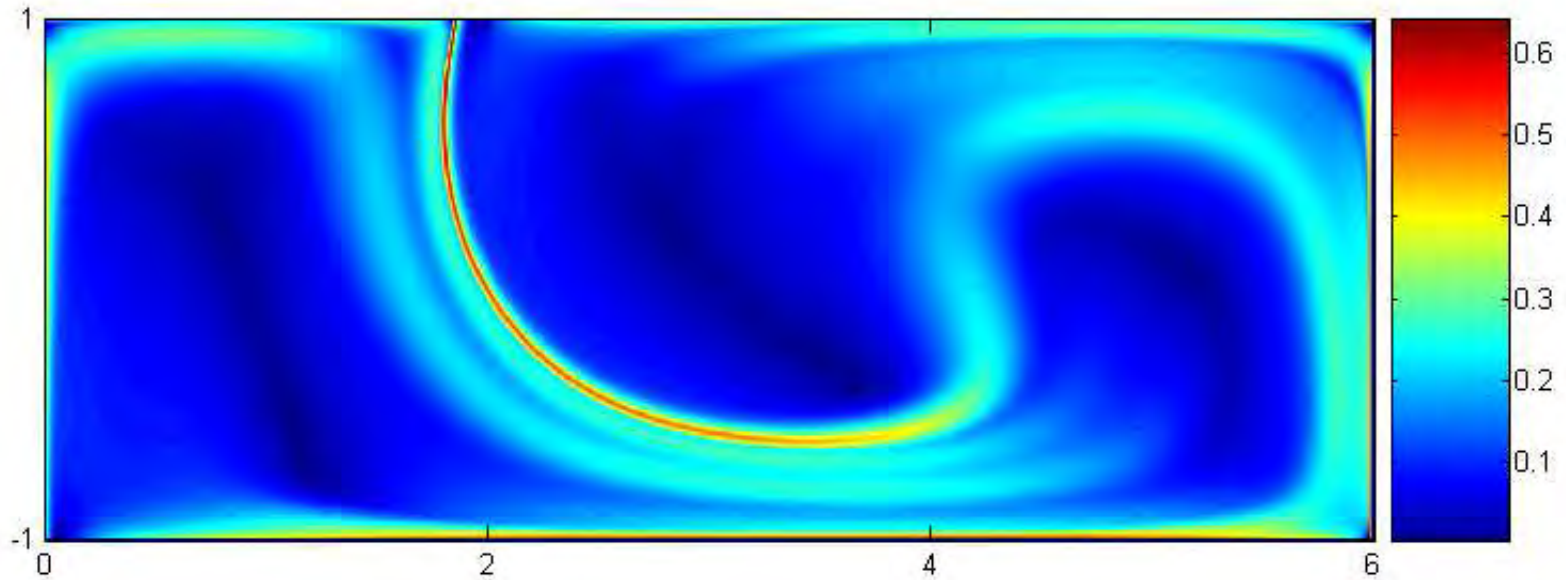


Deformation of a disk under the flow during  $[t, t + T]$

# Coherent sets and set-based definition of FTLE

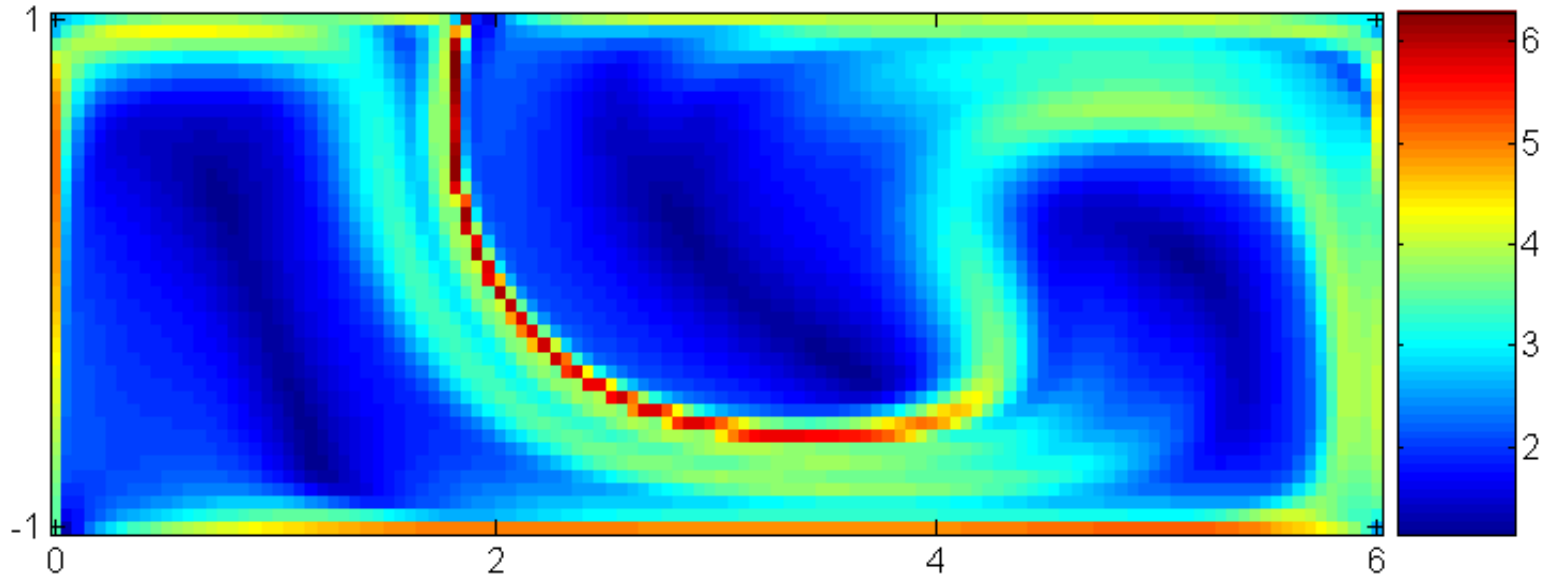
- The **coherence** of a set  $B$  during  $[t, t + T]$  is  $\sigma_I(B, t, T)$ .
- A set  $B$  is **almost-coherent** during  $[t, t + T]$  if  $\sigma_I(B, t, T) \approx 0$ .
- Captures the essential feature of a coherent set: it does not mix or spread significantly in the domain.
- This definition also can identify non-mixing **translating** sets.
- **Values of  $\sigma_I(B, t, T)$  determine the family of sets of various degrees of coherence.**
- Need to set a heuristic threshold on the value of  $\sigma_I(B, t, T)$  to determine coherent sets.
- Notice, coherent sets will be separated by ridges of high FTLE, i.e., LCS

# Coherent sets in lid-driven cavity flow



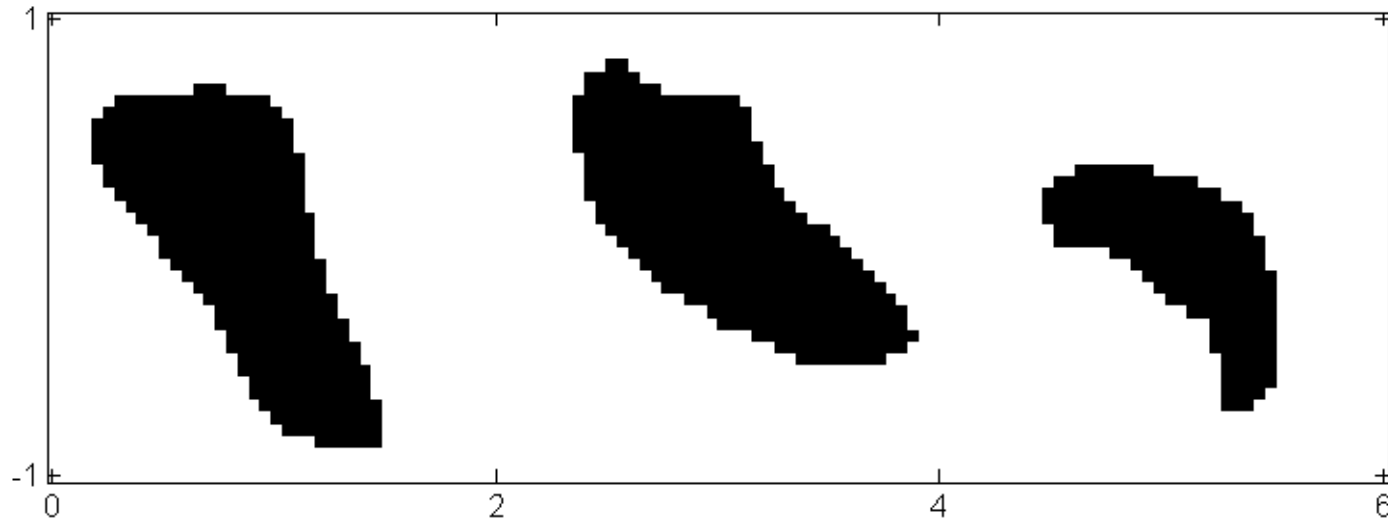
FTLE from line-stretching (conventional) during  $[0, \tau_f]$

# Coherent sets in lid-driven cavity flow



FTLE from covariance-based approach during  $[0, \tau_f]$

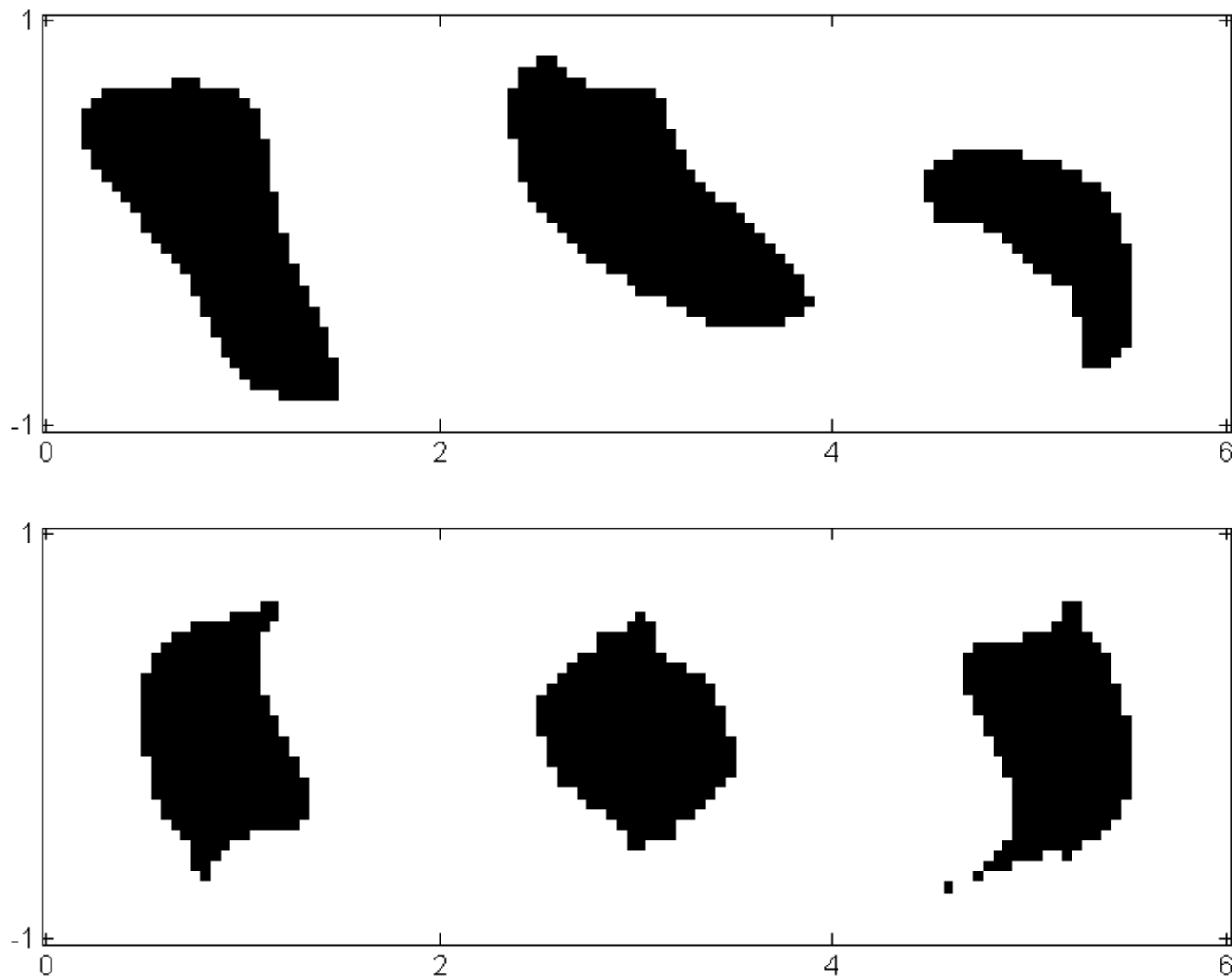
# Coherent sets in lid-driven cavity flow



Sets of coherences  $\sigma_I(0, \tau_f) < 1.6$

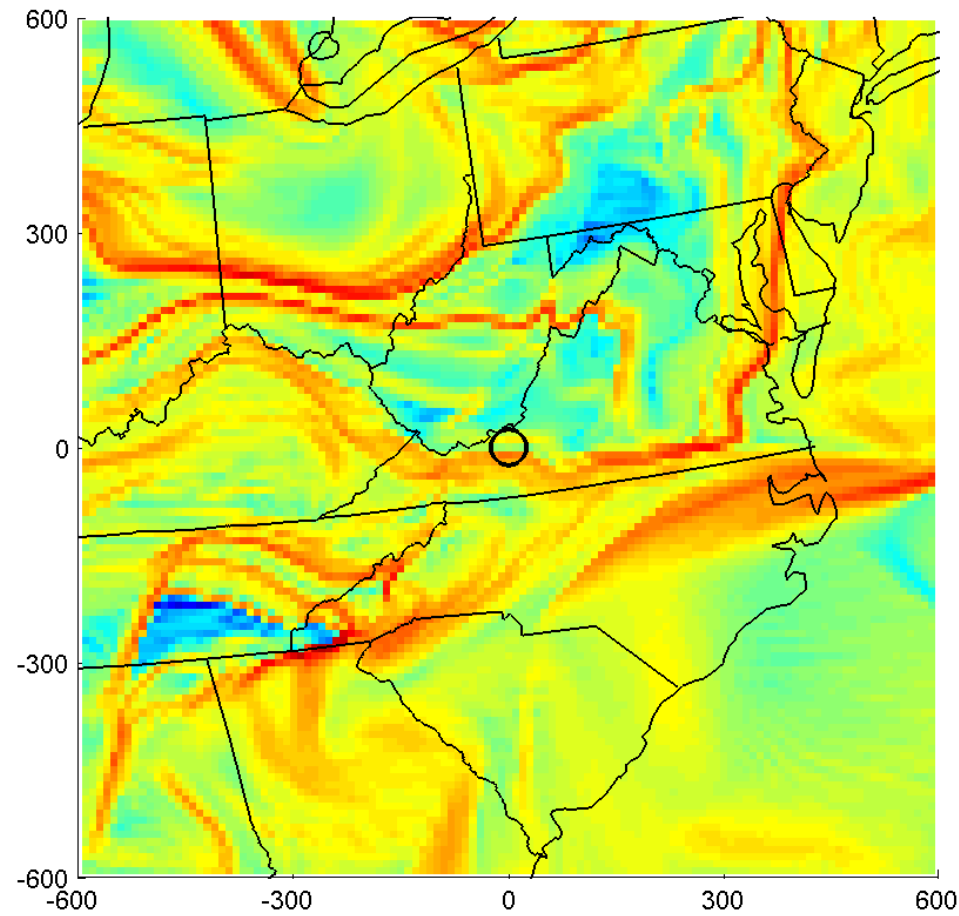


# Coherent sets in lid-driven cavity flow



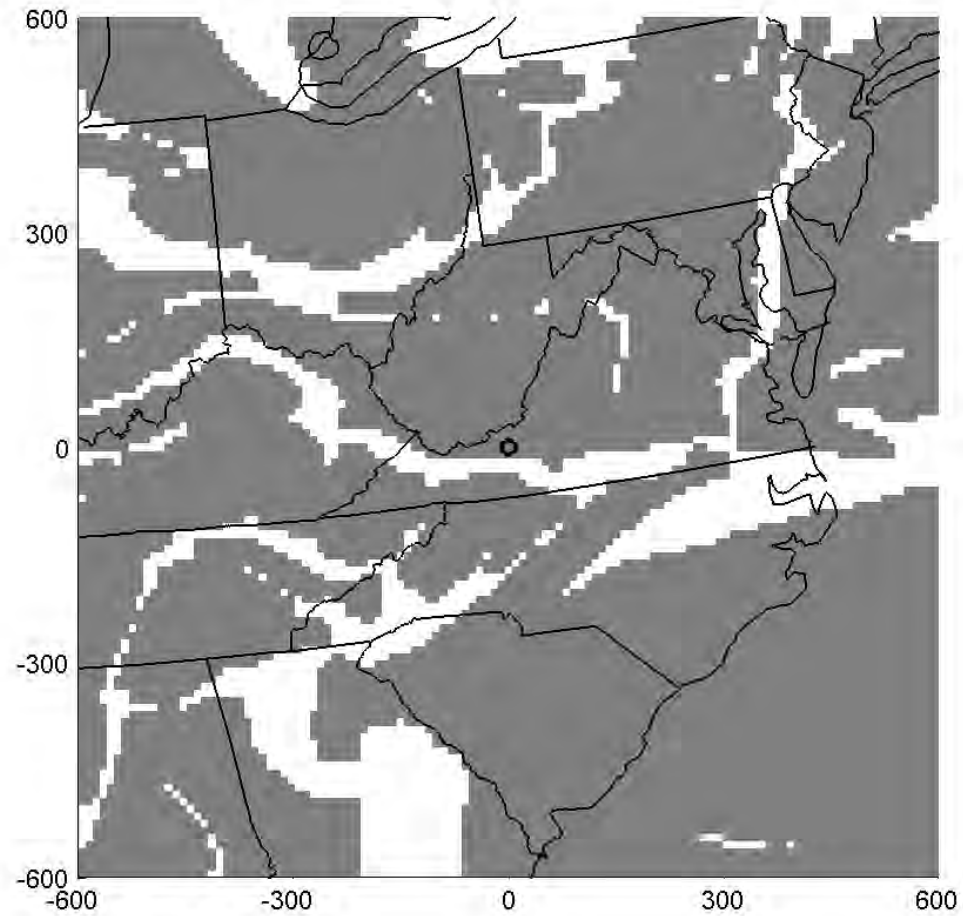
Compare with AIS from second eigenvector of  $P$

# Coherent sets in the atmosphere



- FTLE from covariance during 24 hours starting 09:00 1 May 2007

# Coherent sets in the atmosphere



- Coherent sets during 24 hours starting 09:00 1 May 2007

# Final words on chaotic transport

- What are robust descriptions of transport which work in data-driven aperiodic, finite-time settings?
  - Possibilities: finite-time lobe dynamics / symbolic dynamics may work
    - finite-time analogs of homoclinic and heteroclinic tangles
  - Probabilistic, geometric, and topological methods
    - invariant sets, almost-invariant sets, almost-cyclic sets, coherent sets, stable and unstable manifolds, Thurston-Nielsen classification, FTLE, LCS
  - Many links between these notions — e.g., LCS locate analogs of stable and unstable manifolds
    - boundaries between coherent sets are naturally LCS
    - periodic points  $\Rightarrow$  almost-cyclic sets
    - their ‘stable/unstable invariant manifolds’  $\Rightarrow$  ???

# The End

For papers, movies, etc., visit:

[www.shaneross.com](http://www.shaneross.com)

## Main Papers:

- Stremmer, Ross, Grover, Kumar [2011] Topological chaos and periodic braiding of almost-cyclic sets. *Physical Review Letters* 106, 114101.
- Tallapragada & Ross [2011] A geometric and probabilistic description of coherent sets. Preprint.
- Lekien & Ross [2010] The computation of finite-time Lyapunov exponents on unstructured meshes and for non-Euclidean manifolds. *Chaos* 20, 017505.
- Senatore & Ross [2011] Detection and characterization of transport barriers in complex flows via ridge extraction of the finite time Lyapunov exponent field, *International Journal for Numerical Methods in Engineering* 86, 1163.
- Grover, Ross, Stremmer, Kumar [2011] Topological chaos, braiding and breakup of almost-invariant sets. Preprint.
- Tallapragada & Ross [2008] Particle segregation by Stokes number for small neutrally buoyant spheres in a fluid, *Physical Review E* 78, 036308.